

UNIVERSITEIT VAN STELLENBOSCH  
UNIVERSITY OF STELLENBOSCH

*DISCHARGE MEASUREMENT AT  
NATURAL CONTROLS IN  
WESTERN CAPE RIVERS*



By

M.M. Barnard

Thesis presented in partial fulfilment of the  
requirements for the degree of  
Magister in Engineering (Civil)  
at the University of Stellenbosch

Prof. A. Rooseboom

Study Leader

## **DECLARATION**

I, the undersigned, hereby declare that the work contained in this thesis is my own original work and that I have not previously in its entirety or in part submitted it at any university for a degree.

## **SUMMARY**

This study sets out to explore the possibilities and accuracy of flow measurement at natural controls, focussing specifically on Western Cape cobble-bed rivers. These rivers are regarded as being difficult in terms of flow measurement, mostly due to their large scale roughness and very turbulent and uneven flows.

The aim is to determine a system through which various types of natural controls can be calibrated, by establishing a relationship between the discharge coefficient and the physical characteristics of each control type. This was achieved by conducting an extensive field investigation, focussing on the identification and gauging of both critical and uniform natural controls. Two types of critical controls were identified and investigated, namely step-pool controls and horizontal constriction controls as well as one type of uniform flow control, namely the plane bed control.

Step-pool controls were found to be very robust controls which provided efficient critical controls for a wide range of flows. Horizontal constriction controls proved to be reasonably accurate measurement sites and, because of their physical characteristics, they are able to measure the full range of flows from low to flood flows. Uniform controls are widely used for flow measurements on deep rivers, but such measurements become highly unreliable when flow depths are small and bed roughness high as is the case with cobble-bed rivers. Under conditions of high roughness, generally speaking critical controls can be calibrated more accurately than uniform controls and are therefore to be preferred.

The field study was followed by a series of laboratory tests, focussing on horizontal constriction controls. Calibration equations were derived by which the discharge coefficient value can be determined for a given constriction ratio and upstream energy head.

*Summary*

---

Results from both the fieldwork and laboratory work were analysed and integrated to determine a calibration system applicable to natural controls in Western Cape cobble- and boulder-bed rivers. Reasonably accurate values of the discharge coefficients for different types of natural controls were established, which should be widely applicable.

Additionally, guidelines were drawn up for the measurement of flow at natural controls, to be used by both engineers and non-engineers.

Discharge measurement at natural controls in the Western Cape was found to be a viable and reasonably accurate way of determining river discharge. It proves to be an environmentally acceptable way of measurement, using the natural river characteristics rather than seriously interfering with them or damaging them. These advantages make discharge measurement at natural controls a promising means of determining river discharge in the future.

## **OPSOMMING**

Die beste posisie vir vloeimeting in riviere is waar die topografie van die rivier 'n unieke verhouding tussen die deurstroming en die water diepte bewerkstellig.

Hierdie studie ondersoek die uitvoerbaarheid en akkuraatheid van vloeimeting by natuurlike kontroles met die fokus op Wes-Kaapse spoelklip riviere. Vloeimeting in spoelklip riviere word as baie ingewikkeld beskou weens die grootte van die bedpartikels relatief tot die vloediepte en gevolglike onewe, turbulente vloei.

Die doel van die studie was om 'n stelsel te ontwikkel waardeur verskillende tipes natuurlike kontroles gekalibreer kan word deur verwantskappe te bepaal tussen die deurstromings koëffisiënt en die stroom-op energie hoogte. Bogenoemde is bepaal met behulp van 'n uitgebreide veldstudie waarin die hoof tipes natuurlike kontroles, nl. die kritiese vloei kontrole en die uniforme vloei kontrole, geïdentifiseer en gekalibreer is. Twee tipes kritiese vloei kontroles is ondersoek, naamlik die trap-poel ("step-pool") kontrole en die horisontale vernouing kontrole.

Daar is bevind dat beide die trap-poel kontrole en die horisontale vernouing baie effektiewe kritiese kontroles is, waarmee 'n wye reeks van vloei gemeet kan word. Uniforme vloei kontroles word algemeen vir vloeimeting in diep vloeiende riviere gebruik, maar sulke metings word hoogs onbetroubaar wanner die vloediepte klein is relatief tot die partikel grootte van die rivierbed, soos in die geval van spoelklip riviere. Onder hierdie omstandighede kan kritiese kontroles in die algemeen meer akkuraat gekalibreer word en word hulle gevolglik bo uniforme vloei kontroles verkies.

Die veldstudie is gevolg deur 'n reeks laboratorium toetse, wat fokus op die horisontale vernouing kontrole. Kalibrasie vergelykings is afgelei waarmee die deurstromings koëffisiënt vir 'n gegewe stroom-op energiehogte en vernouings-verhouding bereken kan word.

Resultate van beide die veldstudie en die laboratorium toetse is geanaliseer en geïntegreer om 'n kalibrasie stelsel te bepaal wat van toepassing is op natuurlike

kontroles in Wes-Kaapse spoelklip riviere. Aanvaarbare waardes vir die deurstromings koëffisiente vir verskeie tipes natuurlike kontroles is bepaal, wat algemeen toepasbaar behoort te wees.

Riglyne vir die meting van riviervloei by natuurlike kontroles is opgestel vir die gebruik deur beide ingenieurs en nie-ingenieurs.

Vloei-meting deur middel van natuurlike kontroles is 'n lewensvatbare metingsmetode waarmee riviervloei redelik akkuraat bepaal kan word. Dit is 'n omgewings-aanvaarbare metings metode wat die natuurlike karakter van die rivier gebruik, eerder as om ernstig daarmee in te meng of dit te beskadig. Hierde positiewe eienskappe maak vloei-meting deur middel van natuurlike kontroles 'n belowende metingsmetode vir die toekoms.

## **DEDICATION**

This thesis is dedicated to my husband Ian.

Thank you for your immense support.

## **ACKNOWLEDGEMENTS**

To my Heavenly Father and Creator who gave me the strength to complete this study.

I hereby wish to express my sincerest gratitude to the following people who helped make this study possible:

- Professor Albert Rooseboom for all the time and energy he put into this study. His vast knowledge and experience, combined with his willingness to teach, made working under his guidance a lifelong experience.
- My parents Danie and Marie van Wyk for all their love and support throughout my life.
- My husband Ian for his immense support and help with this study.
- Julia Beck for her friendship and the hours spent discussing the thesis.
- Rodney, Ruth and Kenny for their valuable friendship, support and help.
- Lleana du Preez for making corrections to the thesis in my absence.
- WNK/WRC for the opportunity to conduct this research and their financial support.
- Final year students Stephan van Niekerk, Ryno Nel en Johan Kritzinger for their help with the fieldwork and laboratory work.
- Cape Nature Conservation for access to wilderness areas.
- All the individuals of the Water Division of the Department of Civil Engineering at Stellenbosch, for their general assistance and friendship.



---

**TABLE OF CONTENTS**

	<u>Page</u>
Declaration	
Summary	
Opsomming	
Dedication	
Acknowledgements	
Table of Contents	i
List of Figures	v
List of Tables	viii
List of Symbols	ix
<b>1. INTRODUCTION</b>	
1.1. Aims and Objectives of the Study	1-3
1.2. Methodology	1-3
<b>2. BASIC THEORY</b>	
2.1. Definition of a Control	2-1
2.2. Critical Flow Controls	2-2
2.2.1. Critical Flow Theory	2-2
2.2.2. Head-Discharge Equation at Critical Controls	2-5
2.2.3. Discharge Coefficient, $C_d$	2-7
2.2.4. Standard flow measurement structures	2-8
2.3. Uniform Flow Theory	2-12
2.3.1. Chézy and Manning Formulas	2-13
2.3.2. Applicability of the Chézy and Manning Formulas	2-14
2.3.3. Cobble and Boulder Bed Rivers	2-16
2.3.4. Sand Bed Rivers	2-19

---

<b>3. FIELDWORK</b>	
3.1. Introduction	3-1
3.2. Definitions	3-4
3.2.1. Flow Classification	3-4
3.2.2. Sediment Classification	3-4
3.3. General Criteria for Selecting Natural Control Sites	3-5
3.4. Natural Control Sites Selected for the Study	3-6
3.4.1. Site 1	3-6
3.4.2. Site 2	3-9
3.4.3. Site 3	3-11
3.4.4. Site 4	3-13
3.4.5. Site 5	3-15
3.4.6. Summary	3-16
3.5. Data Collection	3-17
3.5.1. Data Collection Procedure	3-17
3.5.2. Data Collection Points	3-18
3.5.3. Problems Encountered with Collection of Data	3-20
3.5.4. Recommendations	3-21
3.6. Analysis of Field Data	3-22
3.6.1. Calculating Discharge ( $Q$ ) from the Recorded Water Level ( $h$ )	3-22
3.6.1.1. Critical Controls	3-22
3.6.1.2. Uniform Controls	3-23
3.6.2. Determination of the discharge coefficient, $C_d$	3-24
3.7. Summary of Results	3-25
3.7.1. Step-pool Controls	3-25
3.7.2. Horizontal Constriction Control	3-26
3.7.3. Uniform Control	3-28

**4. LABORATORY WORK**

4.1. Introduction	4-1
4.2. Previous Studies	4-2
4.2.1. Hager (1985)	4-2
4.2.2. Hager (1986)	4-3
4.2.3. Hager (1988)	4-5
4.2.4. Samani and Magallanez (1993)	4-7
4.2.5. Samani and Magallanez (2000)	4-8
4.2.6. Malan and Van Huyssteen (1999)	4-10
4.3. Laboratory Tests	4-12
4.3.1. Approach followed	4-12
4.3.2. Laboratory Layout	4-13
4.3.3. Definition of Parameters	4-14
4.3.4. Tests Performed	4-17
4.3.4.1. Test Set 1: Constriction with Vertical Sides	4-17
4.3.4.2. Test Set 2: Constriction with Sloped Sides	4-18
4.3.4.3. Test Set 3: Constriction with Arbitrary Shape	4-19
4.4. Summary of Results	4-20
4.4.1. Test Set 1: Constriction with Vertical Sides	4-21
4.4.2. Test Set 2: Constriction with Sloped Sides	4-23
4.4.3. Test Set 3: Constriction with Arbitrary Shape	4-25

**5. INTEGRATED RESULTS**

5.1. Introduction	5-1
5.2. Step-Pool Controls	5-1
5.3. Horizontal Constriction Controls	5-3
5.3.1. Arbitrarily Shaped Controls	5-3
5.3.2. Non-Arbitrarily Shaped Controls	5-4
5.3.2.1. Vertical Sides Constriction	5-4
5.3.2.2. Sloped Sides Constriction	5-7
5.3.2.3. Laboratory Results compared to Previous Studies	5-10
5.4. Independent Verification of Results	5-13
5.5. Uniform Flow Controls	5-14

---

**6. CONCLUSIONS AND RECOMMENDATIONS**

6.1. Introduction	6-1
6.2. Step-Pool Controls	6-1
6.3. Horizontal Constriction Controls	6-2
6.4. Uniform Controls	6-3
6.5. General Conclusions	6-3
6.6. Recommendations for Further Research	6-4

**7. REFERENCES**

**APPENDIX A:** Guidelines on Flow Measurement at Natural Controls

**APPENDIX B:** Raw Data from Laboratory Test

**APPENDIX C:** Raw Data from Fieldwork

**APPENDIX D:** Calculations

## LIST OF FIGURES

	Page
Figure 2.1: Definition sketch for application of energy equation (Ven Te Chow, 1959).	2-2
Figure 2.2: Variation of Specific energy with depth given a constant discharge (Ven Te Chow, 1959).	2-3
Figure 2.3: Definition sketch for application of the Bernoulli equation.	2-6
Figure 2.4: Definition sketch for uniform flow description (Ven Te Chow, 1959).	2-12
Figure 2.5: Conceptual illustration of the roughness scale (Malan, 2002).	2-15
Figure 2.6: Definition sketch for Jonker's large-scale roughness equation (Jonker, 2002).	2-17
Figure 2.7: Eddy formed in between irregularities on channel bottom.	2-20
Figure 2.8: Bedforms in sand bed rivers (Rooseboom and Le Grange, 2000).	2-21
Figure 2.9: Progressive development of the total flow regime spectrum for a mobile bed consisting of single size particles (Rooseboom and Le Grange, 2000).	2-23
Figure 2.10: Resistance values and bedforms (Rooseboom and Le Grange 2000).	2-25
Figure 3.1: Location of Berg-, Molenaars-, Elandspad- and Jonkershoek Rivers.	3-2
Figure 3.2: Topographical map of Jonkershoek catchment.	3-3
Figure 3.3: Photograph of Site 1 at 0.31 m <sup>3</sup> /s.	3-6
Figure 3.4: Long section of Site 1.	3-7
Figure 3.5: High flow at Site 1, showing submerged boulders and channel control. (8 m <sup>3</sup> /s)	3-7
Figure 3.6: Low flow conditions at Site 1 showing concentrated flow and consequent high velocity flow conditions in the pool area. (0.31 m <sup>3</sup> /s)	3-8
Figure 3.7: Photograph of Site 2 at 0.31 m <sup>3</sup> /s.	3-9
Figure 3.8: Long section of Site 2.	3-10
Figure 3.9: Photograph of Site 3 at 0.31 m <sup>3</sup> /s.	3-11
Figure 3.10: Long section of Site 3.	3-12

Figure 3.11:	Site 3 at high flows. ( $8 \text{ m}^3/\text{s}$ )	3-12
Figure 3.12:	Photograph of Site 4 at $0.31 \text{ m}^3/\text{s}$ .	3-13
Figure 3.13:	Long section of Site 4.	3-14
Figure 3.14:	Flood flows at Site 4.	3-14
Figure 3.15:	Photograph of Site 5 at $0.31 \text{ m}^3/\text{s}$ .	3-15
Figure 3.16:	Long section of Site 5.	3-15
Figure 3.17:	Low flows at Site 5 showing boulders protruding out of water.	3-16
Figure 3.18:	Water level measurement points at Site 1.	3-19
Figure 3.19:	Water level measurement points at Site 3.	3-19
Figure 3.20:	Water level measurement points at Site 4.	3-20
Figure 3.21:	Water level measurement points at Site 5.	3-20
Figure 3.22:	Measured Flow versus Theoretical Flow.	3-27
Figure 4.1:	Transverse sections of trapezoidal, rectangular and U-shaped channels (Hager, 1985).	4-2
Figure 4.2:	Rectangular channel with circular cone constriction (Hager, 1986).	4-3
Figure 4.3:	Discharge correction coefficient $q = Q/Q_0$ as a function of $U$ . From Hager (1986).	4-4
Figure 4.4:	Venturi-type discharge measurement structure with thin-plate constriction (Hager, 1988).	4-5
Figure 4.5:	Coefficient of discharge as a function of relative energy head (Hager, 1988).	4-6
Figure 4.6:	Cross-sectional view of flume (Samani and Magallanez, 1993).	4-7
Figure 4.7:	Relationship between Relative Energy ( $H/B$ ) and Discharge Coefficient ( $C_d$ ) (Samani and Magallanez, 1993).	4-8
Figure 4.8:	Plan view of simple flume (Samani and Magallanez, 2000).	4-8
Figure 4.9:	Discharge coefficient ( $C_d$ ) versus Relative Energy ( $H/B_c$ ).	4-9
Figure 4.10:	Layout of the three basic critical control shapes tested.	4-10
Figure 4.11:	Examples from each laboratory test set.	4-12
Figure 4.12:	Laboratory Layout. (Not to scale)	4-13
Figure 4.13:	Position of measurement points.	4-14
Figure 4.14:	Control and pool sections.	4-15
Figure 4.15:	Constriction with vertical sides ( $B/b = 1.8$ ).	4-17
Figure 4.16:	Constrictions with sloped sides.	4-18

Figure 4.17:	Constrictions with arbitrary shape.	4-19
Figure 4.18:	$C_d$ vs $H/b$ for constriction with vertical sides.	4-22
Figure 4.19:	$C_d$ vs $H/b$ for constriction with sloped sides.	4-24
Figure 4.20:	$C_d$ vs $H/b$ for constrictions with arbitrary shapes.	4-25
Figure 5.1:	Error between measured data and calculated data using $C_d=0.61$ .	5-2
Figure 5.2:	$C_d$ vs $H/b$ for constriction with vertical sides.	5-4
Figure 5.3:	Design curves for Constrictions with Vertical Sides Constrictions.	5-5
Figure 5.4:	Percentage error in using the single design equation – Vertical Sides.	5-6
Figure 5.5:	$C_d$ vs $H/b$ for constriction with Sloped Sides.	5-7
Figure 5.6:	Design curves for Sloped Sides Constrictions.	5-8
Figure 5.7:	Percentage error in using the single design equation – Sloped Sides.	5-9
Figure 5.8:	Comparison between Vertical Sides Laboratory data and data from Hager (1985) and Samani & Magallanez (2000).	5-10
Figure 5.9:	Comparison between Sloped Sides Laboratory data and data from Hager (1986).	5-11
Figure 5.10:	Comparison between Laboratory data and data from Hager (1985,1986) and Samani & Magallanez (2000).	5-12
Figure 5.11:	Streamline curvature for different constrictions.	5-12
Figure 5.12:	Velocity distributions at critical cross section of Circular Cone Constriction. From Hager (1986).	5-13
Figure 5.13:	Comparison between accuracy of calculations using Jonker (2002)'s and Malan (2002)'s discharge equations respectively.	5-14

---

**LIST OF TABLES**

	Page
Table 2.1: Standard Flow Measurement Weirs (From Bos, 1977).	2-9
Table 2.2: Critical Depth Flumes with Various Cross-sectional Shapes (From Clemmens, Bos and Replogle, 1984).	2-10
Table 2.3: Roughness Scale (From Jonker, 2002).	2-15
Table 3.1: Summary of Results obtained from Site 1.	3-26
Table 3.2: Summary of Results obtained from Site 3.	3-26
Table 3.3: % Error in Theoretical Calculation of Discharge.	3-27
Table 3.4: Results using Jonker (2002)'s discharge equation.	3-28
Table 3.5: Results using Malan (2002)'s discharge equation.	3-28
Table 4.1: Discharge coefficients from tests performed by Malan and Van Huyssteen (1999) on basic critical controls.	4-11
Table 4.2: Results from river modelled controls (Malan and Van Huyssteen, 1999).	4-11
Table 4.3: Summary of Results obtained from Test Set 1.	4-21
Table 4.4: Summary of Results obtained from Test Set 2.	4-23
Table 4.5: Summary of Results obtained from Test Set 3.	4-25
Table 5.1: Percentage difference between calculated discharge using $C_d=0.61$ and measured discharge for Step-Pool controls.	5-2
Table 5.2: Percentage Error using a Discharge Coefficient $C_d=1.26$ for Field Results.	5-3



**LIST OF SYMBOLS**

$\bar{y}_c$	=	Average flow-depth of control section
$\bar{y}_p$	=	Average flow-depth of pool section
$\bar{b}$	=	Average width of control section = $A_c / \bar{y}_c$
$A_c$	=	Flow area at control section
$A_p$	=	Flow area at pool section
$H/b$	=	Relative energy head
$\bar{B}/\bar{b}$	=	Constriction ratio
$\bar{B}$	=	Average width of pool section = $A_p / \bar{y}_p$
$A$	=	Cross sectional flow area = $W_T \bar{D}$ [m <sup>2</sup> ]
$A_c$	=	Flow area of critical control section [m <sup>2</sup> ]
$B$	=	Surface width of waterway [m]
$B_c$	=	Surface width at critical control section [m]
$C$	=	Chézy's resistance factor (Chézy's C)
$C_d$	=	Discharge coefficient $C_d = \frac{Q_{real}}{Q_{theoretical}}$
$D$	=	Hydraulic mean depth = $A/B$ [m]
$d_{50}$	=	Median particle diameter [m]
$d_{84}$	=	Particle size for which 84% of the particle sizes are smaller [m]
$E_s$	=	Specific energy [m]
$g$	=	Gravitational acceleration [m/s <sup>2</sup> ]
$H$	=	Energy head [m]
$h_{1 \times h_{max}}$	=	Water head at 1 x $h_{max}$ distance upstream from control section
$h_1$	=	Water depth at stage measurement section [m]
$h_{2 \times h_{max}}$	=	Water head at 2 x $h_{max}$ distance upstream from control section
$h_{3 \times h_{max}}$	=	Water head at 3 x $h_{max}$ distance upstream from control section
$h_{4 \times h_{max}}$	=	Water head at 4 x $h_{max}$ distance upstream from control section
$h_c$	=	Water head at control section

---

$H_c$	=	Energy head at control section = $\bar{y}_c + \frac{v_c^2}{2g}$
$h_{ds}$	=	Water head at downstream section
$h_{max}$	=	Maximum water head at control section
$H_p$	=	Energy head at pool section = $\bar{y}_p + \frac{v_p^2}{2g}$
$h_{V-notch}$	=	Water head at V-notch weir, taken upstream from the weir at a distance equal to 4 times the maximum head to be measured at the weir plate
$k_s$	=	Absolute roughness coefficient
$n$	=	Manning's roughness coefficient (Manning's $n$ )
$Q$	=	Discharge [ $m^3/s$ ]
$Q_c$	=	Discharge through critical control section [ $m^3/s$ ]
$R$	=	Hydraulic radius = $A/P$ [m]
$R/d_{50}$	=	Relative submergence
$S$	=	Energy slope
$S_f$	=	Energy slope
$S_o$	=	Bed slope
$V$	=	Average flow velocity = $Q/A$ [m/s]
$v$	=	Flow velocity [m/s]
$V$	=	Mean flow velocity [m/s]
$v_l$	=	Velocity at stage measurement section [m/s]
$v_c$	=	Velocity at control section [m/s]
$v_{ss}$	=	Average particle settling velocity [m/s] $v_{ss} = \sqrt{\frac{4}{3} \frac{g}{0.4} \left( \frac{\rho_s - \rho}{\rho} \right) d_{50}}$
$y$	=	Flow depth [m]
$y_c$	=	Water depth at control section [m]
$\rho$	=	Density of water = $1000 \text{ kg/m}^3$
$\rho_s$	=	Average mass density of particles, taken as $2450 \text{ kg/m}^3$ for Western Cape rivers

---

## 1 INTRODUCTION

Water is South Africa's most important natural resource. It is the lifeblood of all life and the key to the country's future development and prosperity. At the very heart of this development is the proper management and precise quantification of this resource to ensure survival for man and nature alike.

The new Water Act of South Africa (National Water Act no.36 of 1998) aims to accommodate both human needs as well as ecological protection by implementing a measure called the 'reserve'. With the 'reserve', the Act seeks to allocate adequate water, in terms of quantity and quality, for South Africa's population, as well as its ecosystems. Consequently, the 'reserve' comprises of two distinct parts: the 'basic human needs reserve' and the 'ecological reserve'. The human rights reserve relates to the basic right of all persons to have access to a minimum amount and minimum quality of water for living, whereas the ecological reserve refers to the minimum quantity and minimum quality of water necessary for a healthy ecosystem.

To determine the ecological reserve, detailed environmental studies need to be undertaken to evaluate and understand each unique river ecosystem. The measurement of river discharge plays a pivotal role in these studies. It allows ecologists to relate ecological health and requirements to an easily quantifiable parameter which can be monitored on a continuous basis.

As more and more studies are being conducted on mountainous rivers, the need has increased for flow measurement in these rivers. This has proven to be a difficult exercise due to the complex nature of these rivers. Mountainous rivers mostly have cobbles and boulders as bed-material, causing the flow in the upper reaches of these rivers to be highly non-uniform and turbulent with the steep gradients and series of steps and pools rather than uniform stretches of river. Along reaches where the gradient is reasonably flat, flow is often controlled by large scale roughness effects. There are few existing weirs on these rivers, mainly because they are difficult to construct and to

maintain. Existing gauging weirs are mostly situated lower down on rivers where more tranquil flow conditions exist. There are serious environmental objections to the construction of new weirs. A cost effective and reasonably accurate method to measure river discharge in mountainous rivers, without disturbing the natural river ecology, is therefore sought.

Traditionally flow measurement in South African rivers has been done by means of flow gauging weirs. These include sharp crested weirs, broad crested weirs and various types of flumes (Wessels, 1996). These structures form obstructions in river courses. Being built at right angles to river channels and by constricting flow in the vertical and/or horizontal directions, they form unnatural controls which locally alter the natural flows of rivers. These structures may have a detrimental impact on the ecology e.g. by forming barriers to migrating fish, preventing them from migrating upstream to spawn.

From an engineering perspective, weir structures in rivers pose maintenance problems with large sediment loads silting up weir pools and floods causing structural damage. A natural river is in equilibrium and will therefore try to correct any unnatural slope changes imposed on it.

In the light of the above, an alternative discharge measurement method is being sought which makes use of the natural characteristics and shape of a river rather than by using artificial structures. Natural control sites such as channel constrictions, transverse rock outcrops or stretches where near uniform flow occurs are potential sites for flow measurement without artificial structures. Flow conditions at these sites allow unique relationships to be drawn between stage and discharge, thus making continuous gauging possible by recording flow depths and translating these into discharge values.

Being able to measure discharges at natural controls provides an ecologically acceptable means of determining river discharges without interfering with natural river flows and in a cost effective way. Since the control is part of the natural river channel, costs are limited to those of the stage recorder making such gauging very attractive.

Experience gained with a wide range of gauging structures (Hager, 1985, 1986 and 1988; Samani and Magallanez 1993, 2000) indicated that discharge coefficients for different shapes of structures did not vary greatly. This led to the conclusion that it should be possible to determine discharge coefficients for different natural controls with an acceptable degree of accuracy.

### **1.1 Aims and Objectives of the Study**

This study sets out to explore the possibilities and accuracy of flow measurement at natural controls, focussing specifically on Western Cape cobble-bed rivers. These rivers are regarded as being difficult in terms of flow measurement, mostly due to their large scale roughness and very turbulent and uneven flows.

The aim of the study is to determine a system through which various types of natural controls can be calibrated, by establishing a relationship between the discharge coefficient and the physical characteristics of each control type.

Finally, guidelines will be drawn up for the measurement of flow at natural controls, to be used by both engineers and non-engineers.

### **1.2 Methodology**

The first component of the study comprised an extensive field investigation, focussing on the identification and gauging of both critical and uniform natural controls. At the same time a literature study into various aspects of discharge measurement was conducted. This was followed by a series of laboratory tests based on the literature study as well as results from the fieldwork.

Results from both the fieldwork and laboratory work were analysed and integrated to determine a calibration system applicable to natural controls in Western Cape cobble- and boulder-bed rivers.

## 2 BASIC THEORY

### 2.1 Definition of a control

A control section is defined as being any section in a watercourse where a unique and known relationship between stage ( $h$ ) and discharge ( $Q$ ) exists. This unique relationship enables the discharge to be calculated from the measured water level, making control sites attractive for continuous flow measurement since only stage needs to be recorded which can later be translated into discharge.

Controls most commonly used for discharge measurement are sections where flow passes from subcritical to supercritical. These controls are called critical controls and common examples are weirs, flumes, gates, spillways and free overfalls.

Another, not so commonly used in South Africa, type of control is found where uniform flow occurs for a reasonable length of the watercourse. Uniform flow is not associated with particular localised features, as is the case with critical controls. It is characterised by the constant depth which the flow tends to assume in a long uniform channel, when no other controls are present (Henderson, 1966).

Controls may be either natural or artificial, depending upon whether they are of natural origin or constructed by man. Natural controls can be formed by single topographic features such as reefs of bedrock extending across a stream or clasts of boulders constricting the flow, thus forming a critical control; or by long stretches of river having essentially uniform characteristics, thus inducing uniform flows.

The basic theory of critical- and uniform controls, as used for discharge measurement, is discussed in the following sections. Problems associated with the use of uniform flow equations in cobble and boulder bed rivers, as well as sand bed rivers, are also addressed.

## 2.2 Critical Flow Controls

### 2.2.1 Critical Flow Theory

Flow conditions at a critical control can be defined in terms of the specific energy equation. Specific energy ( $E_s$ ) is the energy head relative to the channel bottom as datum.

Consider flow in an open channel with flow depth  $y$  and flow velocity  $v$  (Ven Te Chow, 1959). See Figure 2.1.

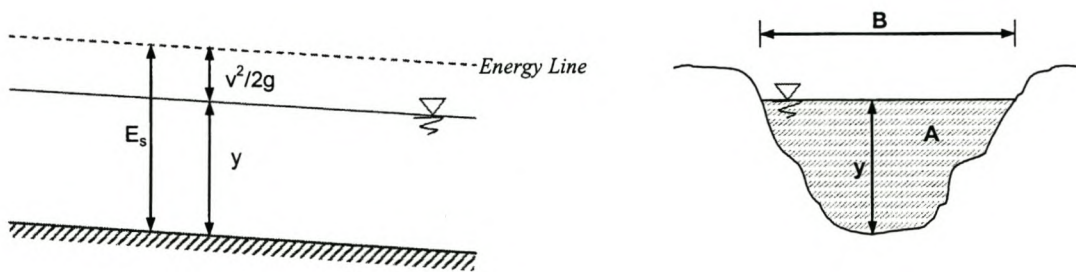


**Figure 2.1: Definition sketch for application of energy equation (Ven Te Chow, 1959).**

The specific energy is thus defined as:

$$E_s = y + \frac{v^2}{2g} \quad \dots 2-1$$

Where

$E_s$	=	Specific energy [m]
$y$	=	Flow depth [m]
$v$	=	Flow velocity [m/s]
$g$	=	Gravitational acceleration [m/s <sup>2</sup> ]

From the continuity equation

$$Q = vA \quad \dots 2-2$$

Where

$Q$	=	Discharge [m <sup>3</sup> /s]
$A$	=	Flow area [m <sup>2</sup> ]

Equation 2-1 can now be written as

$$E_s = y + \frac{\left(\frac{Q}{A}\right)^2}{2g}$$

$$E_s = y + \frac{Q^2}{2gA^2} \quad \dots 2-3$$

Now consider the variation in  $E_s$  with  $y$  for a constant discharge value  $Q$ . Plotting the depths of flow ( $y$ ) against the specific energy ( $E_s$ ) for a given discharge and channel section (Figure 2.2), leads to a graph known as the specific energy curve (Ven Te Chow, 1959).

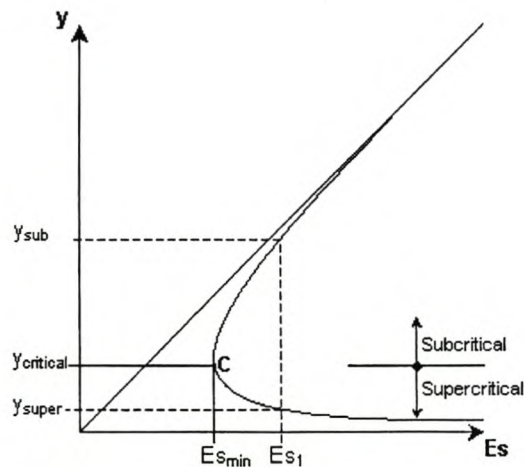


**Figure 2.2: Variation of Specific energy with depth given a constant discharge (Ven Te Chow, 1959).**

The curve indicates that, for a given specific energy value other than the critical value, there are two possible depths of flow known as alternate depths. Two regimes of flow can be distinguished from the curve:

- 1) Fast and shallow (supercritical flow) and
- 2) Slow and deep (subcritical flow).

At point C, the specific energy is a minimum. Here the flow is poised between the two regimes of flow, subcritical and supercritical, and is referred to as 'critical flow'.



For a minimum value of  $E_s$

$$\frac{dE_s}{dy} = 0 \quad \dots 2-4$$

$$\begin{aligned} \therefore \frac{dE_s}{dy} &= 1 + \frac{Q^2}{2g} \frac{d}{dA} \left( \frac{1}{A^2} \right) \frac{dA}{dy} = 0 \\ &= 1 - \frac{Q^2}{gA^3} \frac{dA}{dy} \quad \dots 2-5 \end{aligned}$$

Considering the effect on the area  $A$  of a small increase in depth  $y$ :

$$\therefore dA = Bdy$$

Where

$B$  = Surface width of waterway [m]

Substituting the above into Equation 2-5, leads to

$$\begin{aligned} \therefore \frac{dE_s}{dy} &= 1 - \frac{Q^2}{2g} \frac{2B}{A^3} \\ \therefore \frac{Q^2 B}{gA^3} &= 1 \quad \dots 2-6 \end{aligned}$$

Since the Froude number ( $Fr$ ) is defined as

$$Fr = \frac{V}{\sqrt{gD}} \quad \dots 2-7$$

Where

$V$  = Average flow velocity =  $Q/A$  [m/s]  
 $D$  = Hydraulic mean depth =  $A/B$  [m]

It follows that

$$Fr = \sqrt{\frac{Q^2 B}{gA^3}} \quad \dots 2-8$$

It is clear from Equations 2-6 and 2-8 that, for critical flow conditions the Froude number is equal to unity, which is the defining principle of critical flow.

$$\therefore Fr = 1 \text{ for critical flow}$$

From Equation 2-6 the discharge equation, applicable to all critical control sections, can be established:

$$Q_c = \sqrt{\frac{gA_c^3}{B_c}} \quad \dots 2-9$$

Where

$Q_c$	=	Discharge through critical control section [m <sup>3</sup> /s]
$A_c$	=	Flow area of critical control section [m <sup>2</sup> ]
$B_c$	=	Surface width at critical control section [m]

### 2.2.2 Head-Discharge Equation at Critical Controls

“At a critical control section, the relationship between the depth of flow and the discharge is definitive, independent of the channel roughness and other uncontrollable circumstances. Such a definitive stage-discharge relationship offers a theoretical basis for the measurement of discharge in open channels” (Ven Te Chow, 1959).

For the purpose of flow measurement it is essential that the discharge at the control section is related to the upstream energy head, where stage will be measured. To establish this relationship the Bernoulli equation is applied between the stage measurement section and the control section (Figure 2.3).

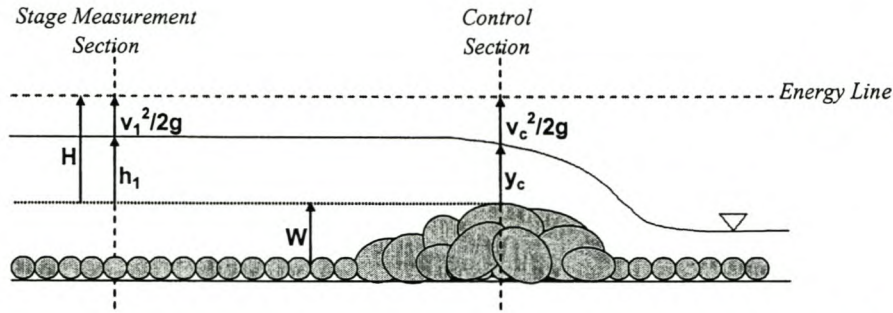


**Figure 2.3: Definition sketch for application of the Bernoulli equation.**

Applying the Bernoulli equation between two sections and assuming ideal flow conditions, thus assuming

- 1) uniform velocity distribution at both sections,
- 2) straight and parallel streamlines, and
- 3) no energy losses between the two sections

leads to the following equation:

$$H = h_1 + \frac{\alpha_1 v_1^2}{2g} = y_c + \frac{\alpha_2 v_c^2}{2g} \quad \dots 2-10$$

Where

$H$	=	Energy head [m]
$h_1$	=	Water depth at stage measurement section [m]
$y_c$	=	Water depth at control section [m]
$v_1$	=	Velocity at stage measurement section [m/s]
$v_c$	=	Velocity at control section [m/s]
$\alpha$	=	Correction coefficient applied to velocity head as calculated from the mean velocity

From the continuity equation it follows that

$$Q = v_1 A_1 = v_c A_c \quad \dots 2-11$$

$$\therefore v_c = \frac{Q}{A_c} \quad \dots 2-12$$

and substituting Equation 2-9 into Equation 2-12, results in

$$v_c = \sqrt{\frac{gA_c}{B_c}} \quad \dots 2-13$$

When substituted into Equation 2-10, Equation 2-10 becomes:

$$H = y_c + \frac{\alpha A_c}{2B_c} \quad \dots 2-14$$

Both  $A_c$  and  $B_c$  are fully determined in terms of  $y_c$ , and it follows that critical flow in the control section is uniquely related to the energy head  $H$ .

Combining Equation 2-10, 2-11 and 2-13 gives the head-discharge equation for critical controls of any shape

$$\begin{aligned} Q &= v_c A_c \\ &= \sqrt{\frac{gA_c}{B_c}} A_c \\ &= \sqrt{\frac{g(H - y_c)2B_c}{\alpha B_c}} A_c \end{aligned}$$

$$Q = A_c \sqrt{\frac{2g}{\alpha}} (H - y_c)^{1/2} \quad \dots 2-15$$

### 2.2.3 Discharge Coefficient, $C_d$

The discharge coefficient is a coefficient that corrects for non-ideal flow conditions. Because the assumptions made in the derivation of the head-discharge equation, namely

- 1) uniform velocity distribution,
- 2) straight and parallel streamlines, and
- 3) no energy losses due to friction or by boundary layer development

are not completely valid, a discharge coefficient ( $C_d$ ) should be incorporated.

The value of  $C_d$  is denoted by

$$C_d = \frac{Q_{real}}{Q_{theoretical}} \quad \dots 2-16$$

The discharge coefficient is generally not constant for all flow depths, and can vary with varying water levels.

The head-discharge equation can now be written as

$$Q = C_d A_c \sqrt{\frac{2g}{\alpha}} (H - y_c)^{1/2} \quad \dots 2-17$$

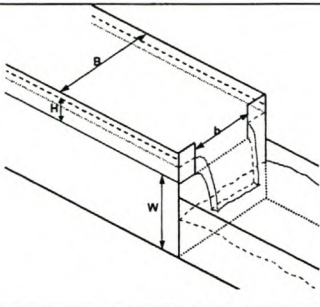
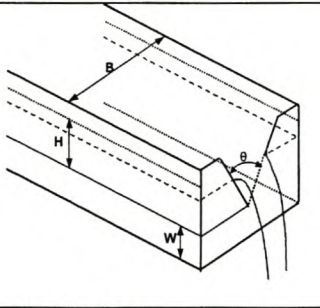
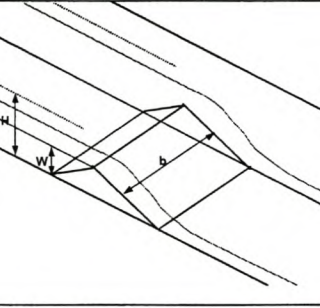
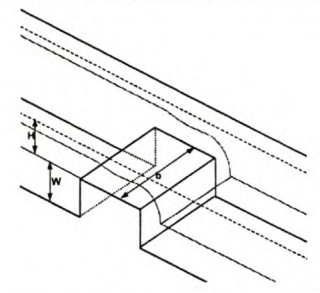
#### 2.2.4 Standard Flow Measurement Structures

In the previous section the head-discharge equation for an arbitrarily shaped critical control was derived. The following two tables give the head-discharge equations of various standard flow measuring structures which are frequently used for discharge measurement.

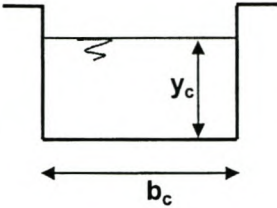
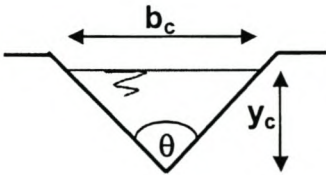
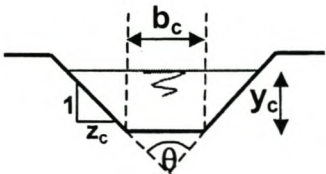
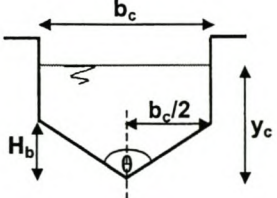
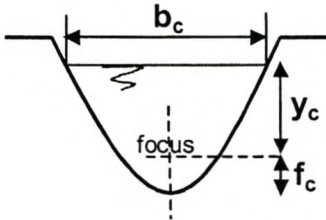
Equations for critical depth flumes exhibit much the same form as Equation 2-17 and may possibly be used to represent conditions at natural controls, provided that corrections are introduced to compensate for the imperfect shapes of the natural control sections. Equations for measurement weirs are somewhat different from Equation 2-17, since the upstream energy head can not be directly derived from the critical flow depth ( $y_c = \frac{2}{3} H$ ) due to the irregular shapes of the control sections.

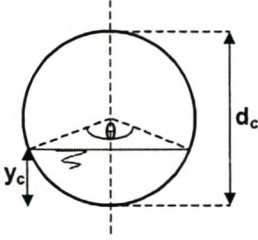
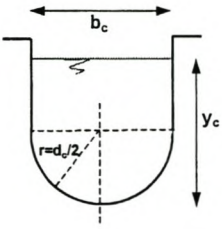
Table 2.1 shows various types of flow measurement weirs and Table 2.2 shows critical depth flumes with different cross sectional shapes.

**Table 2.1: Standard Flow Measurement Weirs (From Bos, 1976).**

Name	Definition Sketch	Head-Discharge Equation
Rectangular Sharp Crested Weir		$Q = C_d \frac{2}{3} \sqrt{2gb} H^{3/2}$
Triangular Sharp Crested Weir		$Q = C_d \frac{8}{15} \tan \frac{\theta}{2} \sqrt{2g} H^{5/2}$
Triangular Profile Weir (Crump)		$Q = C_d \sqrt{gb} H^{3/2}$
Rectangular Profile Weir (Broad Crested)		$Q = C_d \left(\frac{2}{3}\right)^{3/2} \sqrt{gb} H^{3/2}$

**Table 2.2: Critical Depth Flumes with Various Cross-sectional Shapes (From Clemmens, Bos and Replogle, 1984).**

<p>Rectangular</p>		$Q = C_d \frac{2}{3} \sqrt{\frac{2}{3}} g b H^{3/2}$ $y_c = \frac{2}{3} H$
<p>Triangular</p>		$Q = C_d \frac{16}{25} \sqrt{\frac{2}{5}} g \tan \frac{\theta}{2} H^{5/2}$ $y_c = \frac{4}{5} H$
<p>Trapezoidal</p>		$Q = C_d [b y_c + z_c y_c^2] \sqrt{2g} [H - y_c]^{1/2}$ $y_c = \text{variable}$
<p>Compound Triangular / Rectangular</p>		$H \leq 1.25 H_b \quad (y_c = \frac{4}{5} H)$ $Q = C_d \frac{16}{25} \sqrt{\frac{2}{5}} g \tan \frac{\theta}{2} H^{5/2}$ $H \geq 1.25 H_b \quad (y_c = \frac{2}{3} H + \frac{1}{6} H_b)$ $Q = C_d \frac{2}{3} \sqrt{\frac{2}{3}} g b (H - \frac{1}{2} H_b)^{3/2}$
<p>Parabolic</p>		$Q = C_d \sqrt{\frac{3}{4}} f_c g H^2$ $y_c = \frac{3}{4} H$

<p>Circular</p>		$Q = C_d d_c^{5/2} \sqrt{g} [f(\theta)]$ $f(\theta) = \left( \frac{A_c}{d_c^2} \right) \left\{ 2 \left( \frac{H}{d_c} - \frac{y_c}{d_c} \right) \right\}^{1/2}$
<p>U-shaped</p>		$H \leq 0.7 d_c$ $Q = C_d d_c^{5/2} \sqrt{g} [f(\theta)]$ $f(\theta) = \left( \frac{A_c}{d_c^2} \right) \left\{ 2 \left( \frac{H}{d_c} - \frac{y_c}{d_c} \right) \right\}^{1/2}$ $H \geq 0.7 d_c$ $Q = C_d 2 d_c \sqrt{2g} \left( \frac{1}{3} H - 0.0358 d_c \right)^{3/2}$ $y_c = \frac{1}{2} H + 0.152 d_c$

It proves that there is a great deal of communality between formulas for comparable cross sectional shapes. This strengthens the belief that formulas for comparable natural control sections should also follow well-defined patterns.





The best known and the most widely used uniform flow formulas are those of Chézy and Manning.

### 2.3.1 Chézy and Manning Formulas

Chézy Formula:  $V = C\sqrt{RS}$  . . . 2-19

Manning Formula:  $V = \frac{1}{n} R^{2/3} S^{1/2}$  . . . 2-20

Where

$C$  = Chézy's resistance factor (Chézy's  $C$ )  
 $n$  = Manning's roughness coefficient (Manning's  $n$ )

The Manning equation is very sensitive to the value of  $n$ . The choice of an appropriate Manning  $n$  value relies heavily on the experience and judgement of the engineer since there is no exact method of selecting the  $n$  value. The value of  $n$  is highly variable and depends on a number of factors, viz. surface roughness, vegetation, channel irregularities, channel alignment, silting and scouring, obstructions to flow, size and shape of channel, stage and discharge and sediment concentration (Ven Te Chow, 1959). Various tables and graphs are available as guidelines for selecting a Manning  $n$  value and the reader is referred to Ven Te Chow (1959) and Rooseboom et al. (1984) for the most extensive and useful of these.

The Chézy equation, which makes use of an absolute roughness coefficient, was found to be more robust and mathematically correct than the Manning equation (Rooseboom, 1974).

Chézy's  $C$ , for fully rough turbulent flow, can be expressed as follows:

$$C = 18 \log \left( \frac{12R}{k_s} \right) \quad \dots 2-21$$

Where

$k_s$  = Absolute roughness coefficient

It must be kept in mind that the  $k_s$  value is the average size of the eddies which are formed to fit in between the irregularities on the bed (Rooseboom, 1984).

See Figure 2.7. Refer to Rooseboom (1984) for a graph of relevant  $k_s$  values.

### 2.3.2 Applicability of the Chézy and Manning Formulas

The resistance coefficient in both the Chézy and Manning formulas depends upon various factors viz. surface roughness, vegetation, channel irregularities and alignment, silting and scouring, channel size and shape, obstruction to flow and the roughness (Ven Te Chow, 1959). These formulas were developed for conditions of small-scale roughness, where the physical roughness elements are small relative to the flow depth and flow resistance may be attributed mainly to surface drag on the channel boundary. It is recommended by Ven Te Chow (1959) that the standard resistance coefficients be used only when the relative roughness ( $d_{50}/D$ ) is less than 0.3.

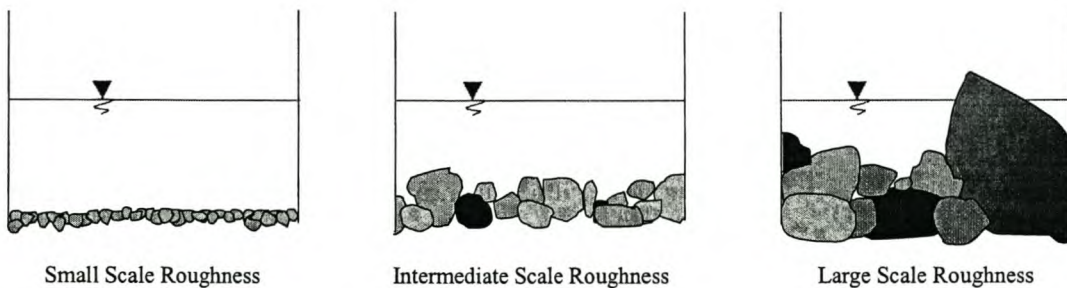
Cobble and boulder bed rivers are characterised by steep gradients and relatively low flow depths in relation to bed particle size, and as a result display complex velocity-depth relationships. Under these large-scale roughness conditions the boundary resistance becomes less dominant, while form drag around the individual particles composing the river bed and disturbance of the free water surface become more significant (Jonker, 2002).

Due to the very different hydraulic mechanisms of flow resistance under conditions of large-scale roughness, conventional friction based uniform flow equations, such as the Chézy and Manning equations, are inaccurate as they may largely underestimate channel resistance (Jonker, 2002).

Table 2.3 provides a scale distinguishing between small, intermediate and large-scale roughness depending on the relative submergence ratios. Figure 2.5 gives a conceptual illustration of the scale.

**Table 2.3: Roughness Scale (From Jonker, 2002).**

Roughness Scale	Relative Submergence	
Small Scale	$\frac{D}{d_{50}} > 7.5$	$\frac{D}{d_{84}} > 4$
Intermediate Scale	$2 < \frac{D}{d_{50}} < 7.5$	$1.2 < \frac{D}{d_{84}} < 4$
Large Scale	$\frac{D}{d_{50}} < 2$	$\frac{D}{d_{84}} < 1.2$

**Figure 2.5: Conceptual illustration of the roughness scale (From Malan, 2002).**

Sand bed rivers, on the other hand, continuously adjust their water- and sediment transport balance. Sediment being transported will lead to a change in the resistance of flow by changing the bed roughness and the suspended sediment concentration. The resistance to flow is a complex function of flow, fluid and sediment characteristics and is dependent on the variations in the bed forms (Rooseboom and Le Grange, 2000).

Changes in flow resistance for a sand bed river under steady flow, are considered to be due to changes in the degree of bed deformation and the consequent roughness of the bed. Bed forms vary as the flow regime varies and their influence in determining the total resistance are far more significant than that of particle roughness within most flow regimes.

---

Studies performed by Jonker (2002), Malan (2002) and Rooseboom and Le Grange (2000) address the problems associated with cobble and boulder bed rivers and sand bed rivers, respectively. Jonker (2002) developed a new equation for calculating the mean velocity in cobble and boulder bed rivers while Rooseboom and Le Grange developed a system from which the appropriate roughness coefficient and the associated bedforms can be determined for sand bed rivers. Their work is discussed briefly in the following two sections.

### 2.3.3 Cobble and Boulder Bed Rivers

Cobble and boulder bed rivers are characterised by steep gradients and relatively low flow depths in relation to bed particle size, and as a result display complex velocity-depth relationships. Flow in these rivers is very turbulent and particularly so at low flows when bed elements protrude out of the water and affect the free water surface. Malan (2002) stated that the bed roughness could be classified as large-scale if the roughness elements affect the free surface.

Under these large-scale roughness conditions the boundary resistance becomes less dominant, while form drag around the individual particles composing the river bed and disturbance of the free water surface become more significant (Jonker, 2002). Malan (2002) stated that in the case of large-scale roughness, the roughness elements tend to act individually and that the total resistance to flow is mainly the sum of their form drags.

As stated before, conventional friction based uniform flow formulas, such as the Chézy and Manning formulas, are not applicable to the large scale roughness situation as these equations underestimate channel resistance significantly (Jonker, 2002). New equations thus had to be formulated of which the most are empirically based. Studies conducted by Jonker (2002) and Malan (2002) formulated discharge equations to be used for large-scale roughness. Both Jonker (2002) and Malan (2002)'s equations are calibrated for Western Cape rivers.

The equations developed by Jonker (2002) and Malan (2002) will be discussed next.

Jonker (2002) developed the following equation from which the discharge can be calculated for a uniform stretch of river with large-scale roughness:

$$Q = A \sqrt{\frac{2gd_{50}S_o}{0.5285\left(\frac{R}{d_{50}}\right)^{-2.166}}} \quad \dots 2-22$$

Where

$Q$	=	Discharge [ $\text{m}^3/\text{s}$ ]
$g$	=	Gravitational acceleration [ $\text{m}/\text{s}^2$ ]
$d_{50}$	=	Median particle diameter [m]
$S_o$	=	Bed slope
$R$	=	Hydraulic radius [m]
$A$	=	Cross sectional flow area = $W_T \bar{D}$ [ $\text{m}^2$ ] (See Figure 2.6)
$R/d_{50}$	=	Relative submergence

This equation is only applicable under conditions of large scale roughness as defined in Section 2.3.2.

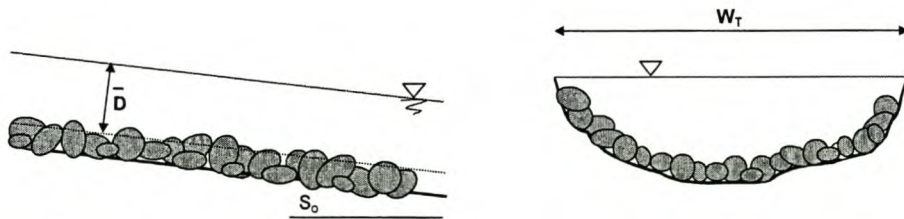


**Figure 2.6: Definition sketch for Jonker's large-scale roughness equation. (Jonker, 2002)**

Jonker proved that the equation is able to consistently provide fairly accurate estimates ( $\pm 25\%$ ) of mean flow velocity under conditions of large-scale roughness. The development of the equation was theoretically based, which makes it more generally applicable than most other, previously developed, empirical and semi-empirical equations, which are site specific.

Malan (2002) found that traditional resistance equations containing parameters of energy slope, bed material gradation and relative submergence correlated well with the data set obtained by him in the Western Cape rivers. An investigation was undertaken to identify the significant parameters influencing the roughness coefficient under Western Cape large-scale roughness conditions and it was found that the following parameters were significant:

- 1) Relative submergence  $\left(\frac{d}{D_{84}}\right)$
- 2) Energy slope ( $S_f$ )
- 3) Bed material size ratio  $\left(\frac{D_{84}}{D_{50}}\right)$
- 4) The ratio between applied stream power and the power required to suspend a particle  $\left(\frac{\sqrt{gRS_f}}{v_{ss}}\right)$ .

Malan (2002) calibrated the following equation in order to calculate discharges in a plane bed, large-scale roughness river in the Western Cape.

$$Q = 115.9 \frac{R^{1.75} S_f^{0.2}}{v_{ss}^{0.5}} \left(\frac{d_{50}}{d_{84}}\right)^{3.84} P \quad \dots 2-23$$

Where

- $d_{84}$  = Particle size for which 84% of the particle sizes are smaller [m]  
 $S_f$  = Energy slope  
 $v_{ss}$  = Average particle settling velocity [m/s]  $v_{ss} = \sqrt{\frac{4}{3} \frac{g}{0.4} \left(\frac{\rho_s - \rho}{\rho}\right) d_{50}}$   
 $\rho_s$  = Average mass density of particles, taken as 2450 kg/m<sup>3</sup> for Western Cape rivers  
 $\rho$  = Density of water = 1000 kg/m<sup>3</sup>  
 $P$  = Wetted perimeter

He also calibrated Chézy's  $C$  for specific use in Western Cape cobble bed rivers:

$$\frac{C}{\sqrt{g}} = 20.9 \left(\frac{\sqrt{gRS_f}}{v_{ss}}\right)^{0.5} \left(S_f^{-0.55} \left(\frac{D_{84}}{D_{50}}\right)^{-3.84}\right) \quad \dots 2-24$$

Thirty percent of the discharge values obtained by using Equation 2-23 were within the 10% accuracy band and 45,5% within the 20% accuracy band (Malan, 2002).

#### 2.3.4 Sand Bed Rivers

“Sand bed rivers continuously adjust their water- and sediment transport balance. This occurs by virtue of the considerable flexibility of an added import variable, namely the form roughness of the bed” (Rooseboom and Le Grange, 2000). Bedform roughness is the result of variations in flow depth, flow velocity and sediment concentration. Sediment being transported will lead to a change in the resistance of flow by changing the bed roughness and the suspended sediment concentration.

A sand bed river is inclined to assume a condition of minimum energy dissipation, i.e. minimization of applied stream power. The presence of sediment in the river provides an alternative mechanism whereby scour is limited through deformation of the river bed. As a river bed is deformed and the value of  $k_s$  increases, the applied unit stream power along the bed is decreased (Rooseboom and Le Grange, 2000).

Rooseboom (1974) stated, “that whenever alternative modes of flow exist, that mode which requires the least amount of applied unit power will be adopted. It follows that fluid flowing over transportable material will not transport such material unless this would result in less power being applied than without sediment transport.”

#### *The influence of sediment transport on flow resistance*

A major problem when working with sand bed rivers is the roughness function. If a river bed is flat and no roughness of the bedform is present, the absolute roughness value  $k_s$  is represented by an equivalent value of the radius  $R_o$  of the eddies formed right next to the bed and having a size of the same order of magnitude as the irregularities on the bed (Figure 2.7). This equivalent roughness  $R_o$  is generally regarded to be a function of the particle diameter  $d$ .



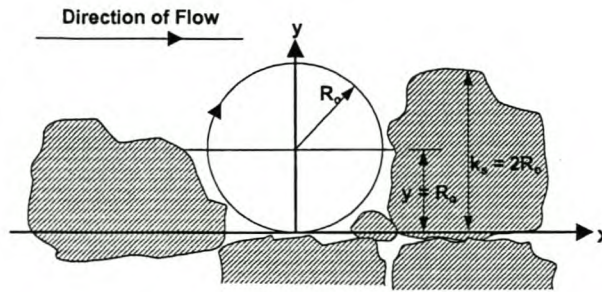


**Figure 2.7: Eddy formed in between irregularities on channel bottom.**

According to the unit stream power theory, the applied stream power will tend to increase as the discharge increases. It is also recognised that increasing flow in an erodible channel generates complex bed forms along the channel bed.

When sediment is being transported, the amount of stream power applied along the bed can be reduced by (Rooseboom, 1974):

- 1) the formation of a pseudo-viscous zone of high concentration suspension along the bed which acts in a similar fashion to a true laminar sub-layer, or
- 2) deformation of the bed through the formation of bed forms whereby eddies with larger radii are formed along the bed i.e. the value of  $k_s$  increases.

When the value of  $k_s$  increases, it represents a decrease in the amount of applied power along the bed for maintaining motion.

The resistance to flow is a complex function of discharge, fluid and sediment characteristics and is dependent on the variations in bed forms. Changes in flow resistance for a sand bed river under steady flow are considered to be due to change in the degree of bed deformation and the consequent roughness of the bed.

Bedforms vary as the flow regime varies and their influence in determining the total resistance is far more significant than that of particle roughness within certain flow regimes.

Rooseboom and Le Grange (2000) separated bedforms into three main categories of flow regimes:

- 1) The lower flow regime (low stream power) consisting of ripples, bars, dunes with ripples superimposed and dunes. See Figure 2.8a, b and c.
- 2) The transition zone comprising a flat bed with no bedforms. See Figure 2.8d.
- 3) The upper flow regime, comprising the upper regime bedforms of plane bed, antidunes (standing waves and breaking antidunes), chutes and pools, etc. See Figure 2.8e and f.

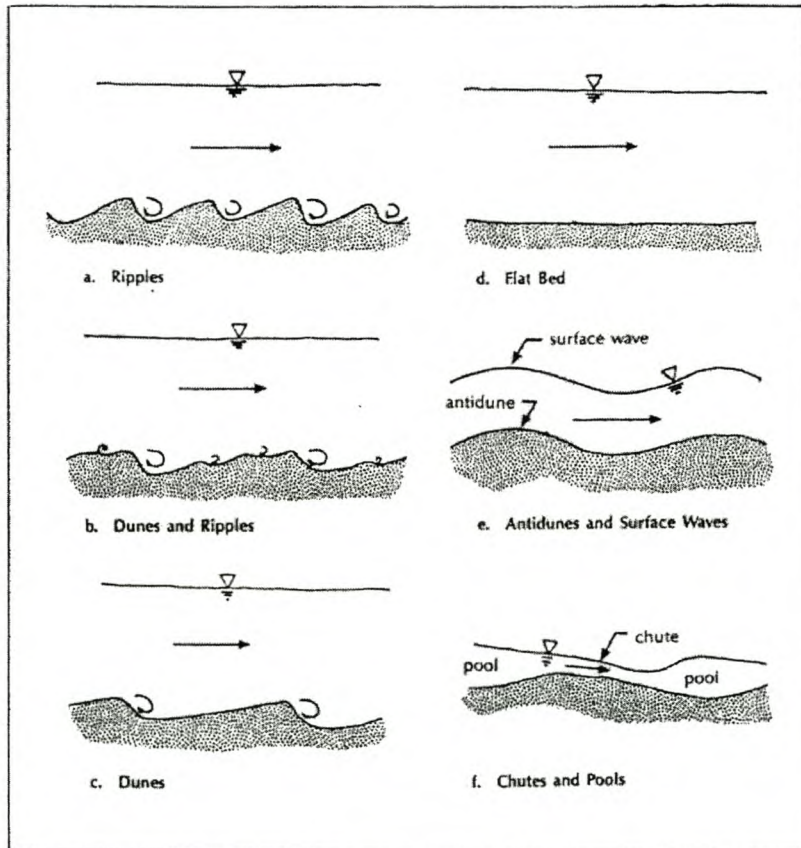


**Figure 2.8: Bedforms in sand bed rivers**  
(From Le Grange, 1994).

At low flows and low sediment transport concentrations, the bed deforms into a series of bedforms known as ripples and dunes. (Figure 2.8)

At higher flows and higher sediment concentrations, the amplitude of the bedforms rapidly become smaller and for fine sands the bedforms may disappear leaving a flat bed with a minimum friction factor for the given flow. (Figure 2.8)

At the upper flow regime, standing waves tend to form with associated bedforms known as antidunes. (Figure 2.8)

At still higher flows, breaking waves form and the flow becomes difficult to describe quantitatively.

At low discharges and depths of flow the resistance to flow is in accordance with the relationships that describe non-sediment carrying flows. At high discharges and depths of flow, however, the friction factors are primarily determined by the interaction between the transported sediment and flowing fluid, i.e. the absolute roughness value  $k_s$ .

Rooseboom and Le Grange (2000) explained the progressive development of the total flow regime spectrum for a mobile bed consisting of a single particle diameter  $d$  by means of a diagram (Figure 2.9) showing the unique relationship between the two parameters  $\frac{\sqrt{gDs}}{v_{ss}}$  (representing the unit power being applied along the bed relative to the power required to suspend the particles of a given density and diameter) and  $\frac{\sqrt{gDs} k_s}{\nu}$  (representing the ratio between applied stream power for laminar conditions and the applied stream power for turbulent boundary conditions along an uneven bed).

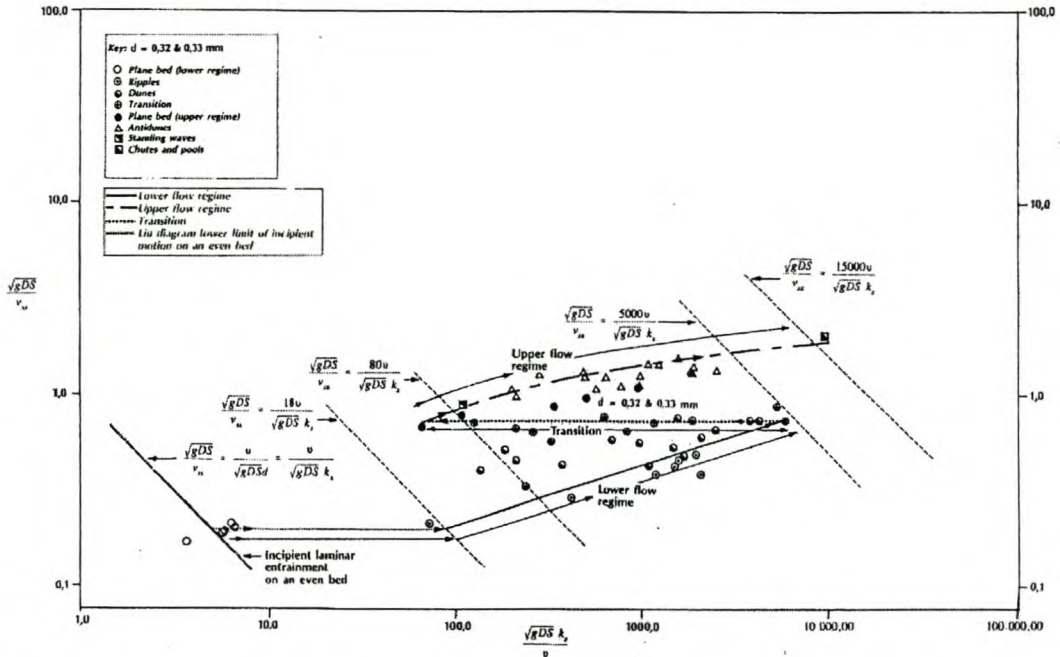


**Figure 2.9: Progressive development of the total flow regime spectrum for a mobile bed consisting of single size particles (Rooseboom and Le Grange, 2000).**

The diagram is explained by Rooseboom and Le Grange (2000) as follows:

Starting at the lower limit of incipient motion and a flat bed, with increasing  $\sqrt{gDs}$  values the mobile bed is deformed under lower flow regime condition into ripples and subsequently dunes. These bedforms go hand in hand with increasing values of  $k_s$  or  $\frac{\sqrt{gDs} k_s}{v}$  values until the right-hand turning point is reached. Bed deformation under the low flow regime reaches a maximum value at this stage.

Transition from the lower to the higher flow regime and associated flattening of the bed is represented by the horizontal part of the line. Whilst  $\frac{\sqrt{gDs}}{v_{ss}}$  values remain constant,  $k_s$ -values decrease dramatically until a new turning point is reached where bed deformation is a minimum for upper regime conditions.

“Lower flow regime bedforms are associated with laminar boundary conditions. As the value of  $\frac{\sqrt{gDs} k_s}{v}$  increases, a point is reached where the laminar stream power

becomes greater than that which is required to maintain turbulent flow at the boundary. Once the boundary conditions in the hollows between the bedforms switch to being turbulent, the bed suddenly becomes unstable. Less power is required to entrain particles when the flow at the bed switches from laminar to turbulent. The existing bedforms are thus seen to be washed away” (Rooseboom and Le Grange, 2000).

Bed deformation again increases from the left hand turning point under upper flow regime conditions, progressing through flat bed, antidunes, standing waves, etc. and associated increases in the value of  $k_s$ .

Rooseboom and Le Grange (2000) translated Figure 2.9 into a user-friendly set of graphs for easy practical application. This diagram (Figure 2.10) provides a complete averaged picture of resistance values and indicates the bedforms that will prevail.

The diagram should be used in the following manner:

- 1) Estimate a value for the flow depth  $D$ .
- 2) Read the corresponding  $\Delta$ -value from the diagram (particle diameter to be known).
- 3) Use the associated  $k_s$  value in the Chézy equation and iterate until it yields the same flow depth estimated in step 1.
- 4) The value of  $k_s$  as found will be the correct roughness coefficient to use under the specified flow conditions.

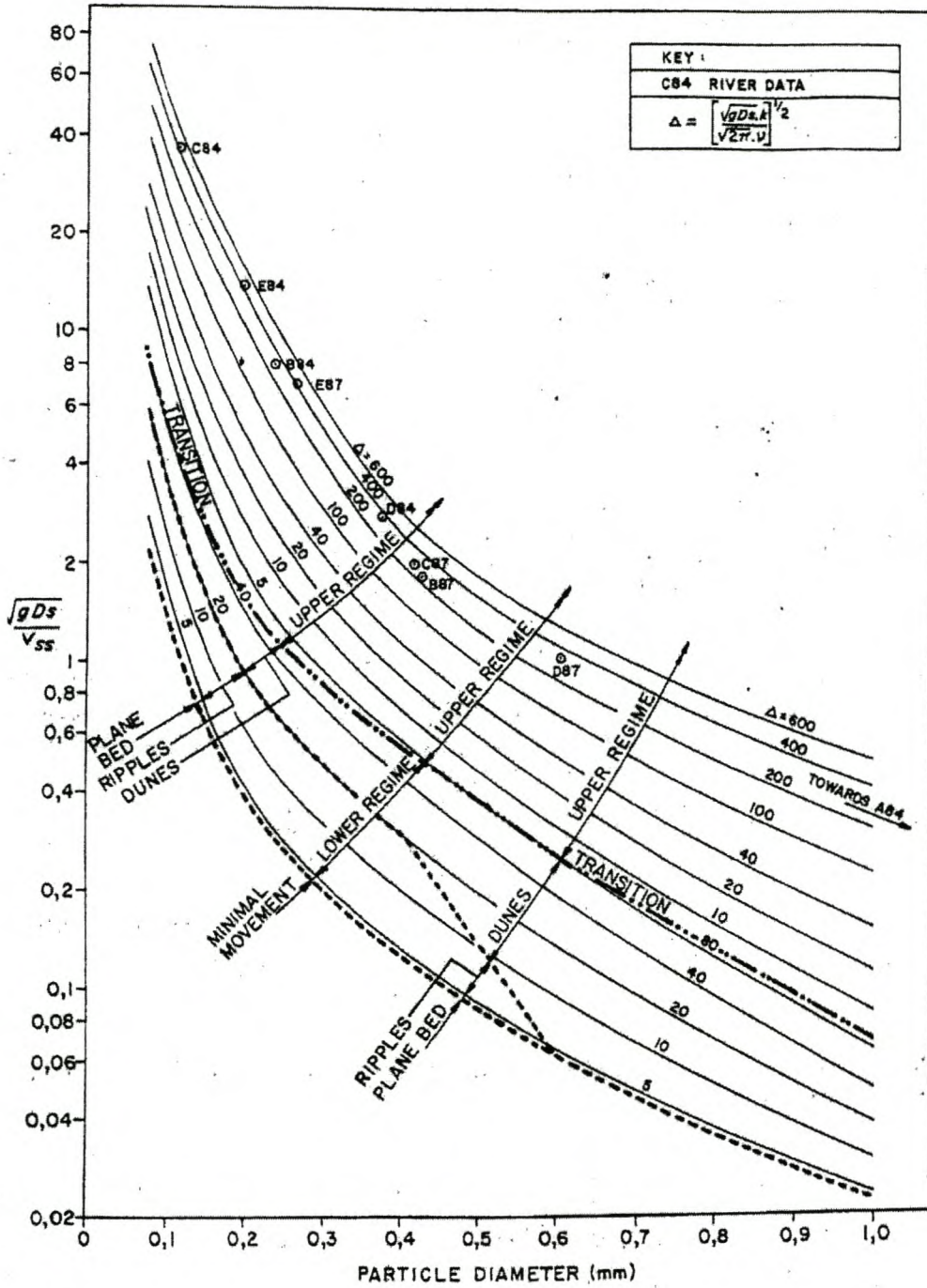


Figure 2.10: Resistance values and bedforms (Rooseboom and Le Grange 2000).

## 3 FIELDWORK

### 3.1 Introduction

Natural controls are natural topographic configurations in a river or stream which, by their character and extent, control the flow conditions at their locations. In order to study the hydraulic character of different natural controls, natural control sites representing critical as well as uniform controls were investigated. As mentioned previously, this study focuses on cobble and boulder bed rivers and specifically those that are found in the mountainous regions of the Western Cape.

A river, representative of a typical Western Cape cobble and boulder bed river with wide inter-annual variation of flows, relatively small dimensions to enable safe entry into the river at higher discharges, and in close proximity of Stellenbosch, had to be found.

The following Western Cape rivers were considered: Berg, Molenaars, Elandspad, and Jonkershoek Rivers (See Figure 3.1). After careful consideration, it was decided to conduct the study in the Jonkershoek River only, with the main reasons being accessibility, travel distance and safety. Sites exhibiting good natural control characteristics on both the Berg and Elandspad rivers are difficult to reach and entailed at least an hour of hiking through rugged terrain carrying surveying equipment. Both rivers are located a substantial distance from Stellenbosch, which increases travelling costs markedly. The Molenaars River is more accessible, but the size of the river made entry into it at higher stages, in order to measure water levels, dangerous.

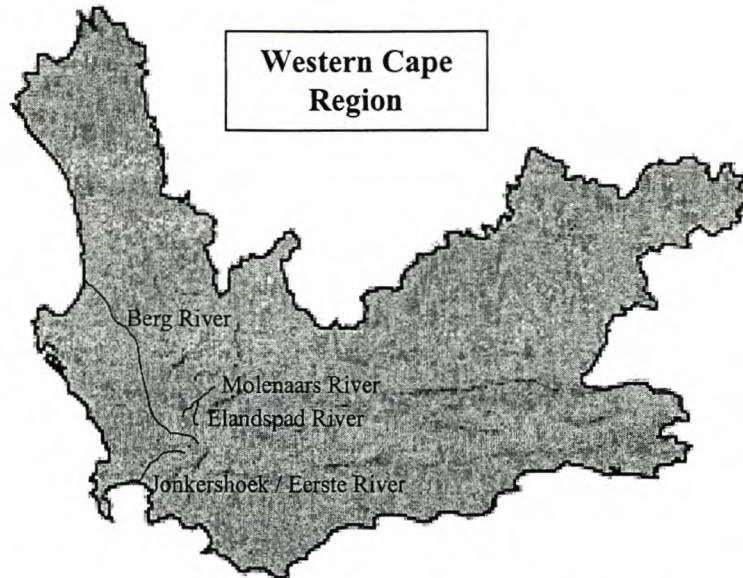


**Figure 3.1: Location of Berg-, Molenaars-, Elandspad- and Jonkershoek Rivers.**

The Jonkershoek River originates high up in the Hottentots Holland Mountains and runs along the bottom of the Jonkershoek Valley to just outside the town of Stellenbosch (Figure 3.2), where it exits the valley and becomes known as the Eerste River. The Jonkershoek catchment is a narrow valley of 21.38 km<sup>2</sup> in size flanked by very high, rocky mountains (1500 m above sea level) with an annual rainfall of 1600 mm/a and a runoff of 24 Mm<sup>3</sup>/a.

Due to the size of the catchment and the steepness of the valley sides and river course, the catchment's runoff response is quick and a wide range of flows could be measured within a single wet season. Most of the catchment area is situated within the Jonkershoek Nature Reserve and the Jonkershoek River is considered to be in pristine condition.



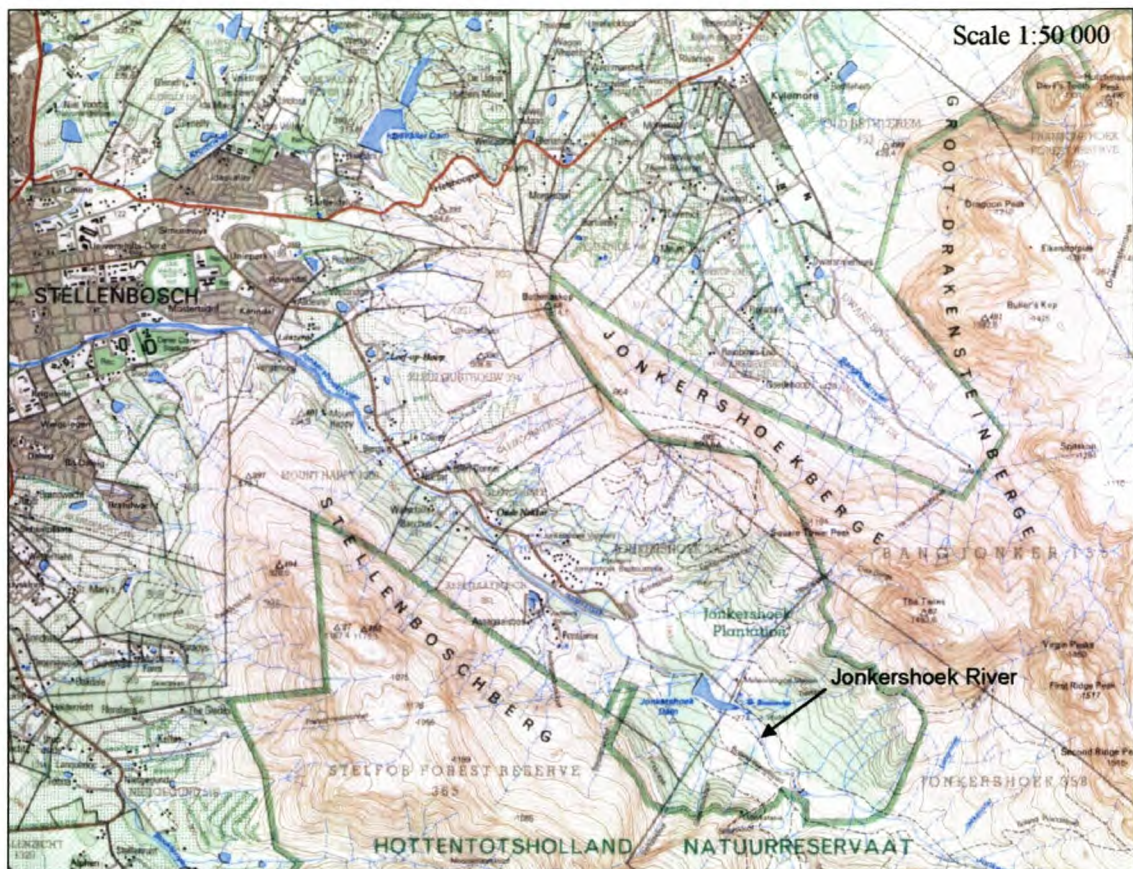


**Figure 3.2: Topographical map of Jonkershoek catchment.**

The Jonkershoek River is characterised by steep bed profiles forming step-pool reaches. Bed particles mainly consist of cobbles and boulders, with the size of the boulders decreasing as the slope decreases. Flow in the river is very turbulent with hydraulic jumps occurring at regular intervals. Even flows along reasonably uniform sections exhibit a pulsating, uneven nature.

Five natural control sites, having different control characteristics, were selected for the study in the Jonkershoek River and these sites will be discussed in the following sections. The general criteria used as guideline in selecting the control sites will be discussed in Section 3.3, after which each individual site's characteristics are described in Section 3.4. Section 3.5 to 3.7 deals with data collection, analysis and results obtained. A brief definition of concepts used in this chapter will be given next.

## 3.2 Definitions

In this chapter certain terms will be used like cobbles, low flows, etc. This section provides short definitions of these terms and other to be used in this chapter for quick referencing.

### 3.2.1 Flow Classification

Low flows:	0 – 0.5 m <sup>3</sup> /s
Medium flows:	0.5 – 1 m <sup>3</sup> /s
Medium high flows:	1 – 5 m <sup>3</sup> /s
High flows:	5 – 27 m <sup>3</sup> /s
Flood flows:	1:2y flood = 27 m <sup>3</sup> /s
	1:10y flood = 36 m <sup>3</sup> /s

### 3.2.2 Sediment Classification

Silt:	< 0.0625 mm in diameter
Sand:	0.0625 mm – 2 mm in diameter
Gravel:	2 mm – 64 mm in diameter
Cobble:	64 mm – 256 mm in diameter
Boulder:	> 256 mm in diameter

(From Rowntree and Wadeson, 1999)

### 3.3 General Criteria for Selecting Natural Control Sites

In searching for suitable natural control sites the following general criteria, as suggested by the USGS (1982), were used as guidelines:

- 1) The general course of the river should be straight for approximately 100m upstream and downstream of the site.
- 2) The total river flow to be measured must be contained in the main channel.
- 3) The streambed should be stable.
- 4) An unchanging natural control must be present.
- 5) A pool must be present upstream from the control at low flows to ensure the recording of stage at these flows and to avoid high velocities in the approach channel during high flows.
- 6) Should a suitable site be situated between two tributaries, it should be far enough downstream from the upper tributary so that flow is fairly uniformly established across the entire width of the river, and far enough upstream from the lower tributary to avoid variable backwater effect.
- 7) Access to the site must be easy.
- 8) All control sites must be in the vicinity of a working gauging weir to establish the real discharge for calibration purposes. There are to be no tributaries entering the river or off-takes from the river between the control sites and the weir and the control site must be far enough upstream from the weir to avoid variable backwater effects.

An ideal measurement site is merely found and judgment had to be exercised in choosing suitable sites, each of which has shortcomings. Adverse conditions existed at all possible sites and a non-ideal site had to be accepted. The physical characteristics and a description of each of the sites chosen for the study will be given in the next section.

### 3.4 Natural Control Sites Selected for the Study

As mentioned previously, five natural control sites were selected in the Jonkershoek River for this study. The following sections provide a description of each site, its location, physical character and response to various flow conditions.

#### 3.4.1 Site 1

Site 1 is classified as a step-pool control (Figure 3.3). Step-pool controls are characterised by large clasts of boulders organised into channel spanning accumulations that form steps behind each of which a scour pool, containing finer material, is present (Wadeson and Rowntree, 1999). The boulder step forms a local maximum of the bed profile and consequently forces the flow through critical depth, i.e. forms a critical control. Boulder sizes at the control section range between 0.7 m and 1.2 m in diameter and the cobbles in the pool are much smaller at 0.25 m in diameter.



**Figure 3.3: Photograph of Site 1 at 0.31 m<sup>3</sup>/s.**

The average slope of the river at Site 1 is steep (3.8%) and the river forms a series of step-pool reaches. Figure 3.4 shows the longitudinal section at Site 1, and the step-pool character of the reach can be clearly seen. The riverbanks are densely vegetated and steep on both sides with no flood plain and the average channel width is 20 m.

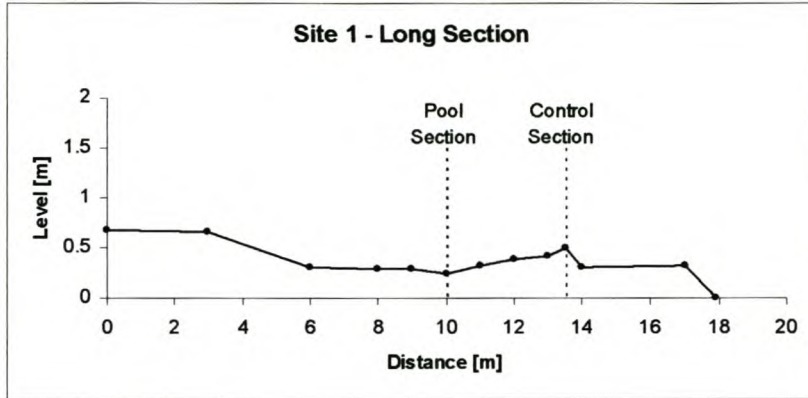


**Figure 3.4: Longitudinal section at Site 1.**

Multiple flow openings are formed at the control section for low to medium flows, as the flow is canalised through openings between adjacent boulders. At high flows the control section becomes submerged, but the local maximum level of the bed profile is still sufficient to form a critical control. High flows, however, cause the boulders to become submerged to such an extent that channel control prevails (Figure 3.5).



**Figure 3.5: High flow at Site 1, showing submerged boulders and channel control. ( $8 \text{ m}^3/\text{s}$ )**

Pool conditions are reasonable and subcritical flow is maintained in the pool for all discharges. At low flows the flow in the control section is concentrated through a single boulder opening on the right hand side of the river and an area of high velocity flow occurs on the right hand side of the pool under these conditions (Figure 3.6).

Site stability was very good and no movement of the boulders forming the control was recorded after flood events.

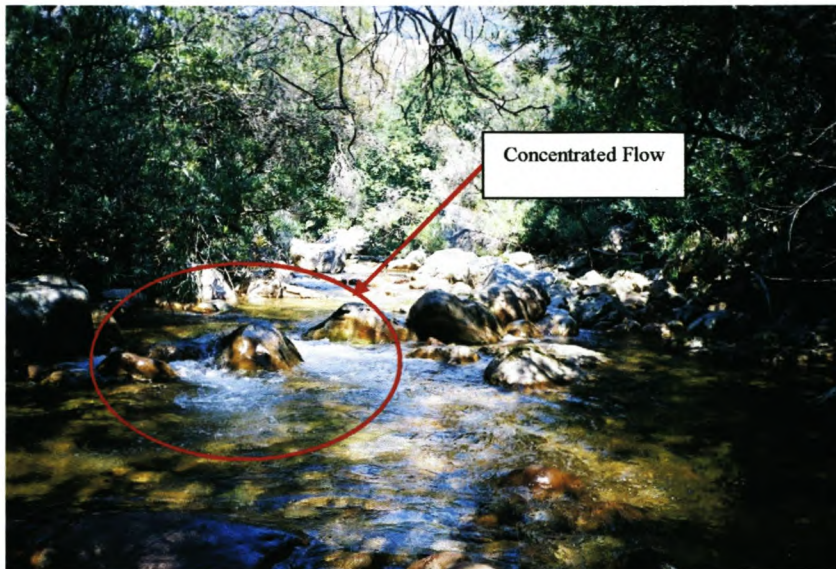


**Figure 3.6: Low flow conditions at Site 1 showing concentrated flow and consequent high velocity flow conditions in the pool area. ( $0.31 \text{ m}^3/\text{s}$ )**

### 3.4.2 Site 2

Site 2 is also classified as a step-pool control. The average size of the boulders comprising the step, however, is 0.5 m in diameter, which is smaller than those at Site 1 and consequently a more even bar is formed across the river (Figure 3.7).



**Figure 3.7: Photograph of Site 2 at 0.31 m<sup>3</sup>/s.**

The average channel width at Site 2 is 15 m with an average channel slope of 4.1%. The reach has the same step-pool character as Site 1, though the steps are much flatter comprising smaller boulders and shallower pools. Figure 3.8 shows the longitudinal section at Site 2. Riverbanks are steep with dense vegetation and no flood plain. Aquatic plants are present in the main channel just upstream of the control section.

Multiple flow openings at the control section are less prominent and flow is more continuous across the control. The pool is not very deep, but stretches far up-stream from the control, allowing subcritical flow to be established before the control section is reached.

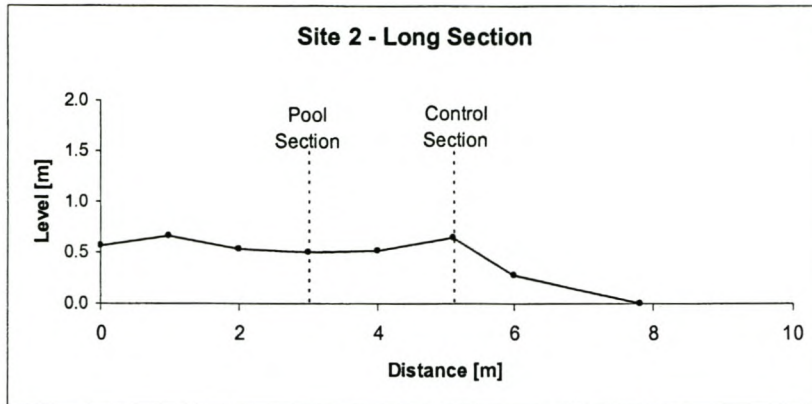


**Figure 3.8: Longitudinal section at Site 2.**

Due to the smaller boulder sizes at the control section, the site only forms a critical control at low flows. During medium to high flows the control becomes completely submerged, with little effect on the flow profile. The boulder seen in Figure 3.7, just downstream of the control section, also creates problems at higher flows causing flow to separate and creating a backwater effect, drowning the control. Movement of the boulders comprising the control was also detected after flood events. Site 2 was found to be unsuitable as a measurement site.



### 3.4.3 Site 3

The critical control at Site 3 is formed by an abrupt break in the channel slope due to an almost continuous bar of large flat boulders across the width of the channel, similar to a broad-crested weir. This is an ideal step-pool control with a deep pool area (0.4 m deep) and an evenly shaped control section (Figure 3.9).



**Figure 3.9: Photograph of Site 3 at  $0.31 \text{ m}^3/\text{s}$ .**

Average channel slope is 6.2%, which is normal for a channel reach having abrupt vertical breaks. The step height is 0.5 m and creates a mini waterfall, establishing an ideal critical control. Figure 3.10 shows the longitudinal section at Site 3. Average channel width is 10 m and though the riverbanks are less steep than at Sites 1 and 2, there is still no noticeable flood plain present.

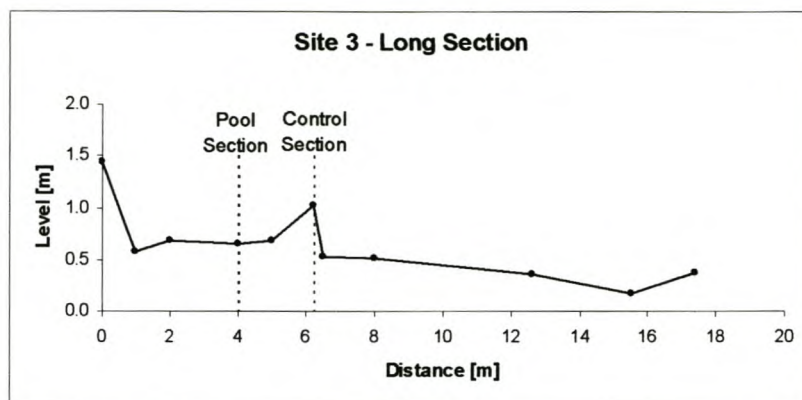


**Figure 3.10: Longitudinal section at Site 3.**

Low flows are concentrated through a V-shaped section in the control enabling fairly accurate measurement of low flows and no drowning of the control took place at high flows. It was thus possible to measure a wide range of flows at this control. Figure 3.11 shows Site 3 at high flows.

The site also exhibits good site stability with no movement of boulders having been detected after flood events.



**Figure 3.11: Site 3 at high flows. ( $8 \text{ m}^3/\text{s}$ )**

#### 3.4.4 Site 4

Site 4 is a constriction in the river comprising a large boulder (3 m diameter) on one side of the river and smaller boulders ( $\pm 1$  m diameter) on the other side. This constriction forms a local narrowing of the channel, forcing the flow through critical depth and thus establishes a critical control (Figure 3.12).



**Figure 3.12: Photograph of Site 4 at  $0.31 \text{ m}^3/\text{s}$ .**

Flow in the pool area upstream of the constriction is deep and tranquil, facilitating the measurement of stage. A large boulder flanks the right hand side of the pool area and effectively canalises low, medium and medium high flows through the constriction opening.

The average channel slope at Site 4 is 2.8%, which is less than that for Sites 1 to 3 and the average width of the river is 10 m. A densely vegetated flood plain with a width of about 10 m is present, flanked by steep riverbanks. Flow only enters the flood plain at high to flood flows. Figure 3.13 shows the longitudinal section at Site 4.

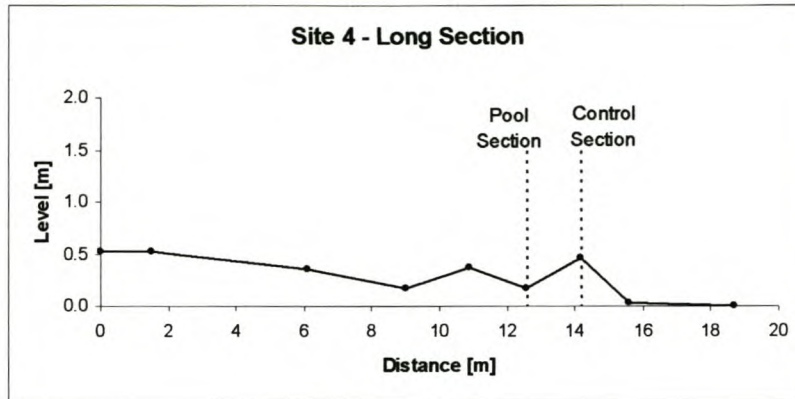


**Figure 3.13: Longitudinal section at Site 4.**

Similar to Site 3, low flows are canalised through a V-shaped portion of the control section allowing these flows to be measured with accuracy. At high flood flows the water level rises above the top level of the right hand side constricting boulder and the control becomes submerged and the constriction loses its effectiveness (Figure 3.14).



**Figure 3.14: Flood flows at Site 4.**

Overall the site was very stable, although some of the smaller cobbles among the smaller boulders on the left were reorganised after flood events. This, however, did not change the basic shape of the constriction and had a minimal effect on the calculations.

### 3.4.5 Site 5

Site 5 is a fairly uniform stretch of river, classified as a plane-bed reach (Figure 3.15). It is characterised by a gradually sloped riverbed, containing bed particles ranging in size from sand and gravel to boulders. The boulders are scattered over the channel bed and project out of the water at low flows (Figure 3.17).



**Figure 3.15: Photograph of Site 5 at 0.31 m<sup>3</sup>/s.**

Flow is contained within the main channel for low to medium flows. At high flows the water level rises into the flood plain, which is densely vegetated and about 10 m wide. The average channel slope is 2.9% and the average size of the bed particles is 0.35 m in diameter. Figure 3.16 shows the longitudinal section at Site 5.

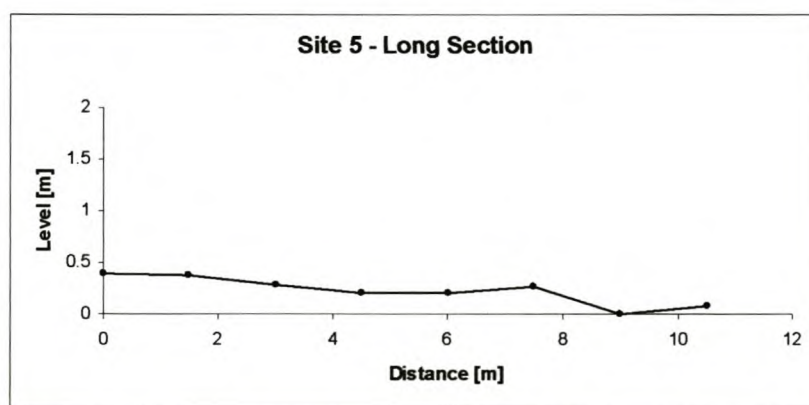


**Figure 3.16: Longitudinal section at Site 5.**



**Figure 3.17: Low flows at Site 5 showing boulders protruding out of water.**

#### 3.4.6 Summary

Of the five sites chosen for the study it was found that, judging from their physical characteristics, only four of these would be suitable as measurement sites. Two distinct types of critical controls were identified (the step-pool controls (Site 1 and 3) and the horizontal channel constriction (Site 4)), as well as a uniform control (Site 5).

The following section is concerned with the data collection at the chosen study sites. It defines the collection procedure, indicates collection points and highlights the problems encountered along with recommendations on how to limit such problems.

## 3.5 Data Collection

### 3.5.1 Data Collection Procedure

The first step in collecting field data was to find river reaches meeting the general criteria set out in Section 3.2, i.e. straight alignment, confined flow, stable controls with pools and free from variable backwater effects.

After suitable control sites were identified they were clearly marked with permanent markings. The surrounding area at each site was explored to ascertain the nature of the river, extent of vegetation, flood plain shape and its overall dimension. Flood plains were investigated to determine the debris line indicating high water marks from previous flood events. Benchmarks were then established and clearly indicated above these debris lines, ensuring that the benchmarks are not compromised by regularly occurring floods. High water marks also provide a good indication of the level at which a permanent stage recorder must be placed to avoid being damaged by floodwaters.

After establishing benchmarks, each site was carefully surveyed at 0.2 m intervals and as much detail as possible was documented. The control section was taken at the section having the minimum flow area and the pool sections were taken in the deepest and slowest flowing parts of the site. The location of each cross-section was clearly marked for re-surveying.

Positions where water levels are to be taken were marked to ensure consistent data collection. Water levels were surveyed at these points for different discharges over a period of seven months, from August 2001 to January 2002. For every water level taken the date, time and benchmark level were recorded. Gauge readings at gauging weir G2H037 were taken before and after water levels were surveyed at the sites, to establish an average, real discharge at the time and to minimize human error in the reading of the gauging plate. The water surface in the pool areas was uneven and at least three stage readings were taken at each site to minimise errors and to determine an average value.

Photos of the sites were taken as frequently as possible and at various discharges. Photos are valuable aids in interpreting the hydraulic behaviour of the controls.

### 3.5.2 Data Collection Points

The location of the water level measurement position materially affects the calculated discharge. If the water level is taken too close to the control section the water surface profile forms a drawdown curve and pressures are not hydrostatic. If it is taken too far upstream from the control section the frictional forces produce a water surface slope towards the control section (Ackers et al., 1978). An appropriate water level measurement position should avoid the area of drawdown, but should not be too far upstream from the control section to allow frictional losses to play a significant role.

For weirs and flumes it is common practice to specify the distance from the structure as a multiple of the maximum head to be expected at the structure. Current recommendations for standard measurement structures, as provided by Ackers et al. (1978), are as follows:

- 1) Thin plate weirs: 3 to 4 times the maximum head upstream from the crest.
- 2) Triangular-profile weirs: 2 times the maximum head upstream from the crest.
- 3) V-form, triangular-profile weirs: 10 times the height of the V upstream from the crest.
- 4) Rectangular-profile weirs: 2 to 3 times the maximum head upstream from the upstream face of the weir.
- 5) Round-nosed horizontal crested weirs: 2 to 3 times the maximum head upstream from the upstream face of the weir.
- 6) Trapezoidal and U-shaped flumes: 3 to 4 times the maximum head upstream from the leading edge of the entrance transition.

The recommendations given above were used as guideline in selecting suitable water level measuring positions at each site. Stage measurements were taken in the deepest and most tranquil parts of the pool areas and it was checked that the positions are at



least 2 times the maximum head expected but not further than 3 times. The measurement positions for each site are shown in Figures 3.18-3.21.

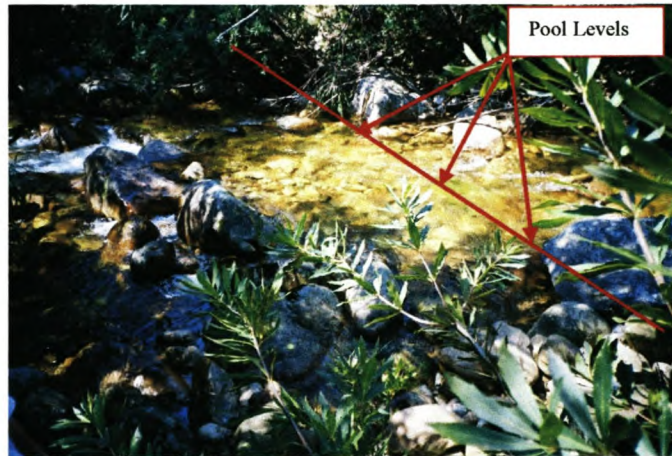


**Figure 3.18: Water level measurement points at Site 1**



**Figure 3.19: Water level measurement points at Site 3**

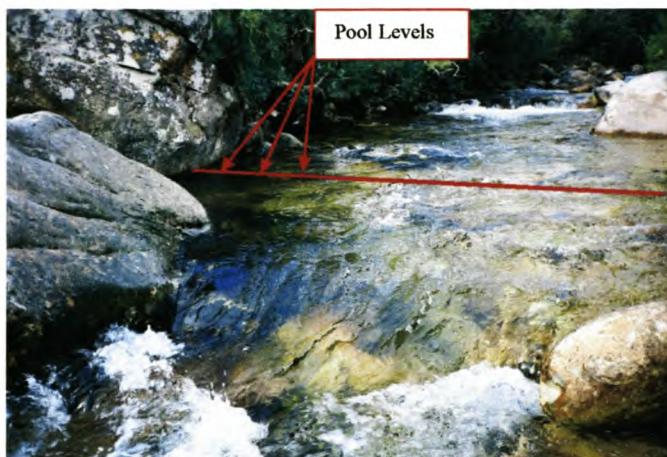


**Figure 3.20: Water level measurement points at Site 4**

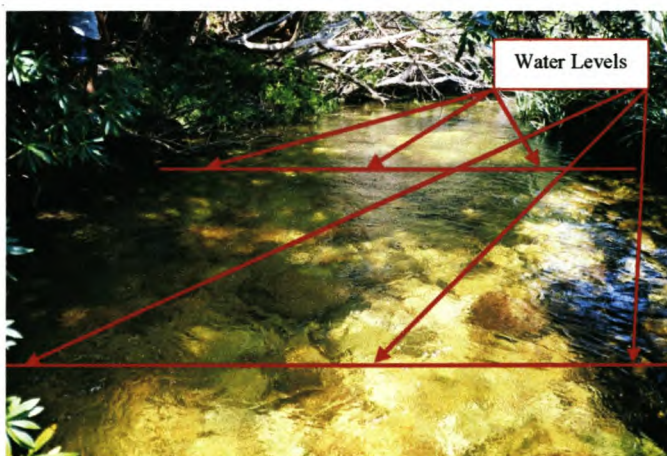


**Figure 3.21: Water level measurement points at Site 5**

More than one measurement point was used to ensure an average reading and to minimise human error. Water levels were also taken at the control section to give an indication of the critical depth. Downstream water levels were also taken to determine the modular limit of the control.

### 3.5.3 Problems Encountered with Collection of Data

Water surfaces in the pools were very unstable and surveying was difficult. Multiple readings had to be taken to ensure an average value and to minimise error. This was a lengthy process and very time consuming.

In order to survey the water levels, a person had to physically enter the river and hold the staff in the pool. This seriously limited the range of flows that could be measured. High flow velocities and the slippery surface of cobbles and boulders made it unsafe for entry even at moderate flows.

Human error caused readings to be discarded because benchmark levels were not surveyed along with the water levels and levels could not be compared to other measurements.

#### 3.5.4 Recommendations

It is strongly recommended that a permanent gauging plate be installed at study sites. This will eliminate the need to physically enter the river and will greatly increase the range of flows that can be measured and save time.

Regular surveys of the sites should be done, especially after a high flow- or flood event occurred to determine the stability of the site. Controls consisting of bedrock outcrops or large boulders are much less susceptible to cross-sectional changes than controls formed by cobbles or smaller boulders. Key cross-sectional boulders should be marked and photos taken of the site at regular intervals, especially after a high flow event. These photos can then be compared digitally to determine if movement of the boulders had taken place.

Should a control to be used for long-term measurement consist of a combination of large and small boulders or cobbles, it is advised that the small boulders or cobbles be stabilised or fastened in some way to establish site stability.

Surveying of the site should preferably be done in the dry season to capture as much detail as possible. During the wet season most of the site is likely to be under water and detailed surveying is difficult. Should surveying be done in the wet season, it must be repeated in the dry season.

### 3.6 Analysis of Field Data

After the data was collected it was analysed to determine the section's suitability as a flow measurement site. Theoretical discharges were calculated and compared to the discharges obtained from the gauging weir and relationships established between the physical parameters of the sections and the discharge coefficient. The following sections describe how the theoretical discharges and the discharge coefficients were determined.

#### 3.6.1 Calculating Discharge ( $Q$ ) from the recorded water level ( $h$ )

##### 3.6.1.1 *Critical Controls*

In order to determine the theoretical discharge ( $Q$ ) from the measured stage ( $h$ ) the energy equation needed to be balanced between the pool section and the control section. It is assumed that critical flow occurs in the control section and that energy losses between the two sections are negligible. Because the flow area in the control section does not change proportionally to a change in flow depth, the procedure is iterative.

The iterative procedure is as follows:

- 1) Estimate a value for flow depth in the control section ( $y_c$ ).
- 2) Determine the flow area in the control section ( $A_c$ ) and surface width of flow ( $B_c$ ) for flow depth  $y_c$ .
- 3) Calculate the discharge by assuming critical flow ( $Fr = 1$ ) in the control section:

$$Q = \sqrt{\frac{gA_c^3}{B_c}}$$

- 4) Calculate velocity head at control section: Equal to  $\frac{v_c^2}{2g}$
- 5) Calculate the energy head at control section:  $H_c = y_c + \frac{v_c^2}{2g}$
- 6) Determine the flow area in the pool section ( $A_p$ ) from the measured stage ( $h$ ).

- 7) Calculate the flow velocity in the pool section:  $v_p = \frac{Q}{A_p}$
- 8) Calculate the velocity head in the pool section: Equal to  $\frac{v_p^2}{2g}$
- 9) Determine the energy head at the pool section:  $H_p = y_p - W + \frac{v_p^2}{2g}$
- 10) Compare  $H_c$  and  $H_p$ . If  $H_c$  and  $H_p$  are not equal, estimate another value for  $y_c$  and iterate until  $H_c$  equals  $H_p$ , i.e. until the energy equation is balanced, between the pool and control sections.

### 3.6.1.2 Uniform Controls

The theoretical discharge was calculated using the equations for large-scale roughness as provided in Chapter 2, Section 2.3.3. The following input data for the equations were collected and determined:

1. Median size of the bed material ( $d_{50}$ ) as well as the size for which 84% of the particles are smaller ( $d_{84}$ ) were determined by measuring the size of the particles.
2. Flow area, width of flow, hydraulic radius and wetted perimeter for each measured water level ( $y$ ) were determined by means of the AutoCAD drawing programme.

Discharge was calculated using both the equations of Jonker (2002) and Malan (2002) as given in Chapter 2. The two equations are as follows:

Jonker (2002): 
$$Q = A \sqrt{\frac{2gd_{50}S_o}{0.5285\left(\frac{R}{d_{50}}\right)^{-2.166}}}$$

Malan (2002): 
$$Q = 115.9 \frac{R^{1.75} S_f^{0.2}}{v_{ss}^{0.5}} \left(\frac{d_{50}}{d_{84}}\right)^{3.84} P$$

### 3.6.2 Determination of the Discharge Coefficient, $C_d$

As mentioned in Chapter 2, the discharge coefficient is a coefficient that corrects for non-ideal flow conditions and is calculated by the ratio  $\frac{Q_{real}}{Q_{theoretical}}$ .

The real discharge was measured at the gauging station G2H037 close to the study sites. The theoretical discharge was calculated using the procedure stated in the previous section.

For every measurement taken at the site the real discharge was obtained from the gauging weir and the theoretical discharge calculated and the discharge coefficient determined.

The discharge coefficient obtained was then related to the physical character of the section to try and establish a relationship between the parameters describing the physical character of the section and its discharge coefficient. The results of these investigations are discussed in the following section.

### 3.7 Summary of Results

The results obtained from the analysis of the field data are discussed in the following sections. Results are grouped according to the type of control under consideration:

1) Step-pool controls, 2) Horizontal constriction controls, and 3) Uniform controls.

It must be emphasized that this is only a summary of the results, a detailed discussion of all the results obtained from the field and laboratory work and how they correlate with each other and with previous studies will be given in Chapter 5.

#### 3.7.1 Step-Pool Controls

The step-pool controls were analysed assuming critical flow conditions at the control sections and the theoretical discharge was calculated as explained in Section 3.6.

As was to be expected the results obtained from Site 1 and 3 correlated very well due to the fact that they are both step pool reaches. The theoretical discharge calculated was equal to an average of 60% of the real measured discharge, and this deviation was reasonably constant for all the calculations done and an overall first estimate of the discharge coefficient equal to 0.6 can be employed to calibrate this type of control.

The discharge coefficient of 0.6 also corresponds well with the discharge coefficient determined for broad crested weirs, which could be expected due to the similar shapes. Further research should be done into the correlation between  $C_d$  and characteristics of these controls. Table 3.1 and 3.2 shows the results obtained from these two sites.

**Table 3.1: Summary of Results obtained from Site 1.**

$h_{\text{measured}}$ [m]	Theoretical Discharge [m <sup>3</sup> /s]	Real Discharge [m <sup>3</sup> /s]	$C_d$ Discharge Coefficient
0.320	0.142	0.092	0.645
0.380	0.338	0.264	0.782
0.391	0.389	0.220	0.567
0.456	0.816	0.428	0.525
0.474	1.010	0.577	0.572
			<b>0.618</b> = Average $C_d$

**Table 3.2: Summary of Results obtained from Site 3.**

$h_{\text{measured}}$ [m]	Theoretical Discharge [m <sup>3</sup> /s]	Real Discharge [m <sup>3</sup> /s]	$C_d$ Discharge Coefficient
0.525	0.379	0.220	0.582
0.564	0.503	0.311	0.617
0.622	0.785	0.428	0.545
0.653	1.015	0.577	0.569
0.662	1.060	0.623	0.588
0.778	2.121	1.489	0.702
			<b>0.601</b> = Average $C_d$

### 3.7.2 Horizontal Constriction Control

Excellent results were obtained from measurements taken at the horizontal constriction at Site 4. Without calibration and assuming critical flow in the constriction, the discharge could be calculated theoretically with a maximum and average error of 25% and 21% respectively (See Figure 3.22). The result obtained from the very lowest discharge (shaded grey in the table) was discarded due to the fact that the accuracy of the gauging weir at these low discharges is very poor.

Further research was conducted into this type of controls as a result of the good results obtained in the field. This research will be discussed in Chapter 4.



**Table 3.3: % Error in Theoretical Calculation of Discharge.**

$Q_{theory}$	$Q_{real}$	$C_d$	% Deviation
0.057	0.092	1.600	38%
0.173	0.220	1.273	21%
0.345	0.428	1.242	20%
0.423	0.564	1.334	25%
0.460	0.610	1.326	25%
1.252	1.489	1.189	16%
0.255	0.311	1.221	18%
			<b>21%</b> Average % Error
			<b>25%</b> Max % Error

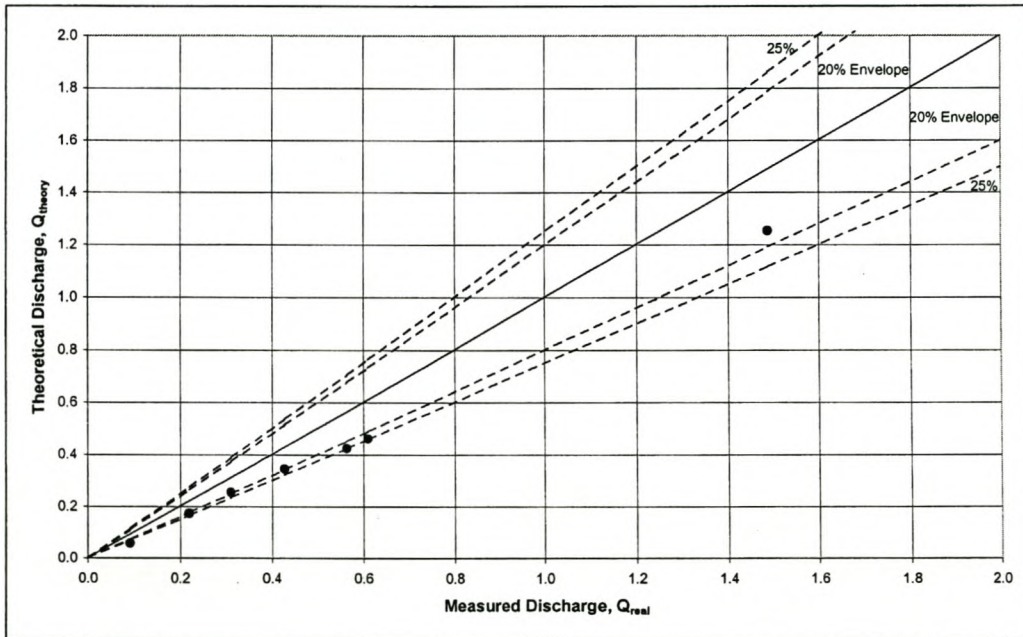


**Figure 3.22: Measured Flow versus Theoretical Flow.**

### 3.7.3 Uniform Control

Reasonable correlation at higher flows was obtained at the uniform control site. See Tables 3.4 and 3.5. The equation calibrated by Jonker (2002) yields better results than Malan's (2002) equation. Malan's (2002) equation consistently overestimates the flows at this section, though the percentage error becomes smaller with increasing discharge. This suggests that the equation becomes more accurate at higher flows. Discharge calculation at low flows is less accurate with most of the boulders protruding out of the water at these levels (See Figure 3.17) and as a result causes complicated flow patterns and uneven water levels.

Further field-testing to confirm the accuracy of these equations is recommended. It is also advised that better particle sampling be done to determine the particle distribution. Particle sampling for this study was only done on the cross-sections and should rather be done over the whole river reach to get a better spatial distribution.

**Table 3.4: Results using Jonker (2002)'s discharge equation.**

Depth [m]	Area [m <sup>2</sup> ]	Wetted Perimeter [m]	Hydraulic Radius [m]	Theoretical Discharge [m <sup>3</sup> /s]	Measured Discharge [m <sup>3</sup> /s]	% Error [%]
0.423	1.364	4.782	0.285	0.224	0.036	522.2
0.454	1.507	4.880	0.309	0.270	0.092	193.1
0.632	2.358	5.329	0.443	0.623	0.428	45.6
0.671	2.550	5.418	0.471	0.720	0.545	32.2
0.687	2.659	5.475	0.486	0.777	0.623	24.7
0.696	2.704	5.496	0.492	0.801	0.678	18.2
0.843	3.416	5.815	0.588	1.227	1.357	-9.6
0.913	3.779	5.975	0.632	1.470	1.949	-24.6

$d_{50} =$	0.30 m
$S_o =$	0.0027

**Table 3.5: Results using Malan (2002)'s discharge equation.**

Depth [m]	Area [m <sup>2</sup> ]	Wetted Perimeter [m]	Hydraulic Radius [m]	Theoretical Discharge [m <sup>3</sup> /s]	Measured Discharge [m <sup>3</sup> /s]	% Error [%]
0.423	1.364	4.782	0.285	0.680	0.036	1789.0
0.454	1.507	4.880	0.309	0.797	0.092	766.4
0.632	2.358	5.329	0.443	1.634	0.428	281.8
0.671	2.550	5.418	0.471	1.850	0.545	239.5
0.687	2.659	5.475	0.486	1.975	0.623	217.1
0.696	2.704	5.496	0.492	2.028	0.678	199.2
0.843	3.416	5.815	0.588	2.927	1.357	115.7
0.913	3.779	5.975	0.632	3.422	1.949	75.6

$d_{50} =$	0.30 m
$S_f =$	0.0027
$v_{ss} =$	3.77 m/s
$\rho_s =$	2450 kg/m <sup>3</sup>
$\rho =$	1000 kg/m <sup>3</sup>
$d_{84} =$	0.60 m

## 4 LABORATORY WORK

### 4.1 Introduction

Following the good results obtained from measurements taken at the horizontal constriction control at Site 4 in the Jonkershoek River, it was decided to further investigate this type of control. The first step was an extensive literature search on channel constrictions and though literature dealing with natural control constrictions as such was scarce, extensive literature was found on man-made constrictions for the purpose of discharge measurement. These included studies into various commonly known flumes such as the Parshall-, Venturi- and Cutthroat-flumes as well as other, not so commonly known, critical depth flumes making use of cylinders, half-cylinders, iron-angles, etc. to create a constriction in the channel and consequently forcing the flow through critical depth.

Studies done by Samani and Magallanez (1993, 2000) and Hager (1985, 1986, 1988), in which they tested the performance of various critical depth flumes, were found to be the most applicable to the natural control situation. A brief discussion of their work will be given in the next sections.

Malan and Van Huyssteen (1999) conducted an exploratory study into the use of natural controls for the measurement of discharge. They identified and commented on a few natural controls found in Western Cape rivers and conducted introductory laboratory tests. Unfortunately the raw data from the laboratory work were not properly documented and as a result the tests were of little use outside the scope of their investigation. Their findings will also be discussed in the following section.

The second step in the investigation, into horizontal constrictions as discharge measurement devices, was to conduct a series of laboratory tests to evaluate the hydraulic characteristics of such controls and their correlation with physical parameters. These tests were performed in the Hydraulics Laboratory of the University of Stellenbosch and the tests and its results will be discussed in detail in this chapter.

## 4.2 Previous Studies

### 4.2.1 Hager (1985)

The investigation deals with a modified Venturi channel having the constriction along the channel axis instead of at its sidewalls by positioning a cylinder axially into the channel. It considered three types of prismatic channels, namely: rectangular, trapezoidal and U-shaped (Figure 4.1).

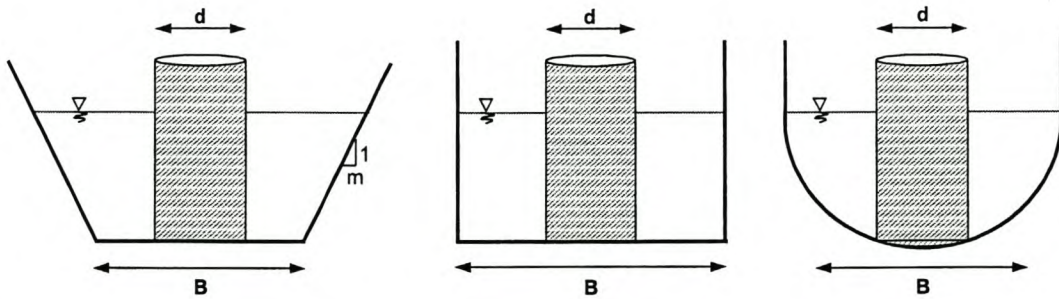


**Figure 4.1: Transverse sections of trapezoidal, rectangular and U-shaped channels (Hager, 1985).**

Discharges for the respective channel shapes can be calculated as follows:

*Trapezoidal Cross-section:*

$$Q^2 = \frac{[y(1+y)]^3}{1+2y}, \quad y = \frac{mh}{b} \quad \dots 4-1$$

*U-shaped Cross-section:*

$$\frac{H}{B} = y + \frac{\frac{Q^2}{gB^5}}{2 \left[ \frac{4}{3} y^{3/2} \left( 1 - \frac{y}{3} \right) - \beta y + \frac{\beta^3}{12} \right]^2}, \quad h < \frac{B}{2} \quad \dots 4-2$$

$$\frac{H}{B} = y + \frac{\frac{Q^2}{gB^5}}{2 \left[ \frac{\pi - 4}{8} + y(1 - \beta) + \frac{\beta^3}{12} \right]^2}, \quad h \geq \frac{B}{2} \quad \dots 4-3$$

with

$$y = \frac{h}{B}, \quad \beta = \frac{d}{B},$$

$h$  = Water depth [m]

$b$  = Constricted width =  $B - d$  [m]

$H$  = Energy head [m]

$m$  = Side slope

*Rectangular Cross-section:*

$$Q = \left(\frac{2}{3}\right)^{3/2} b \sqrt{gh^3} \left(1 + \frac{2b^2}{9B^2}\right) \quad \dots 4-4$$

#### 4.2.2 Hager (1986)

Experiments were conducted to evaluate the flow patterns resulting from a circular cone immersed in a rectangular channel under critical flow conditions (Figure 4.2).

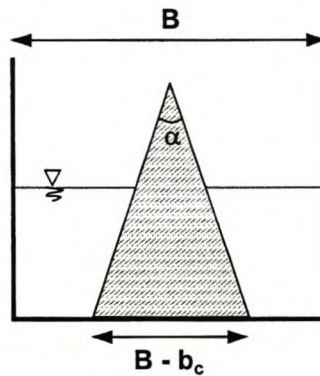


**Figure 4.2: Rectangular channel with circular cone constriction (Hager, 1986).**

Two different circular cones of angles  $\alpha = 2.18^\circ$  and  $\alpha = 2.29^\circ$  were inserted in a rectangular channel of width 0.5 m. Discharges were varied between 0.01 and 0.2 m<sup>3</sup>/s. Discharges could be approximated within  $\pm 2\%$  accuracy with the following equations:

$$Q = \left(\frac{2}{3}\right)^{3/2} b \sqrt{gH^3} \left(1 + \frac{2mH}{3b}\right), \quad 0 < \frac{mH}{b} < 1 \quad \dots 4-5$$

$$Q = \left(\frac{4}{5}\right)^{5/2} m \sqrt{\frac{gH^5}{2}} \left(1 + \frac{5b}{4mH}\right), \quad \frac{mH}{b} \geq 1 \quad \dots 4-6$$

$$C_d = q = 1 + \frac{14U}{243 \left(1 + \frac{U}{27}\right)} \quad ; \quad S = 0 \quad \dots 4-7$$

$$C_d = q = 1 + \frac{U}{27 \left(1 + \frac{U}{27}\right)} \quad ; \quad S > 0.5 \quad \dots 4-8$$

with

$$U = \frac{H}{bR}$$

$$R = \frac{B-b}{2}$$

$$S = \frac{mH}{b}$$

$m$  = Side slope of cone

The discharge coefficient  $C_d (=q)$  was plotted relative to the value of  $U$  and the resultant graph is shown in Figure 4.3.

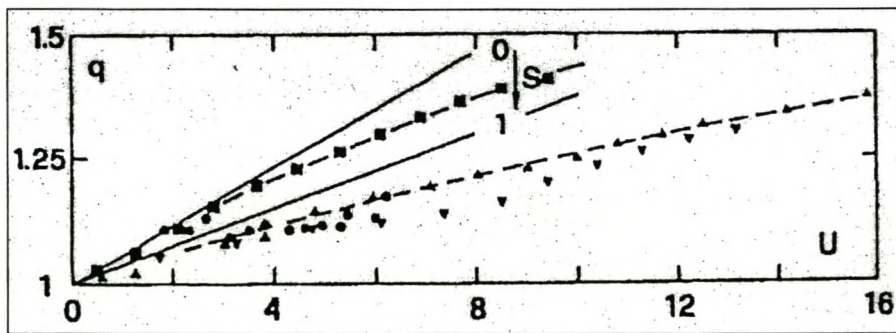
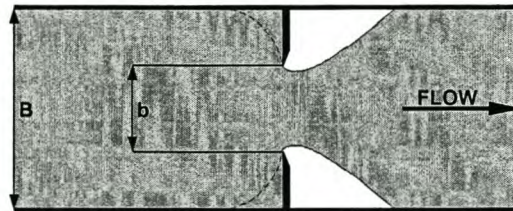


Figure 4.3: Discharge correction coefficient  $q = Q/Q_0$  as a function of  $U$ .  
From Hager (1986).

### 4.2.3 Hager (1988)

The study presented a modified Venturi-type discharge measurement structure with side contractions formed by two symmetrical thin-plate, sharp-edged vertical walls (Figure 4.4).



**Figure 4.4: Venturi-type discharge measurement structure with thin-plate constriction (Hager, 1988).**

Test observations were made in a horizontal, rectangular channel of width 0.5 m and height 0.7 m. Discharges were varied between 10  $\ell/s$  and 240  $\ell/s$ . Rectangular, sharp-edged plates of widths 0.05 m, 0.075 m and 0.1 m were placed at each side of the channel creating channel constrictions ( $B/b$ ) equal to 1.25, 1.43 and 1.67 respectively.

Difficulties associated with this type of control section, are mainly due to the abrupt change of the channel width and the associated fluid separation from the two plates. The flow cannot follow the thin plates at the constriction and the fluid separates up- and downstream of the plates, causing the space downstream of the constriction to be free of water as shown in Figure 4.4. At the upstream zone an eddy forms, while the fluid contracts to a minimum  $\mu b$  value (*with  $\mu < 1$* ) at the downstream constriction zone, which is smaller than the constriction width  $b$  created by the plates.

The discharge coefficient ( $C_d$ ) was plotted as a function of the relative energy head ( $H/b$ ) for different constriction ratios, as shown in Figure 4.5. It can be seen that the discharge coefficient ( $C_d$ ) increases steadily with growing  $H/b$ . Discharges can be calculated using the following equation:

$$Q = C_d b \sqrt{g} \left( \frac{2}{3} H \right)^{3/2} \quad \dots 4-9$$

with

$$C_d = \left[ 0.828 + 0.057(\psi + 2\psi^4) \right] \left( 1 + \frac{(W)^2}{3 + 5(W)^2} \right) \quad \dots 4-10$$

$$\psi = \frac{b}{B}$$

$$W = \frac{H}{b}$$

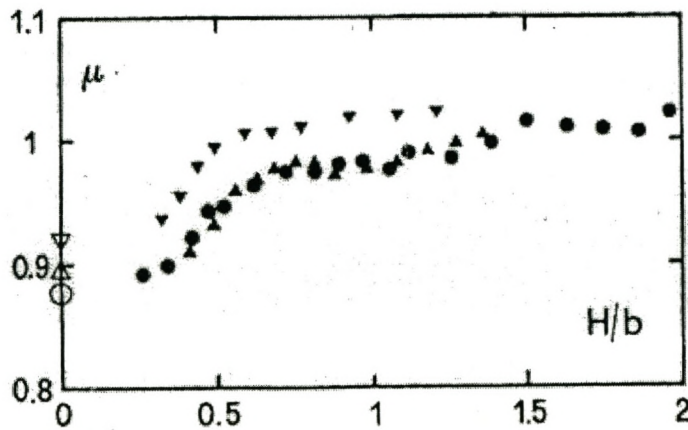
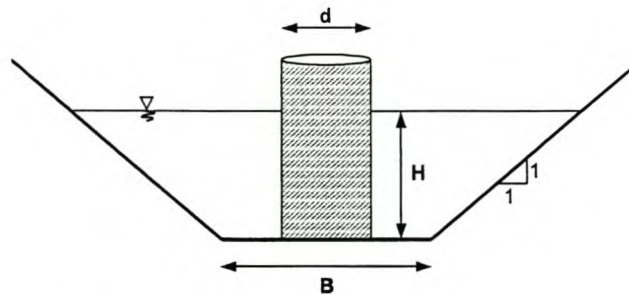


Figure 4.5: Coefficient of discharge as a function of relative energy head (Hager, 1988).



#### 4.2.4 Samani and Magallanez (1993)

Laboratory experiments were conducted to evaluate the hydraulic characteristics of a flume consisting of a pipe installed axially inside a trapezoidal channel (Figure 4.6). The pipe constricted the channel width sufficiently to force the flow through critical depth. The research followed on previous work presented by Hager (1985, 1988) discussed previously.



**Figure 4.6: Cross-sectional view of flume (Samani and Magallanez, 1993).**

Tests were performed at the New Mexico State University hydraulics laboratory in a plywood trapezoidal channel having a length of 5 m, width of 0.1715 m and side slopes of 1/1. Two diameters of polyvinyl chloride pipes (0.155 m and 0.168 m) were respectively installed axially at the downstream end of the canal and critical flow is enforced at the smallest cross section between the column and the canal sides.

Discharges were calculated using the conventional energy equation and taking the Froude number equal to unity. A dimensionless curve was developed by plotting the relative energy ( $H/B$ ) versus the discharge coefficient ( $C_d = Q_{measured} / Q_{calculated}$ ) as shown in Figure 4.7. An equation was developed based on the data shown in Figure 4.7 as follows:

$$C_d = 1.121 \left( \frac{H}{B} \right)^{0.0701} \quad \dots 4-11$$

The maximum submergence ratio for this flume was equal to 81%. The flume was also field-tested and the maximum error for calculated discharges was less than 5.1%.

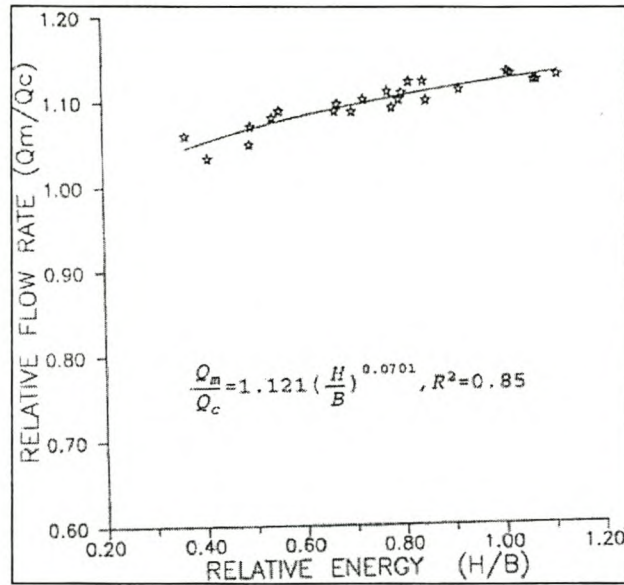


**Figure 4.7: Relationship between Relative Energy ( $H/B$ ) and Discharge Coefficient ( $C_d$ ) (Samani and Magallanez, 1993).**

#### 4.2.5 Samani and Magallanez (2000)

Samani and Magallanez (2000) conducted a series of laboratory tests in the hydraulics laboratory at Mexico State University. The tests investigated the performance and characteristics of a simple critical flume constructed by attaching two polyvinyl chloride half-cylinders to the sidewalls of a rectangular, 3 m long and 0.28 m wide wooden channel. Figure 4.8 shows a plan view of the flume.

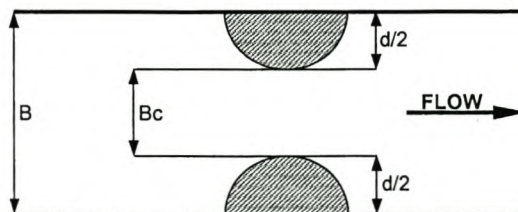


**Figure 4.8: Plan view of simple flume (Samani and Magallanez, 2000).**

Discharges in the flume were varied between 0.8 l/s and 26 l/s and three different cylinder sizes (0.114 m, 0.152 m and 0.168 m) were tested. Water levels, contraction ratios and the real discharges were measured for each set of tests and the theoretical discharges calculated from the equation  $Q = B_c \sqrt{g \left( \frac{2H}{3} \right)^3}$  where  $H$  = upstream energy head,  $B_c$  = contracted width and  $g$  = acceleration of gravity ( $9.81 \text{ m/s}^2$ ).

For each test the discharge coefficient ( $C_d$ ) was calculated as the ratio  $\frac{Q_{\text{Measured}}}{Q_{\text{Theoretically Calculated}}}$ .

Hager (1986) showed that this discharge coefficient is a function of the upstream energy head ( $H$ ) and the contracted channel width ( $B_c$ ).

Using their laboratory data, Samani and Magallanez (2000) developed a dimensionless curve plotting the discharge coefficient ( $C_d$ ) at various discharge rates versus the relative energy ( $H/B_c$ ) for each contraction ratio ( $d/B$ ). The resulting graph is shown in Figure 4.9.

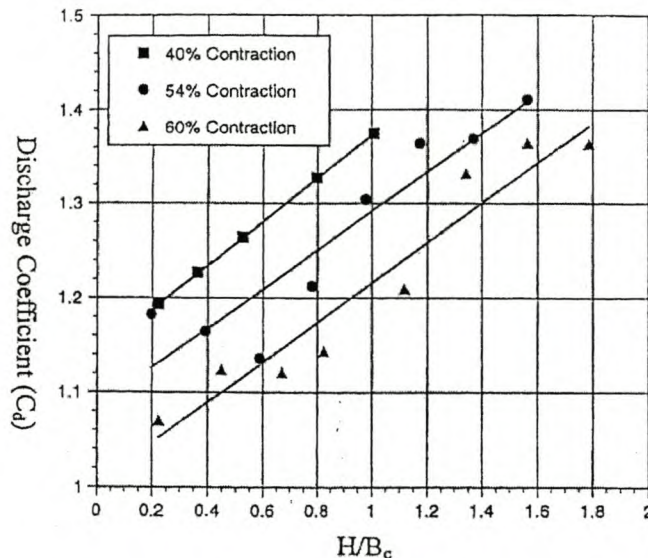


**Figure 4.9: Discharge coefficient ( $C_d$ ) versus Relative Energy ( $H/B_c$ ) (Samani and Magallanez, 2000).**

The data in Figure 4.9 were compiled into a single equation:

$$C_d = 1.33 - 0.44 \frac{d}{B} + \sin \left( 0.21 \frac{H}{B_c} \right) \quad \dots 4-12$$

The flume was field tested in a 1.2 m long, 0.76 m wide and 0.91 m deep canal. Discharges could be measured with less than 5% error.

#### 4.2.6 Malan and Van Huyssteen (1999)

This introductory study into natural controls investigated the potential of natural controls for discharge measurement. Different types of control sections were identified in rivers and modelled in the laboratory. Discharge characteristics of basic prismatic control shapes were determined by laboratory tests as well as two controls modelled from the controls identified in rivers.

Three basic critical controls were investigated: The vertical constriction, the horizontal constriction and a combination of the two. See Figure 4.10. Table 4.1 shows the resultant discharge coefficient values for each cross section.

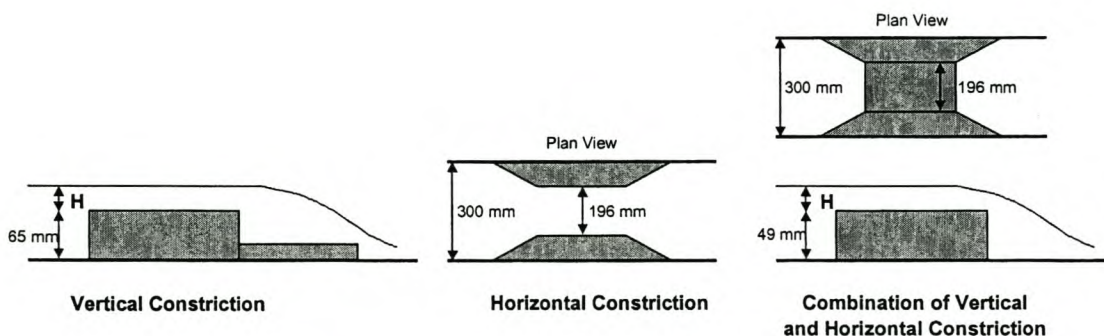


**Figure 4.10: Layout of the three basic critical control shapes tested.**

**Table 4.1: Discharge coefficients from tests performed by Malan and Van Huyssteen (1999) on basic critical controls.**

Vertical Constriction	Horizontal Constriction	Vertical and Horizontal Constriction
1.18	1.014	1.08
0.98	1.010	1.07
0.94	1.014	1.12
0.93	1.014	1.13
0.96	1.011	1.17
		1.13
<b>Average <math>C_d</math>: 0.95</b>	<b>Average <math>C_d</math>: 1.01</b>	<b>Average <math>C_d</math>: 1.12</b>

Two cross sections modelling the controls identified in the rivers were also tested and results are shown in Table 4.2.

**Table 4.2: Results from river modelled controls (Malan and Van Huyssteen, 1999).**

Vertical and Horizontal Constriction	Horizontal Constriction
1.23	1.26
1.34	1.15
1.22	

Unfortunately the raw data from the laboratory tests conducted by Malan and Van Huyssteen (1999) was not documented in sufficient detail and could not be used by the author to extend current laboratory results.

### 4.3 Laboratory Tests

#### 4.3.1 Approach followed

A series of laboratory tests were undertaken at the hydraulics laboratory of the University of Stellenbosch, South Africa. The objective was to determine the discharge characteristics of a horizontally constricted channel.

Using the work of Samani and Magallanez (2000) as starting point, horizontal constrictions were created in a rectangular glass flume using cobbles instead of PVC pipes.

Three sets of tests were performed. The first test set consisted of constrictions having vertical sides, the second having sloped sides and the last having arbitrarily shaped cross-sections (Figure 4.11).



**Figure 4.11: Examples from each laboratory test set.**

The laboratory layout will be discussed next followed by definitions of all the parameters used in the analysis of the tests as well as a description of the measurement points. A short summary of each individual test set will be given in Section 4.3.4.

### 4.3.2 Laboratory Layout

Tests were performed in a 40 m long, 1 m wide and 1.5 m deep glass flume. Figure 4.12 shows a diagram of the laboratory layout. Water was pumped from underground storage reservoirs to a constant head tank  $\pm 5$  m above the flume and distributed through a 0.3 m diameter pipeline to a concrete stilling tank at the upstream end of the flume.

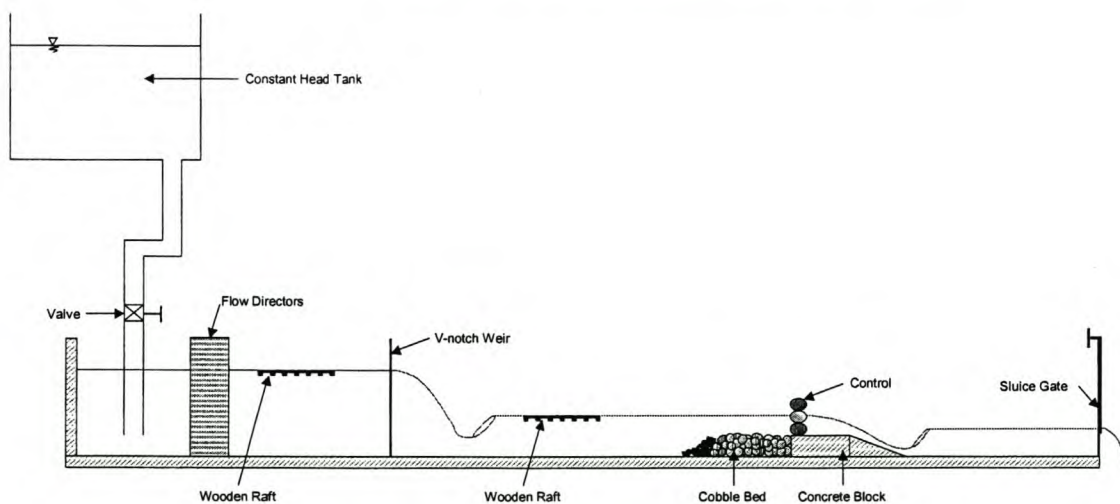


**Figure 4.12: Laboratory Layout. (Not to scale)**

From the stilling tank water flows into the glass flume via a set of flow directors, comprising a wall of pipes stacked on top of each other. A wooden raft was placed just downstream of the flow directors to eliminate surface waves.

Discharge was measured by means of a  $90^\circ$  V-notch sharp crested weir placed 5 m downstream of the flow directors. A wooden raft was placed downstream of the V-notch weir to calm the surface waves caused by the hydraulic jump downstream of the weir.

The channel constriction was concreted on top of a concrete block situated 20 m downstream of the weir. A 2.8 m long cobble bed was placed upstream and to the same level of the concrete block. This was done to create a more natural approach condition, similar to those found in mountain-rivers. A gravel transition was placed between the flume bottom and the start of the cobble bed.

Downstream water levels were controlled by a sluice gate situated at the end of the channel, from which the water exits the flume and flows back into the underground storage reservoirs.

Definitions of the parameters used in the analysis of the tests are given in the next section, followed by a short description of each test set.

### 4.3.3 Definition of Parameters

For each test, the cross-sections of the control section and the pool sections were imported into the computer programme AutoCAD. From the programme it was easy to calculate the flow area and average flow depth for each section once the water level is known. The average width was calculated dividing the flow area by the average flow depth.

Definitions of the parameters used in the analysis will be given in the next paragraphs. Figures 4.13 and 4.14 provide definition sketches.

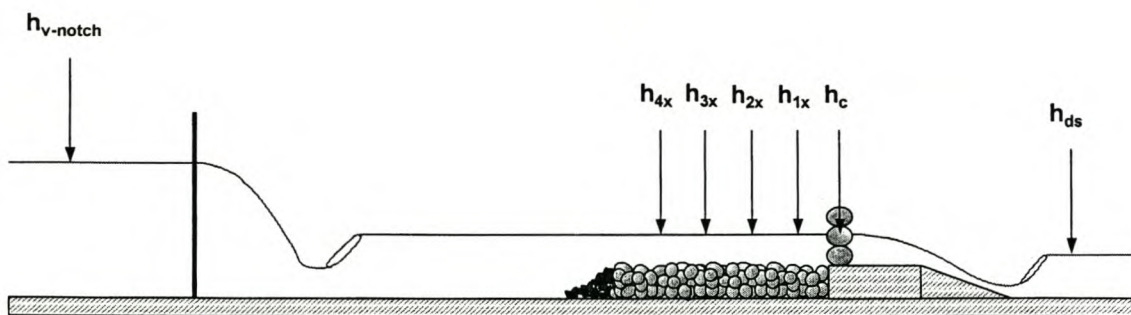


**Figure 4.13: Position of measurement points.**



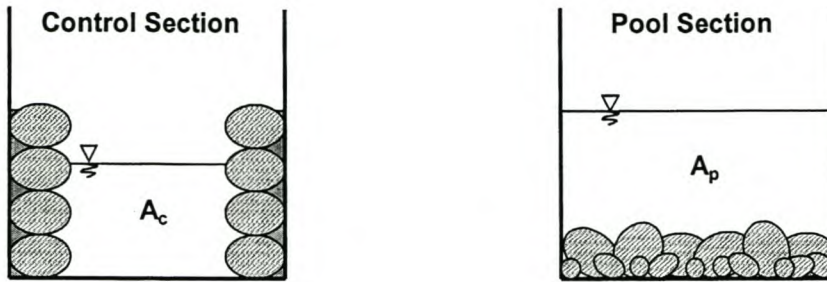


Figure 4.14: Control and pool sections.

$A_c$  = Flow area at control section.

$A_p$  = Flow area at pool section.

$\bar{y}_c$  = Average flow-depth of control section. Calculated using AutoCAD.

$\bar{b}$  = Average width of control section =  $A_c / \bar{y}_c$ .

$\bar{y}_p$  = Average flow-depth of pool section. Calculated using AutoCAD.

$\bar{B}$  = Average width of pool section =  $A_p / \bar{y}_p$ .

$h_c$  = Water head at control section.

$h_{max}$  = Maximum water head at control section.

$h_{1 \times h_{max}}$  = Water head at 1 x  $h_{max}$  distance upstream from control section.

$h_{2 \times h_{max}}$  = Water head at 2 x  $h_{max}$  distance upstream from control section.

$h_{3 \times h_{max}}$  = Water head at 3 x  $h_{max}$  distance upstream from control section.

$h_{4 \times h_{max}}$  = Water head at 4 x  $h_{max}$  distance upstream from control section.

$h_{ds}$  = Water head at downstream section.

$h_{V-notch}$  = Water head at V-notch weir, taken upstream from the weir at a distance equal to 4 times the maximum head to be measured at the weir plate.

$H_c$  = Energy head at control section =  $\bar{y}_c + v_c^2 / 2g$ .

$H_p$  = Energy head at pool section =  $\bar{y}_p + v_p^2 / 2g$ .

$H = H_c = H_p$  = Total energy head.

$H/b$  = Relative energy head.

---

$$\frac{\bar{B}}{b} = \text{Constriction ratio.}$$

Pool stage measurements were taken at distances of 1,2,3 and 4 x  $h_{\max}$  upstream of the control section, for the first set of tests, to determine what influence the draw down towards the control section has on the stage measurements. It was found that the stage values between 2 and 3 x  $h_{\max}$  remained constant. Values between 1 and 2 x  $h_{\max}$  decreased towards the control section, indicating the presence of draw down towards the control and the consequent influence on water levels in its vicinity. Water levels increased slightly from 3 to 4 x  $h_{\max}$ , which is due to the surface roughness influencing the slope of the water.

It is recommended that stage measurements be taken at least 2 x  $h_{\max}$  upstream from the control section, but not further than 3 to 4 x  $h_{\max}$  (preferably 3 x  $h_{\max}$ ) to ensure accurate readings.

#### 4.3.4 Tests Performed

##### 4.3.4.1 Test Set 1: Constriction with Vertical Sides

The constrictions in this set of tests were created by mounting cobbles of approximately equal size on top of each other, forming a constriction with vertical sides and a constant constriction ratio (Figure 4.15). The discharge was increased stepwise up to a maximum value of  $0.18 \text{ m}^3/\text{s}$  (the maximum discharge which could be accommodated by the V-notch weir), and the water levels were measured for each discharge.



**Figure 4.15: Constriction with vertical sides ( $B/b = 1.8$ ).**

Four different constriction ratios were tested, viz. 1.5, 1.8, 2.3, and 3.2. For each discharge, the water level in the pool was measured and the corresponding flow area calculated. The critical depth and theoretical discharge was calculated iteratively by balancing the energy equation between the pool section and the control section in the same manner as was done for the prototype sites described in Chapter 3. A summary of the results is shown in Section 4.4.

The theoretically calculated discharge was compared to the real discharge as measured by means of the V-notch weir and the discharge coefficient ( $C_d$ ) calculated. The discharge coefficients of all the tests were compared to each other and the results are discussed in Section 4.4 and Chapter 5.

For each constriction ratio a test was done to determine the modular limit of the control. The downstream water level was raised by regulating the sluice gate situated at the far end of the glass flume. The upstream and downstream water levels were recorded each time the downstream water level had been raised until the upstream water level became influenced by the downstream water level. This indicates the modular limit of the control. Tables indicating the modular limit of each constriction ratio are shown in Appendix B.

#### 4.3.4.2 Test Set 2: Constriction with Sloped Sides

The constrictions were formed in the same manner as in the previous tests except that the sides of the constrictions were sloped and not vertical. Discharge was again varied stepwise and measurements taken at the same places as in the first set of tests.

Three side-slope angles were tested, viz.  $53^\circ$ ,  $45^\circ$  and  $38^\circ$  (Figure 4.16). The iterative method as described in Chapter 3 was once again used to calculate the critical depth at the control as well as the theoretical discharge. The results are shown in Section 4.4 and Chapter 5.



Side-slope =  $53^\circ$

Side-slope =  $45^\circ$

Side-slope =  $38^\circ$

**Figure 4.16: Constrictions with sloped sides.**

#### 4.3.4.3 Test Set 3: Constriction with Arbitrary Shape

A third set of tests were conducted using two arbitrary shaped control sections formed by boulders approximately 0.3 m in diameter. The two controls are shown in Figure 4.17. Tests were performed in the same manner as the previous two sets. These tests were done to compare the geometric control results with the arbitrary shaped control.

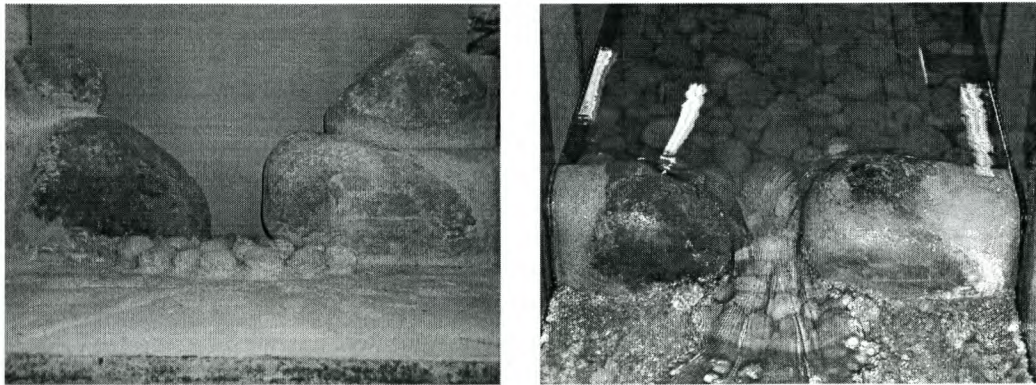


**Figure 4.17: Constrictions with arbitrary shape.**

#### 4.4 Summary of Results

The reader is once again reminded that this is only a summary of the results obtained from the laboratory tests. In Chapter 5 all the results obtained from the study will be discussed in detail and compared to results from previous studies.

The results of the tests were combined into graphs by plotting the discharge coefficient ( $C_d$ ) against the relative energy ( $H/b$ ) value for each constriction ratio. The resultant graphs are shown in Figure 4.18, 19 and 20. From the graphs it is clear that there is a linear relationship between these values for each constriction ratio. The results show the same pattern as those obtained by Samani and Magallanez (2000).

It can also be seen that the slope of the linear relationship is steeper for the constriction with sloped sides than for the constriction with vertical sides, which in turn is steeper than the slopes obtained by Samani and Magallanez (2000).

4.4.1 Test Set 1: Constriction with Vertical Sides**Table 4.3: Summary of Results obtained from Test Set 1.**

TEST NO. 1-1				
$Q_{\text{theory}}$ [m <sup>3</sup> /s]	$Q_{\text{real}}$ [m <sup>3</sup> /s]	$C_d$	B/b	H/b
0.04	0.03	0.93	1.5	0.27
0.06	0.6	1.01	1.5	0.34
0.09	0.09	1.01	1.5	0.40
0.12	0.12	1.05	1.5	0.45
0.14	0.16	1.07	1.5	0.50
0.16	0.18	1.09	1.5	0.53

TEST NO. 1-3				
$Q_{\text{theory}}$	$Q_{\text{real}}$	$C_d$	B/b	H/b
0.01	0.01	0.80	2.3	0.27
0.01	0.01	0.89	2.3	0.33
0.02	0.02	0.86	2.3	0.40
0.03	0.03	0.92	2.3	0.45
0.04	0.04	0.95	2.3	0.51
0.05	0.05	1.00	2.3	0.59
0.06	0.07	1.09	2.3	0.65
0.08	0.08	1.03	2.3	0.71
0.09	0.09	1.05	2.3	0.77
0.10	0.11	1.06	2.3	0.82
0.11	0.12	1.07	2.3	0.88
0.14	0.15	1.09	2.3	0.98
0.16	0.18	1.11	2.3	1.01

TEST NO. 1-2				
$Q_{\text{theory}}$ m <sup>3</sup> /s]	$Q_{\text{real}}$ [m <sup>3</sup> /s]	$C_d$	B/b	H/b
0.07	0.06	0.84	1.6	0.39
0.16	0.17	1.07	1.8	0.70
0.14	0.15	1.06	1.8	0.65
0.09	0.09	1.03	1.8	0.52
0.12	0.12	1.04	1.8	0.59
0.03	0.03	0.91	1.8	0.34
0.03	0.02	0.93	1.8	0.30
0.02	0.01	0.83	1.8	0.25
0.02	0.02	0.93	1.8	0.28
0.01	0.01	0.8	1.8	0.21

TEST NO. 1-4				
$Q_{\text{theory}}$	$Q_{\text{real}}$	$C_d$	B/b	H/b
0.01	0.01	0.80	3.2	0.44
0.02	0.02	0.97	3.2	0.62
0.04	0.04	1.01	3.2	0.82
0.06	0.06	1.08	3.2	1.02
0.08	0.09	1.14	3.2	1.18
0.10	0.12	1.19	3.2	1.34
0.13	0.16	1.22	3.2	1.48

The average modular limit for this type of control is 71%.

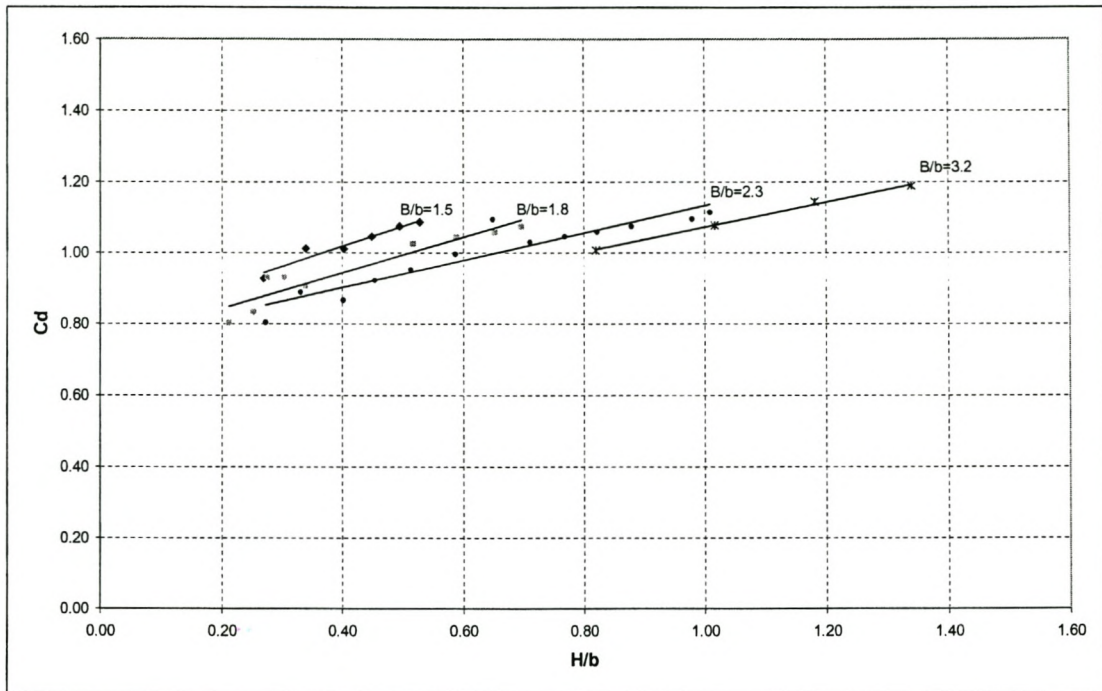


Figure 4.18:  $C_d$  vs  $H/b$  for constriction with vertical sides.



4.4.2 Test Set 2: Constriction with Sloped Sides**Table 4.4: Summary of Results obtained from Test Set 2.**

TEST NO. 2-1				
$Q_{\text{theory}}$ [m <sup>3</sup> /s]	$Q_{\text{real}}$ [m <sup>3</sup> /s]	$C_d$	B/b	H/b
0.09	0.13	1.46	2.2	1.00
0.07	0.11	1.47	2.2	0.94
0.05	0.07	1.43	2.3	0.89
0.04	0.06	1.48	2.8	1.03
0.03	0.05	1.43	3.0	1.02
0.02	0.02	1.48	3.3	0.95
0.01	0.01	1.37	6.2	1.51
0.01	0.01	1.07	7.6	1.64

TEST NO. 2-2				
$Q_{\text{theory}}$ m <sup>3</sup> /s]	$Q_{\text{real}}$ [m <sup>3</sup> /s]	$C_d$	B/b	H/b
0.13	0.15	1.10	1.4	0.47
0.10	0.10	1.04	1.4	0.42
0.07	0.07	1.00	1.6	0.42
0.05	0.04	0.94	1.6	0.37
0.03	0.02	0.90	2.0	0.37
0.01	0.01	0.82	2.2	0.32
0.01	0.01	0.79	2.3	0.28

TEST NO. 2-3				
$Q_{\text{theory}}$ [m <sup>3</sup> /s]	$Q_{\text{real}}$ [m <sup>3</sup> /s]	$C_d$	B/b	H/b
0.11	0.13	1.18	1.4	0.50
0.09	0.10	1.17	1.5	0.51
0.07	0.07	1.13	1.7	0.51
0.04	0.04	1.06	2.0	0.49
0.02	0.02	1.01	2.5	0.51
0.01	0.01	0.89	2.9	0.50
0.01	0.01	0.86	3.4	0.47

The average modular limit for this type of control is 56%.

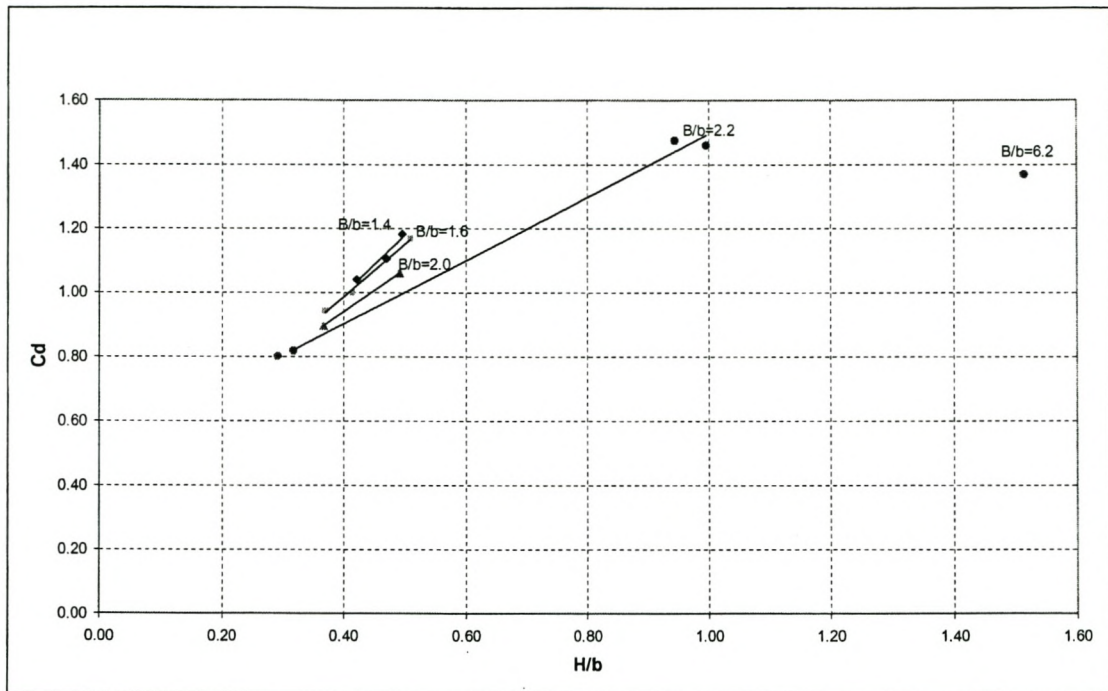


Figure 4.19:  $C_d$  vs  $H/b$  for constriction with sloped sides.

#### 4.4.3 Test Set 3: Constriction with Arbitrary Shape

The arbitrarily shaped controls seem to generate the same pattern as did the vertical and sloped sides. Unfortunately the  $B/b$  ratio changes quickly as the discharge increases and it is difficult to obtain matching values in order to establish a relationship. From the data that did match, it is clear (Figure 4.20) that the controls will form much the same pattern as was found with the previous control shapes.

**Table 4.5: Summary of Results obtained from Test Set 3.**

SHAPE NO. 1					SHAPE NO. 2				
$Q_{\text{theory}}$ [m <sup>3</sup> /s]	$Q_{\text{real}}$ [m <sup>3</sup> /s]	$C_d$	$B/b$	$H/b$	$Q_{\text{theory}}$ m <sup>3</sup> /s]	$Q_{\text{real}}$ [m <sup>3</sup> /s]	$C_d$	$B/b$	$H/b$
0.03	0.05	1.61	2.2	0.82	0.08	0.10	1.3	2.1	1.00
0.03	0.04	1.44	4.0	1.45	0.08	0.10	1.3	2.1	1.01
0.02	0.03	1.19	5.6	1.86	0.07	0.09	1.3	2.1	0.98
0.02	0.02	1.14	5.9	1.92	0.07	0.09	1.28	2.1	.97
0.02	0.02	1.14	6.3	1.95	0.05	0.07	1.28	2.1	0.91
0.01	0.02	1.11	6.7	1.99	0.06	0.08	1.29	2.1	0.95
0.01	0.01	1.06	7.8	2.12	0.06	0.07	1.29	2.1	0.93
0.01	0.01	1.01	8.5	2.14	0.04	0.05	1.31	2.3	0.92
0.01	0.01	0.93	8.6	1.93	0.04	0.05	1.30	2.3	0.92
0.01	0.01	0.93	8.6	1.87	0.03	0.05	1.30	2.4	0.94
					0.03	0.03	1.22	4.5	1.61

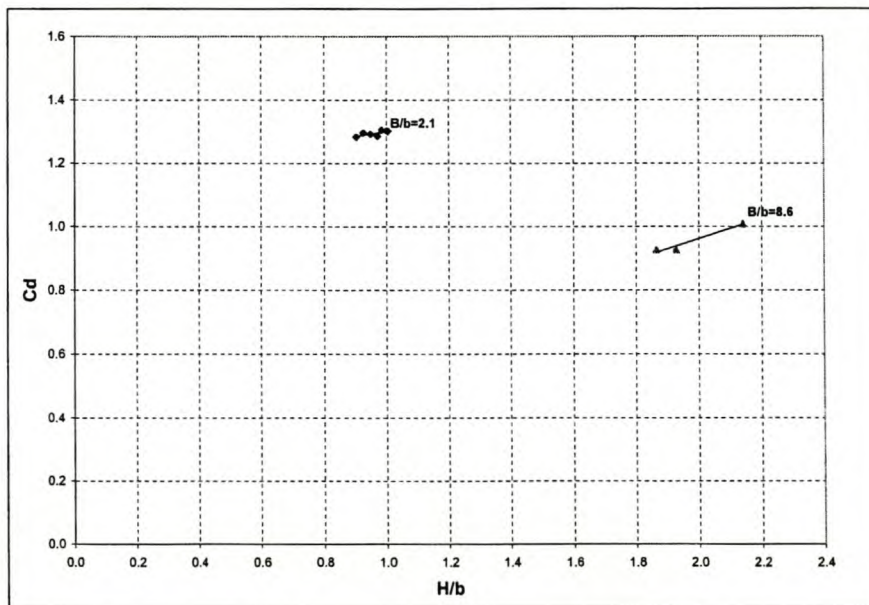


**Figure 4.20:  $C_d$  vs  $H/b$  for constrictions with arbitrary shapes.**

## 5 INTEGRATED RESULTS

### 5.1 Introduction

In the previous two chapters a summary of the results obtained from the field- and laboratory work, was given. The purpose of this chapter is to analyse and discuss these results and to determine how they can be integrated to form a guideline from which appropriate discharge coefficients can be obtained, based on the physical character of the control in question.

### 5.2 Step-pool Controls

Wessels (1996) stated that discharge coefficients at vertically constricted controls are mainly contraction coefficients correcting for the idealised assumptions of a horizontal water surface and straight streamlines between the pool and control section. Thus discharge coefficients for these controls should be similar in value to the contraction coefficient for a rectangular orifice, which is in the order of 0.6.

The average discharge coefficient obtained from the two sites in the field is 0.61 (See Tables 3.1 and 3.2). This result agrees with and confirms the above statement by Wessels. It is recommended that a first estimate value of 0.61 be used as discharge coefficient for step-pool controls.

Applying this average discharge coefficient ( $C_d = 0.61$ ) to the original field data, it was found that the discharge could be predicted with an average error of 9.1%. Table 5.1 and Figure 5.1 show the average percentage errors for both sites as well as maximum percentage errors.

**Table 5.1: Percentage difference between calculated discharge using  $C_d = 0.61$  and measured discharge for Step-Pool controls.**

	Discharge [ $m^3/s$ ]			% Error		
	Theory	$C_d \times$ Theory	Real			
Site 1	0.142	0.087	0.092	5.48		
	0.338	0.206	0.264	22.04		
	0.389	0.237	0.220	-7.64		
	0.816	0.498	0.428	-16.23	11.6 %	Average % Error
	1.010	0.616	0.577	-6.72	22.0 %	Maximum % Error
Site 2	0.379	0.231	0.220	-4.90		
	0.503	0.307	0.311	1.20		
	0.785	0.479	0.428	-11.88		
	1.015	0.619	0.577	-7.27		
	1.060	0.647	0.623	-3.78	7.0 %	Average % Error
	2.121	1.294	1.489	13.09	13.1 %	Maximum % Error
				<b>9.3 %</b>	<b>Overall Average % Error</b>	

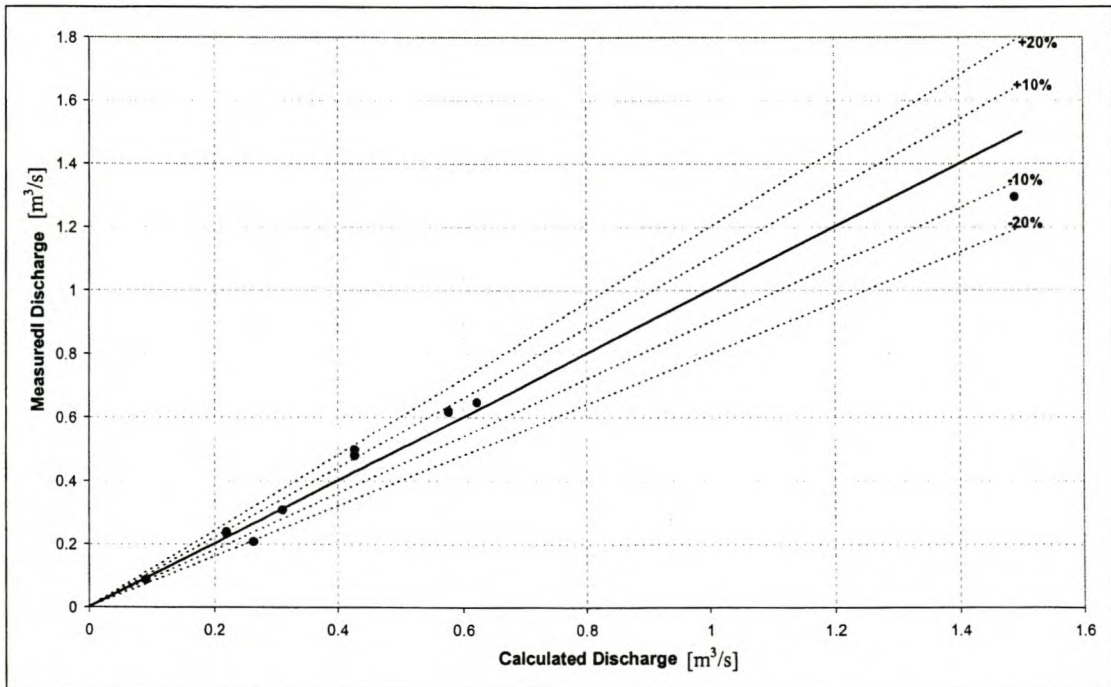


**Figure 5.1: Error between measured data and calculated data using  $C_d=0.61$ .**

### 5.3 Horizontal Constriction Controls

#### 5.3.1 Arbitrarily Shaped Constrictions

Field results from the horizontal constriction correlate well with the results obtained from the laboratory test in which an arbitrarily shaped control was used. The theoretically calculated discharge at this control in the field, consistently underestimates the measured value by an average of 21% (See Table 3.3) without employing a discharge coefficient.

Unfortunately too little data points were available over too wide a range of  $B/b$  values to establish a definite pattern between the discharge coefficient and the relative energy ( $H/b$ ). Although no definite pattern could be established, the discharge coefficient values all lie within the range  $C_d = 1.18$  to  $1.33$ . An average discharge coefficient value equal to  $1.26$  was employed and by using this value the accuracy of measurement was improved to an average error of 3.7% and a maximum error of 6%, bringing it well within 10% accuracy (Table 5.2).

**Table 5.2: Percentage Error using a Discharge Coefficient  $C_d = 1.26$  for Field Results.**

$Q_{\text{Theory}}$ [ $\text{m}^3/\text{s}$ ]	$C_d \times Q_{\text{Theory}}$	$Q_{\text{Real}}$ [ $\text{m}^3/\text{s}$ ]	% Error		
0.173	0.218	0.220	1.00		
0.255	0.321	0.311	-3.22		
0.345	0.434	0.428	-1.42		
0.423	0.533	0.564	5.58		
0.460	0.580	0.610	4.96	3.7%	Average % Error
1.252	1.578	1.489	-6.00	6.0%	Maximum % Error

Results from the laboratory tests yielded an average  $C_d$  value of  $1.29$  (See Table 4.5), which correlates well with the field results described above. It is thus recommended that a  $C_d$  value between  $1.26$  and  $1.29$  be used as a first estimate to determine the discharge at a horizontal constriction having an arbitrary shape.

### 5.3.2 Non-Arbitrarily Shaped Constrictions

#### 5.3.2.1 *Vertical Sides Constriction*

The following graph (Figure 5.2) shows the results obtained from the laboratory tests with vertical side constrictions. It clearly shows the linear relationship between the discharge coefficient ( $C_d$ ) and the relative energy ( $H/b$ ). The linear equation for each constriction ratio is given below Figure 5.2.

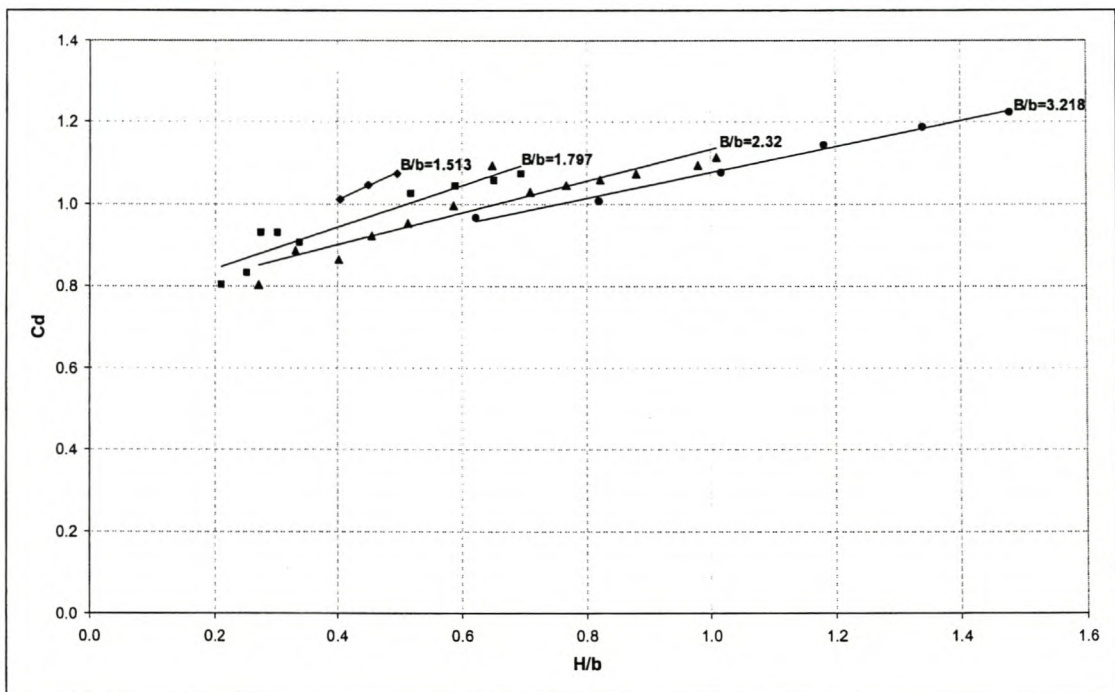


**Figure 5.2:  $C_d$  vs  $H/b$  for constriction with vertical sides.**

Linear equations for each respective constriction ratio:

$$\bar{B}/\bar{b} = 1.513: C_d = 0.7309 + 0.6949(H/\bar{b})$$

$$\bar{B}/\bar{b} = 1.797: C_d = 0.7409 + 0.5042(H/\bar{b})$$

$$\bar{B}/\bar{b} = 2.320: C_d = 0.7464 + 0.3858(H/\bar{b})$$

$$\bar{B}/\bar{b} = 3.218: C_d = 0.7605 + 0.3154(H/\bar{b})$$

These lines were interpolated and smoothed into dimensionless design curves having the following equations:

$$C_d = a + b(H/\bar{b})$$

B/b	a	b
1.4	0.725770	0.808681
1.5	0.731319	0.702005
1.6	0.734355	0.620604
1.7	0.736697	0.557897
1.8	0.738965	0.50908
1.9	0.741259	0.470731
2.0	0.743524	0.440358
2.1	0.745686	0.416119
2.2	0.747691	0.396636
2.3	0.749514	0.380865

B/b	a	b
2.3	0.749514	0.380865
2.4	0.751147	0.368013
2.5	0.752595	0.357472
2.6	0.753872	0.348772
2.7	0.754993	0.341548
2.8	0.755975	0.335515
2.9	0.756836	0.33045
3.0	0.757589	0.326173
3.1	0.758249	0.322546
3.2	0.758829	0.319454

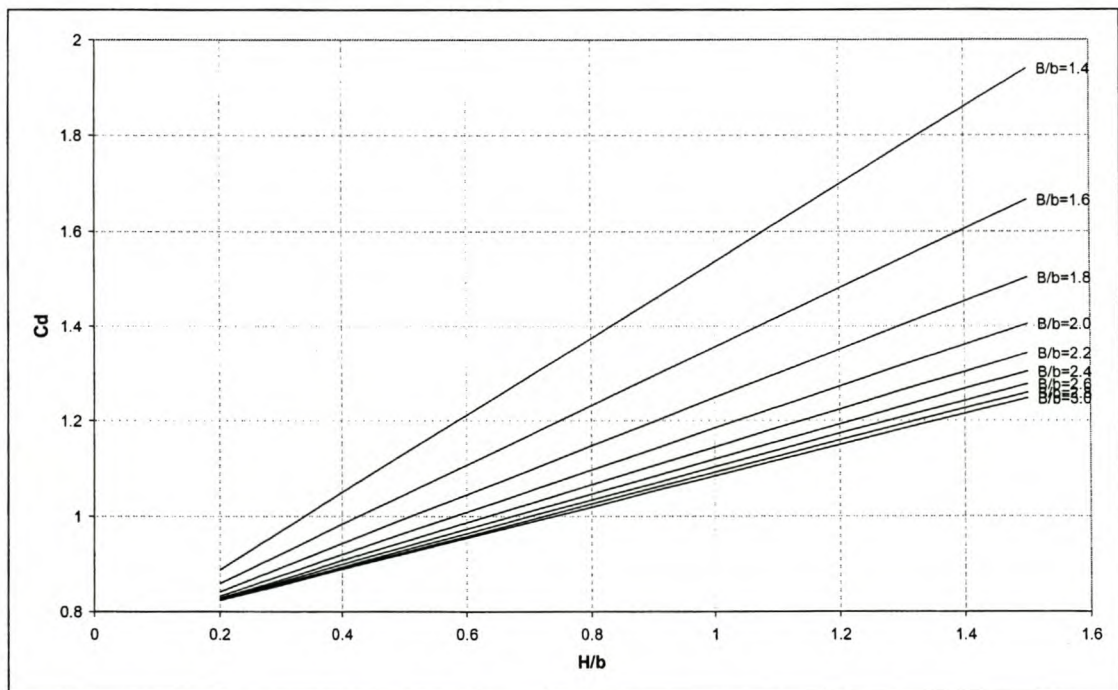


**Figure 5.3: Design curves for Constrictions with Vertical Sides Constrictions.**

There is a distinct relationship between every coefficient and the  $B/b$  value, which allows the use of a single equation to represent the above design curves. There is a quadratic relationship between coefficient  $a$  and  $B/b$  and a sigmoidal relationship between coefficient  $b$  and  $B/b$ . The single equation can be written as follows:



$$C_d = \alpha + \beta(H/\bar{b})$$

$$\alpha = 0.6727 + 0.0498(B/\bar{b}) - 0.0072(B/\bar{b})^2 \quad \dots 5-1$$

$$\beta = \frac{0.4628 + 3.7711(B/\bar{b})^{-3.8657}}{1.5704 + (B/\bar{b})^{-3.8657}}$$

Using this single design equation the average error in calculating the discharge coefficient is 2.1 %. The following graph shows the %error spread when using the single design equation to calculate the discharge coefficient.

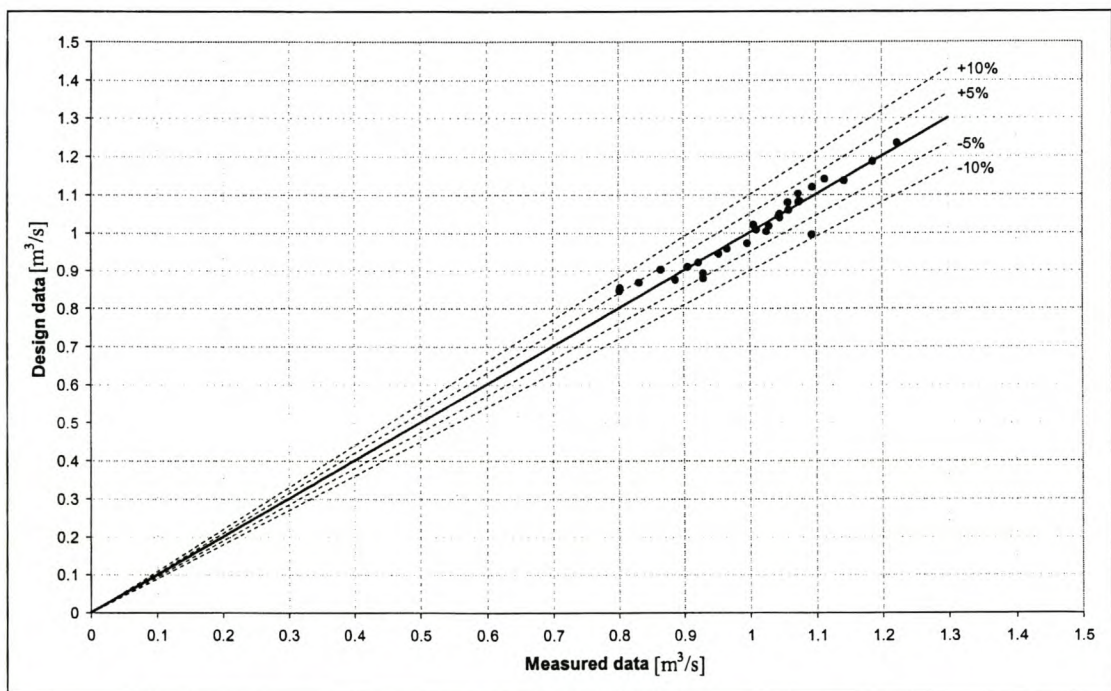


**Figure 5.4: Percentage error in the value of the design  $C_d$  – Vertical Sides.**

### 5.3.2.2 Sloped Sides Constriction

The following graph (Figure 5.5) shows the results obtained from the laboratory tests with sloped side constrictions. As in the case of the Vertical Sides constrictions, it shows a linear relationship between the discharge coefficient ( $C_d$ ) and the relative energy ( $H/b$ ). The graph is followed by the linear equations for each constriction ratio.

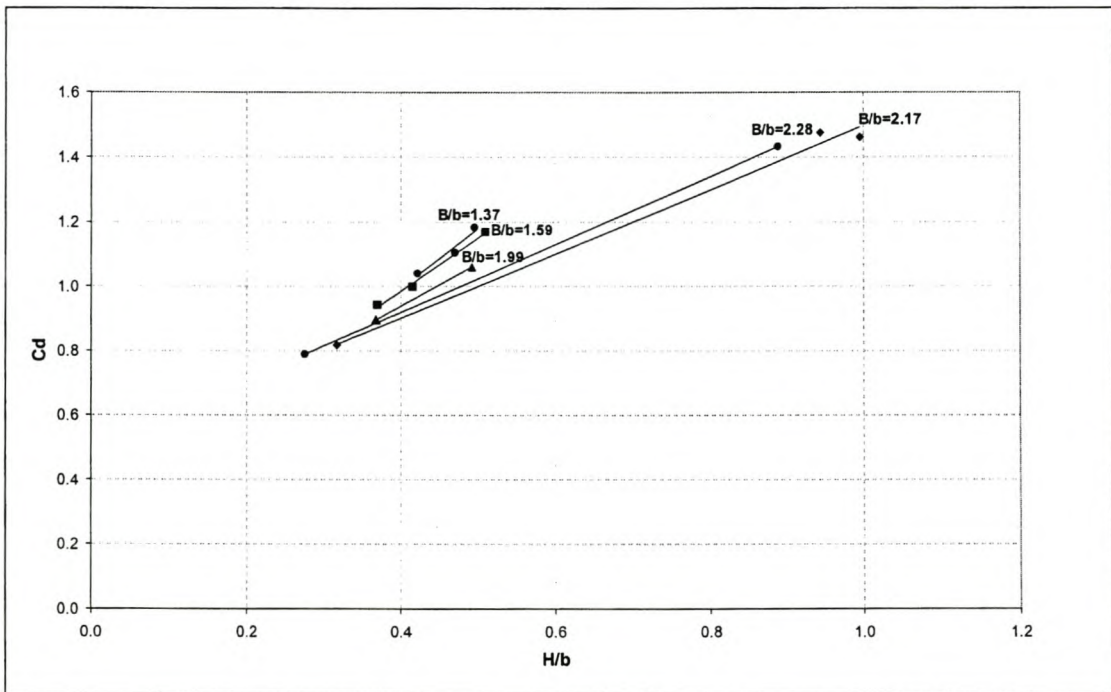


**Figure 5.5:  $C_d$  vs  $H/b$  for constriction with Sloped Sides.**

The linear equation for each constriction ratio is given below:

$$\bar{B}/\bar{b} = 1.37: C_d = 0.2560 + 1.8432(H/\bar{b})$$

$$\bar{B}/\bar{b} = 1.59: C_d = 0.3204 + 1.6573(H/\bar{b})$$

$$\bar{B}/\bar{b} = 1.99: C_d = 0.4050 + 1.3320(H/\bar{b})$$

$$\bar{B}/\bar{b} = 2.17: C_d = 0.5034 + 0.9923(H/\bar{b})$$

$$\bar{B}/\bar{b} = 2.28: C_d = 0.4969 + 1.0534(H/\bar{b})$$

As before, these lines were interpolated and smoothed into dimensionless design curves having the following equations:

$$C_d = a + b\left(H/\bar{b}\right)$$

B/b	a	b
1.00	0.227442	1.902816
1.20	0.240065	1.884494
1.37	0.261765	1.833168
1.40	0.267052	1.818145
1.59	0.308682	1.680536
1.60	0.311161	1.671584
1.80	0.365121	1.472431

B/b	a	b
1.99	0.422934	1.271518
2.00	0.426118	1.261109
2.17	0.481775	1.090319
2.20	0.491831	1.061604
2.28	0.518882	0.987334
2.40	0.559916	0.882273

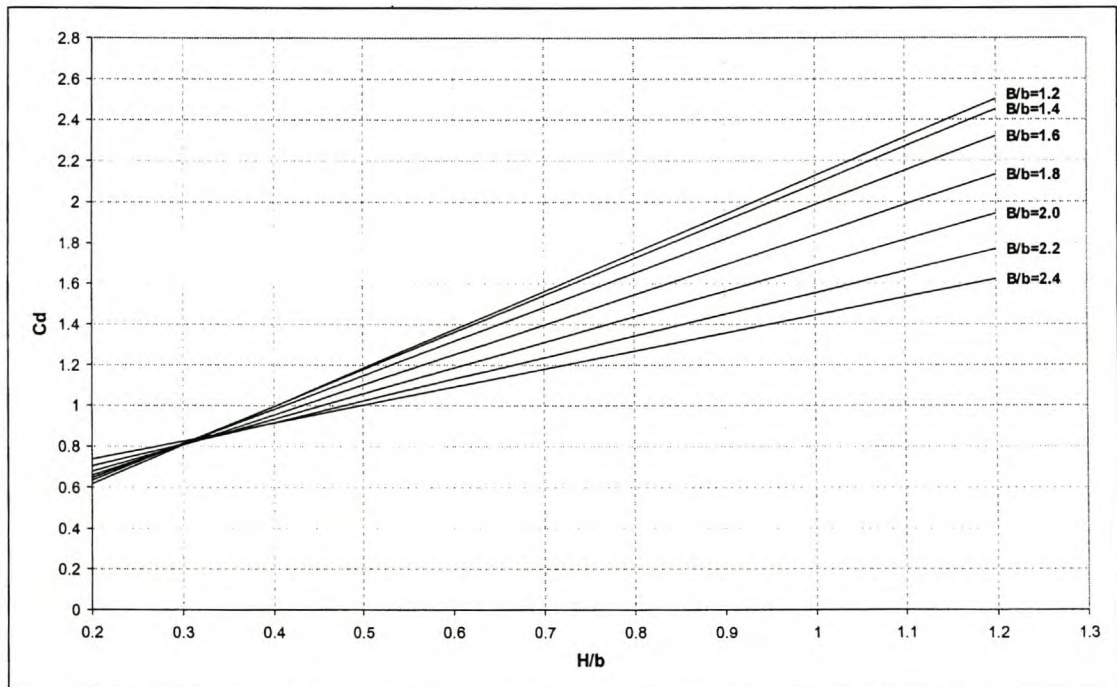


**Figure 5.6: Design curves for Sloped Sides Constrictions.**

There is a distinct relationship between every coefficient and the  $B/b$  value, which allows the use of a single equation to represent the above design equations. There is a quadratic relationship between coefficient  $a$  and  $B/b$  and a sigmoidal relationship between coefficient  $b$  and  $B/b$ . The single equation can be written as follows:

$$C_d = \alpha + \beta(H/\bar{b})$$

$$\alpha = 0.2547 - 0.1516(B/\bar{b}) + 0.1175(B/\bar{b})^2 \quad \dots 5-2$$

$$\beta = \frac{0.0061 + 1.9302(B/\bar{b})^{-6.3549}}{0.0113 + (B/\bar{b})^{-6.3549}}$$

Using this single design equation, the average error in calculating the discharge coefficient is 1.6 %. The following graph shows the %error spread when using the single design equation to calculate the discharge coefficient.

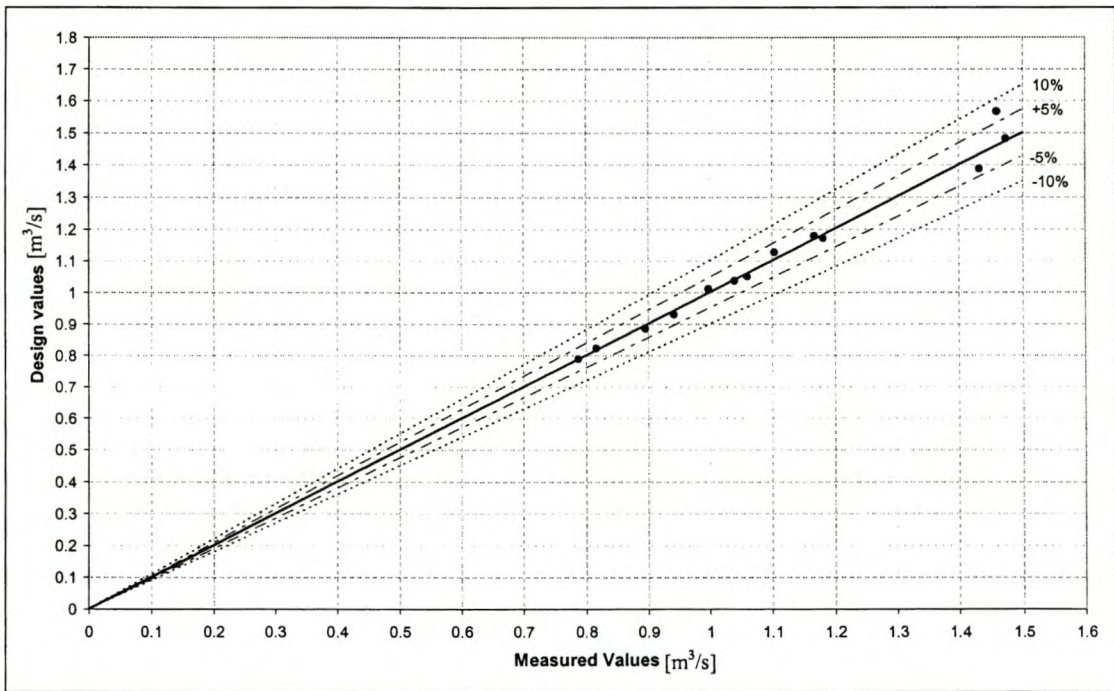


**Figure 5.7: Percentage error in the value of the design  $C_d$  - Sloped Sides.**

### 5.3.2.3 Laboratory Results Compared to Previous Studies

Results from both the constrictions with vertical sides and sloped sides, showed the same linear relationships as results from tests performed by Samani and Magallanez (2000), described in Chapter 4. The  $C_d$  values of each constriction ratio follow a linear relationship with the relative energy ( $H/b$ ). There is also a decrease in the slope of this linear relationship as the constriction ratio increases.

Raw data from the laboratory tests conducted by Hager (1985, 1986) and Samani and Magallanez (2000) were used to calculate discharge coefficient values, using the same iterative procedure employed in this study as described in Chapter 2. These results were compared to the results obtained from the laboratory tests and graphed in Figures 5.8 and 5.9. It is clear from the two graphs that for each set of data the discharge coefficient values ( $C_d$ ) follow a linear relationship with the relative energy ( $H/b$ ) for a given constriction ratio, though the slopes are different for each set. There is a definite slope change between each type of control and the slope decreases with an increase in constriction ratio.

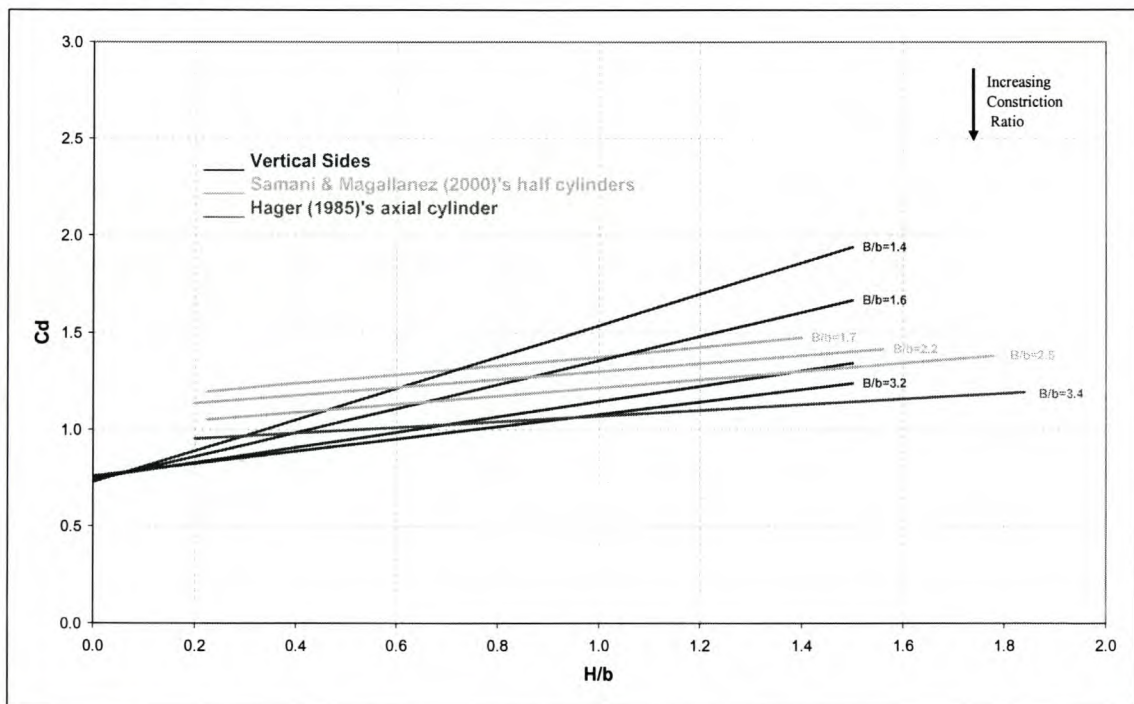


**Figure 5.8: Comparison between Vertical Sides Laboratory data and data from Hager (1985) and Samani & Magallanez (2000).**

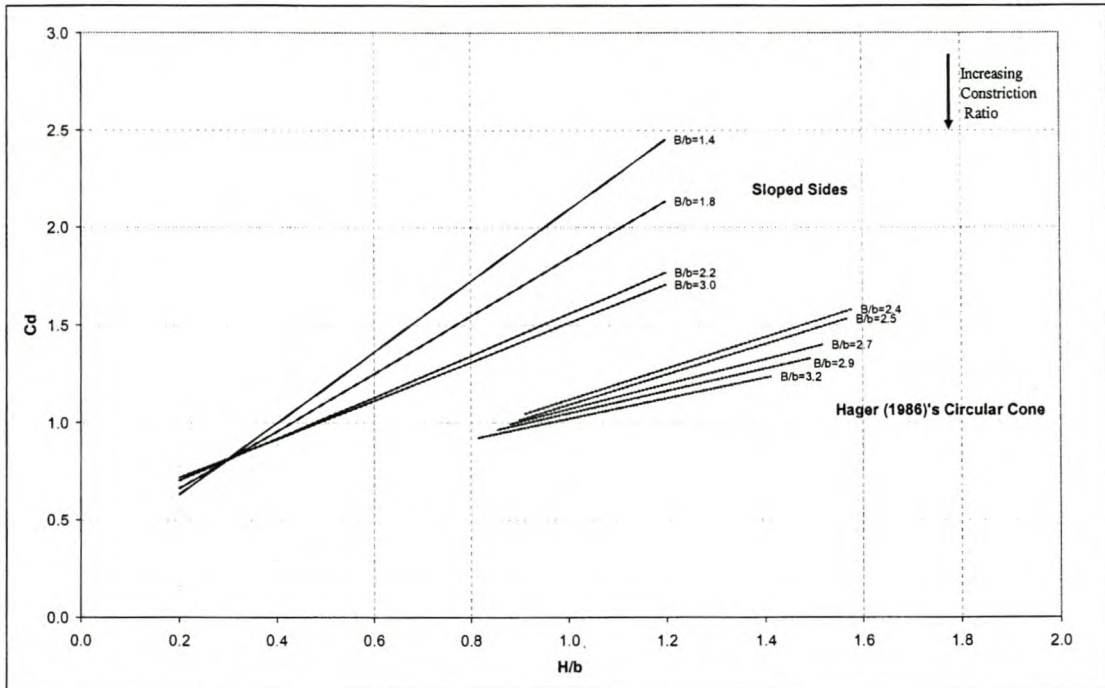


**Figure 5.9: Comparison between Sloped Sides Laboratory data from this study and data from Hager (1986).**

Results from Hager (1985)'s axially mounted cylinder and Samani and Magallanez (2000)'s half cylinders to the side of the channel, yielded similar slopes. This can be attributed to the fact that the two types of constrictions are hydraulically similar. In both cases the constriction is formed by two half cylinders, though their positioning across the channel are different; hence the similar results.

It was stated previously that the discharge coefficient is a function of the upstream energy head and the contracted channel width. From Figures 5.3, 5.6, 5.8 and 5.9 it can be seen that the slope of the linear relationship between the discharge coefficient values and the relative energy head decreases as the channel constriction increases. This would suggest that, as the constriction ratio increases, the value of the discharge coefficient becomes less influenced by the upstream energy head and more influenced by the physical channel contraction. In the case of Hager (1985) and Samani and Magallanez (2000)'s studies it almost follows a horizontal line, reflecting a constant value of  $C_d$ .

The general increase in slope between the different types of constrictions (Figure 5.10) can be attributed to the difference in abruptness of the constriction and its influence on the streamlines. Consider the case of the rounded constriction of Samani and Magallanez (2000). The streamlines are bent gradually around the half cylinders (Figure 5.11), allowing them to follow the edges of the constriction with little vortex formation behind the constriction, resulting in smaller energy losses.

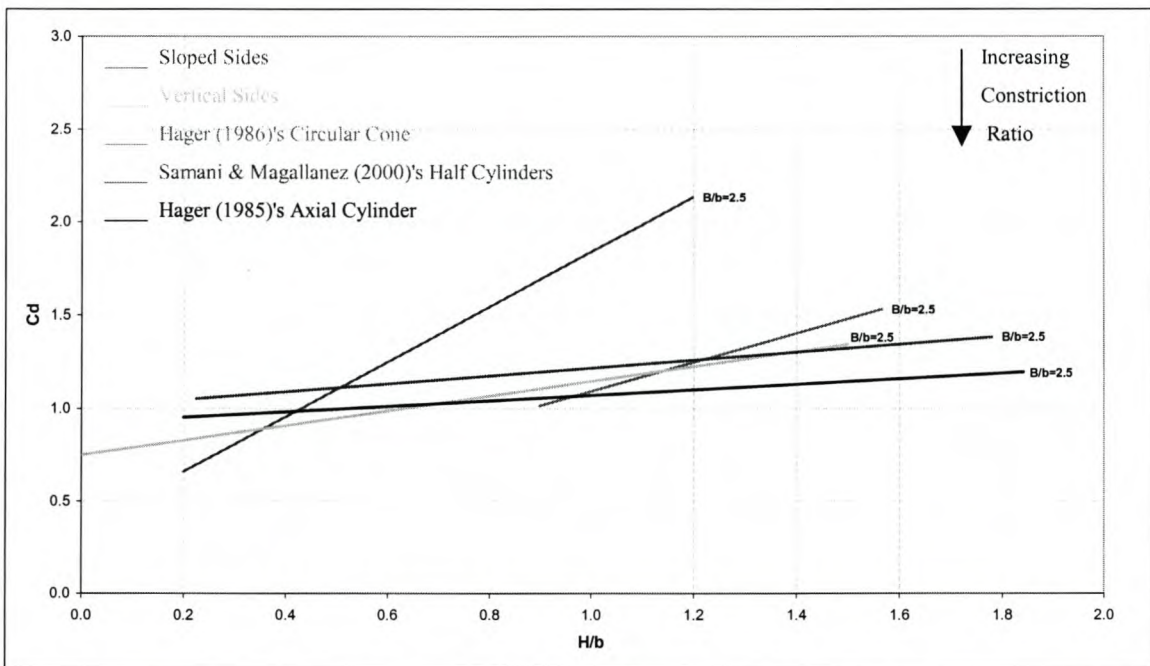


**Figure 5.10: Comparison between laboratory data and data from Hager (1985, 1986) and Samani & Magallanez (2000).**

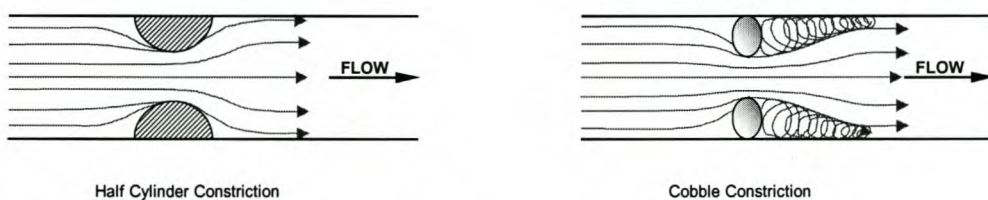


**Figure 5.11: Streamline curvature for different constrictions.**

In the case of the Vertical Sides constrictions the constriction is more sudden, causing the flow lines to be bent more and the flow to separate from the edges behind the constriction resulting in larger energy losses.

This situation becomes less and less ideal as the upstream energy head increases and the assumptions of straight and parallel streamlines, uniform velocity distribution and no energy losses between the pool and constriction sections, become increasingly unrealistic. The discharge coefficient needs to compensate for these assumptions and thus, as the assumptions become more unrealistic, the value of the discharge coefficient will increase.

This increase in the value of discharge coefficient with increasing upstream energy head is steepest for the Sloped Sides and Circular Cone constrictions. The V-shaped geometry of this type of control causes the streamlines at the bottom of the control to be bent even more than in the case of vertical sides. Hager (1986) also showed that the velocity distribution at the critical point for the Circular Cone constriction is far from being uniform (Figure 5.12). A sharper increase in discharge coefficient with upstream energy head is thus noticed for this type of control.

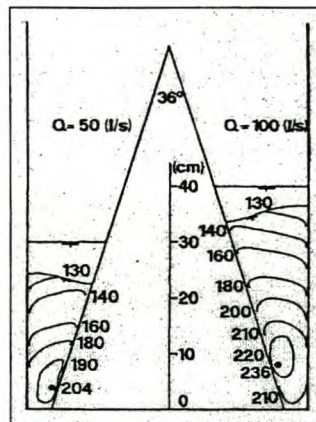


**Figure 5.12: Velocity distributions at critical cross section of Circular Cone Constriction. From Hager (1986).**

#### 5.4 Independent Verification of Results

Independent verification of results was not part of this study. This, along with further calibration, will form part of the next phase of the Water Research Commission's program for investigating natural controls for discharge measurement.



## 5.5 Uniform Flow Controls

Only a limited field study was done on this type of control. Plane bed controls (controls where near uniform flow occurs over a stretch of river having large scale roughness) is a unique and intricate study field and Jonker (2002) has done extensive research on this topic and this research is continuing.

This study identified a near uniform stretch of river (See section 3.4.5 and Figures 3.15 - 17) and applied Jonker's discharge equation as well as Malan's (2002) equation to the section to determine the accuracy of these equations under the study conditions. The following graph (Figure 5.13) shows the difference between the calculated discharge using the two equations and the measured discharge. As mentioned in Chapter 3 Malan's equation consistently overestimates the measured flows, but seem to become more accurate as the discharge increases. Values calculated by means of Jonker's equation, are more accurate and evenly spread around the measured values, suggesting that the equation is applicable to a wider range of flows than in the case of Malan's equation.

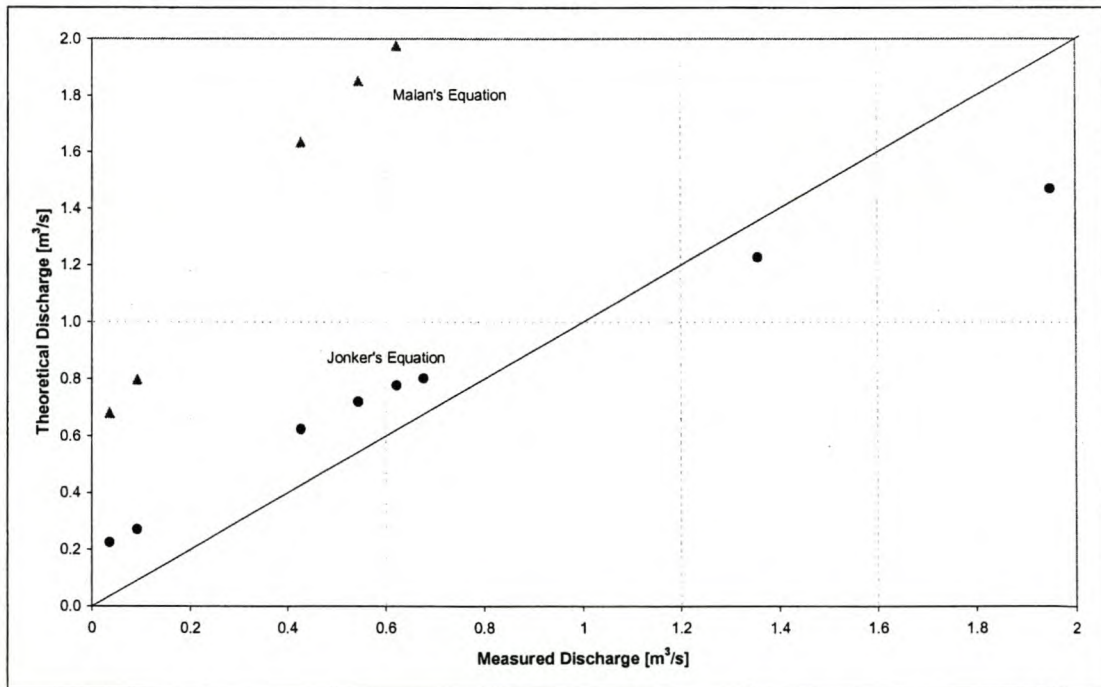


**Figure 5.13: Comparison between accuracy of calculations using Jonker's (2002) and Malan's (2002) discharge equations respectively.**

## 6 CONCLUSIONS AND RECOMMENDATIONS

### 6.1 Introduction

Natural controls can be used for discharge measurement in steep Western Cape and other similar rivers, providing reasonably accurate results at relatively low cost. It proves to be an environmentally acceptable way of measurement, using the natural river characteristics rather than seriously interfering with them or damaging them. These advantages make discharge measurement at natural controls a promising means of determining river discharge in the future.

The following sections present the conclusions reached for each type of natural control which has been considered. Recommendations are made regarding the accuracy, suitability and applicability of each control as well as identifying areas for further research. Lastly overall conclusions are reached regarding the use of natural controls for the measurement of discharge in Western Cape Rivers.

### 6.2 Step-Pool Controls

Step-pool controls were found to be very robust controls which provided efficient critical controls for a wide range of flows. Cross sectional stability at this type of control is very good, with no damage or boulder movement having been detected even after flood events.

Field tests were done under modular flow conditions only. No measurements could be taken during flood flows, more specifically under drowned circumstances. Further investigation into this aspect is needed before this type of control can be used to measure accurately under drowned conditions.

A single discharge coefficient for this type of control was found through field and laboratory tests. This discharge coefficient is equal to 0.61 and is consistent with the contraction coefficient of a rectangular orifice. It is recommended that this value be

used provisionally as the discharge coefficient for step-pool controls. Though these results still need to be tested in other similar cobble and boulder bed rivers, it is believed that this discharge coefficient value is globally applicable on all step-pool controls.

By using this discharge coefficient, it was found that discharges could be calculated with an average accuracy of  $\pm 10\%$  for the study reach. Should a more accurate determination of discharge be needed, it is advised that each site be calibrated separately by means of physical model study.

### 6.3 Horizontal Constriction Controls

This type of control yielded three main results. It was found that for an arbitrary shaped control, a general discharge coefficient  $C_d = 1.26$  can be used. Discharges obtained using this discharge coefficient, were well within  $\pm 10\%$  accuracy. Horizontal constriction controls thus prove to be reasonably accurate measurement sites and, because of their physical characteristics, they are able to measure the full range of flows from low to flood flows. There is most certainly a relationship to be found between the discharge coefficient and the relative energy head for different constriction ratios, but due to the limited results available no definite pattern could be established.

A definite linear relationship, however, was established between the discharge coefficient ( $C_d$ ) and relative energy head ( $H/b$ ) for controls having a definite shape that changes evenly with the depth of flow. Two types of constrictions were tested, those having vertical sides and those having sloped sides. Both showed the same linear relationship though the slopes of the relationship were different for each type. These results were compared to previous experiments done with geometrical shapes forming the constriction and found that they all show a unique linear relationship for each constriction ratio.

Equation 5-1 should be used to calculate the discharge coefficient for a constriction having vertical sides and Equation 5-2 for sloped sides. It is recommended that these equations should not be used outside the range of  $B/b$  and  $H/b$  values indicated, because

no data is available outside these boundaries yet. The accuracy of discharge measurement using these equations is within  $\pm 5\%$ .

#### **6.4 Uniform Controls**

Whilst uniform controls are widely used for flow measurements on deep rivers, such measurements become highly unreliable when flow depths are small and bed roughness high. Under conditions of high roughness, generally speaking, critical controls can be calibrated more accurately than uniform controls and are therefore to be preferred.

Care must be taken when determining the physical parameters for uniform controls, especially the sampling of the bed material sizes, as this can greatly influence the accuracy of the discharge equations.

It is recommended that the discharge equation developed by Jonker (2002) be used for these controls, bearing in mind that calculations become highly unreliable at low flow depths.

#### **6.5 General Conclusions**

Discharge measurement at natural controls in the Western Cape was found to be a viable and reasonably accurate way of determining river discharge. Measurements at these controls were reasonably accurate and consistent.

Discharge coefficients and relationships between discharge coefficients and the physical characteristics of the controls were established. Reasonably accurate values of discharge coefficients of different types of natural controls were established, which should be widely applicable.

### 6.6 Recommendations for further research

- 1) It is recommended that the field study be extended to more cobble and boulder bed rivers within and outside the Western Cape, to broaden the available field data set.
- 2) Both the step-pool and horizontal constriction controls showed promising results as measurement sites. Further study into these controls are recommended to establish a solid database and to verify results obtained in this study.
- 3) Further investigations into the linear relationships between the discharge coefficient  $C_d$  and the relative energy head  $H/b$ , could allow interpolation of results for different shapes of constrictions.

## 7 REFERENCES

Ackers, P., W.R. White, J.A. Perkins and A.J.M. Harrison. *Weirs and Flumes for Flow Measurement*. New York: John Wiley and Sons, 1978.

Issam A. Al-Khatib, "Head-Discharge Relationship in Flumes of Compound Sections," *Journal of Irrigation and Drainage Engineering* 124, no. 3 (1998) : 177-179.

Wubbo Boiten and Remmet H. Pitlo, "The V-Shaped Broad-Crested Weir," *Journal of the Irrigation and Drainage Division Proceedings ASCE* 108, no. 2 (1982) : 142-160.

Bos, M.G. *Discharge Measurement Structures*. Wageningen: International Institute for Land Reclamation and Improvement/ILRI, 1<sup>st</sup> ed.1976; 2<sup>d</sup> ed. 1978; 3<sup>rd</sup> Revised ed. 1989.

Bos, M.G., J.A. Replogle and A.J. Clemmens. *Flow Measuring Flumes for Open Channel Systems*. New York: John Wiley and Sons, 1984.

British Standards Institution, BS3680: Part 4: 1981 *Methods for Measurement of Liquid Flow in Open Channels*

Chadwick, A. and J. Morfett. *Hydraulics in Civil and Environmental Engineering*. London: E & FN Spon, 1998.

Clark, D. *Plane and Geodetic Surveying*. London: Constable and Company Ltd, 1957.

A. J. Clemmens and M. G. Bos, "Critical Depth Relations for Flow Measuring Design," *Journal of Irrigation and Drainage Engineering* 118, no. 4 (1992) : 640-644.

Featherstone, R.E. and C. Nalluri. *Civil Engineering Hydraulics*. Oxford: Blackwell Science Ltd, 1995.

Vito Ferro, "Friction Factor for Gravel-bed Channel with high Boulder Concentration," *Journal of Hydraulic Engineering* 125, no. 7 (1999) : 771-778.

Vito Ferro, "Flow Measurement with Rectangular Free Overfall," *Journal of Irrigation and Drainage Engineering* 118, no. 6 (1992) : 956-964.

Mustafa Gögüş and Dogan AltmBILEK, "Flow Measurement Structures of Compound Cross Section for Rivers," *Journal of Irrigation and Drainage Engineering* 120, no. 1 (1994) : 110-127.

Mustafa Gögüş and Issam A. Al-Khatib, "Flow Measurement Flumes of Rectangular Compound Cross Section," *Journal of Irrigation and Drainage Engineering* 121, no. 2 (1993) : 135-142.

Grover, N.C. and A.W. Harrington. *Stream Flow*. New York: John Wiley and Sons, 1949.

W.H. Hager, "Venturi Flume of Minimum Space Requirements," *Journal of Irrigation and Drainage Engineering* 114, no. 2 (1988) : 226-243.

Willi H. Hager, "Hydraulics of plane free overfall," *Journal of Hydraulic Engineering* 109, no.12 (1983) : 1683-1697.

W. Hager, "Modified, Trapezoidal Venturi Channel," *Journal of Irrigation and Drainage Engineering* 112, no. 3 (1986) : 225-241.

W.H. Hager, "Modified Venturi Channel," *Journal of Irrigation and Drainage Engineering* 111, no. 1 (1985) : 19-35.

Henderson, F.M. *Open Channel Flow*. New York: Macmillan Company, 1966.

Institute for Water and Environmental Engineering in association with the South African National Committee on Large Dams. 2002. *Design and Rehabilitation of Dams*. University of Stellenbosch, Stellenbosch.

International Association for Hydraulic Research. *Hydraulic Structures Design Manual: Discharge Characteristics*. Rotterdam: A.A. Balkema, 1994.

Robert D. Jarrett, "Hydraulics of High-Gradient Streams," *Journal of Hydraulic Engineering* 110, no. 11 (1984) : 1519-1539.

Jonker, V., A. Rooseboom and A.H.M. Görgens. *Environmentally Significant Morphological and Hydraulic Characteristics of Cobble and Boulder Bed Rivers in the Western Cape*. Pretoria: Water Research Commission, 2002.

Le Grange, A. Du P. *Techniques for Predicting the Deformation and Hydraulic Resistance of Sand-bed Flow Channels*. Dissertation, 1994. University of Stellenbosch.

Lotriet, H.H. 1996. *River Discharge Measurement at South African Compound Weirs in Rivers with High Sediment Loads: The Development of an Improved Method for Measurement*. Ph.D. diss., Department of Civil Engineering, University of Stellenbosch, Stellenbosch.

Lotriet, H.H. and A. Rooseboom. *River Discharge Measurement in South African Rivers: The Development of Improved Measuring Techniques*. Pretoria: Water Research Commission, 1995.

Malan, J.G. 2002. *Flow resistance of large-scale roughness in mountain rivers of the Western Cape*. MscIng Thesis, Department of Civil Engineering, University of Stellenbosch, Stellenbosch.

Malan, J.G. and J.W. van Huyssteen. 1999. *Vloeiemeting deur middel van Natuurlike Kontroles*. B.Sc. Eng final year essay, Department of Civil Engineering, University of Stellenbosch, Stellenbosch.

Rooseboom *et al.* 1984. *National Transport Commission: Road Drainage Manual*. 1<sup>st</sup> ed. Pretoria: National Transport Commission. Directorate Land Transport.

- Rooseboom, A. 2001. *Class notes for Advanced Hydraulics MT06*. Stellenbosch : University of Stellenbosch.
- Rooseboom, A. *Open Channel Fluid Mechanics*. Pretoria: Department of Environment Affairs, 1974.
- Rooseboom, A. and A duP Le Grange. "The Hydraulic Resistance of Sand Stream Beds under Steady Flow Conditions," *Journal of Hydraulic Research* 38, no. 1 (2000) : 27-35.
- Rowntree, K.M. and R.A. Wadeson. 1999. *A Hierarchical Geomorphological Model for the Classification of Selected South African Rivers*. Report no. 497/1/99, Water Research Commission, Pretoria.
- M. B. Rubin, "Relationship of Critical Flow in Waterfall to Minimum Energy Head," *Journal of Hydraulic Engineering* 123, no. 1 (1997) : 82-84.
- Z. Samani, S. Jorat and M. Yousaf, "Hydraulic Characteristics of Circular Flume," *Journal of Irrigation and Drainage Engineering* 117, no. 4 (1991) : 558-566.
- Z. Samani and H. Magallanez, "Measuring Water in Trapezoidal Canals," *Journal of Irrigation and Drainage Engineering* 119, no. 1 (1993) : 181-186.
- Z. Samani and H. Magallanez, "Simple Flume for Flow Measurement in Open Channel," *Journal of Irrigation and Drainage Engineering* 126, no. 2 (2000) : 127-129.
- South African Department of Transport. Directorate: Roads. 1997. *Road Drainage Manual*. Pretoria.
- United States Department of the Interior, United States Geological Survey. Geological Survey Water-Supply Paper 2175. 1982. *Measurement and Computation of Streamflow*. Washington, D.C.: Government Printing Office.
- Vicente L. Lopes and Edward D. Shirley, "Computation of Flow Transitions in Open Channels with Steady Uniform Lateral Inflow," *Journal of Irrigation and Drainage Engineering* 119, no. 1 (1993) : 187-200.
- Ven Te Chow. *Open-Channel Hydraulics*. New York: McGraw-Hill Book Company Inc., 1959.
- Webber, N.B. *Fluid Mechanics for Civil Engineers*. London: Chapman and Hall, 1971.
- Wessels, P. 1996. The Calibration of Compound Crump and Sharp-Crested Gauging Weirs in South Africa. Ph.D. diss., Department of Civil Engineering, University of Stellenbosch, Stellenbosch.

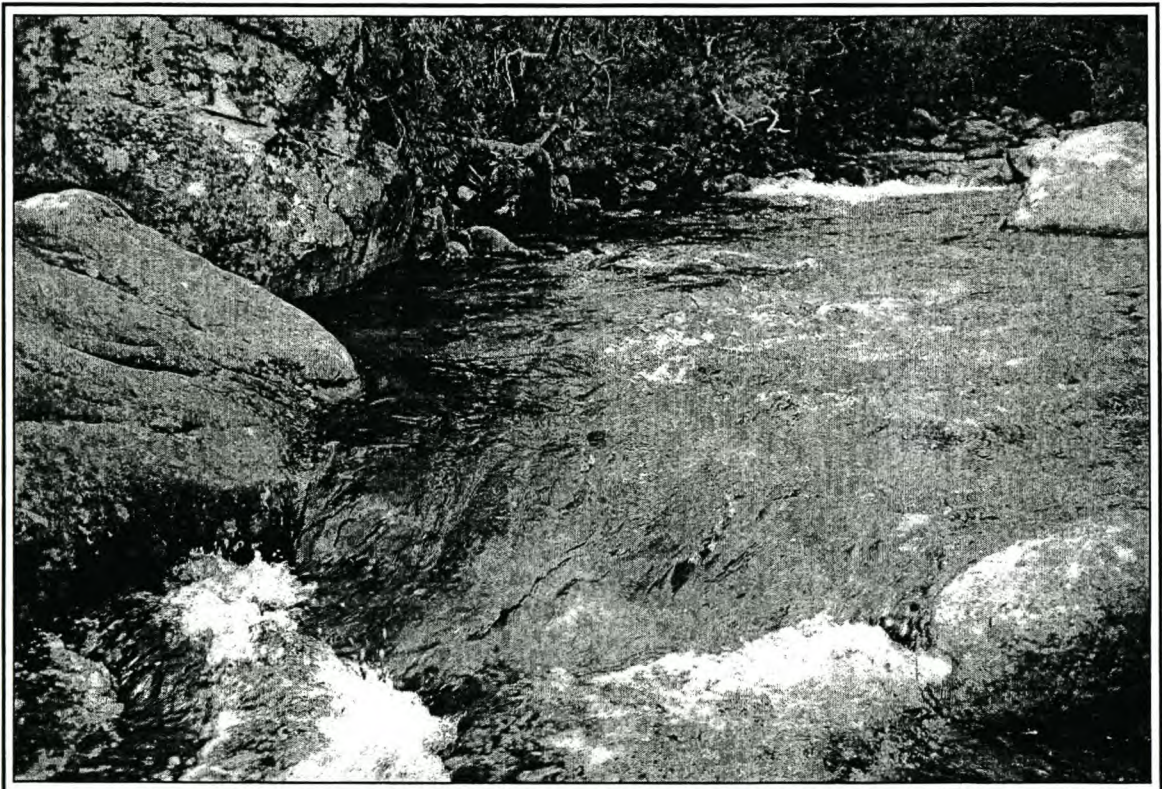


## **APPENDIX A**

### **Guidelines on Flow Measurement at Natural Controls**

---

***CONCEPT  
GUIDELINES ON FLOW  
MEASUREMENT AT NATURAL  
CONTROLS***



September 2003

## 1 PURPOSE OF THIS DOCUMENT

The purpose of this document is to serve as a guideline to the use of Natural Controls for discharge measurement in Western Cape rivers. It explains the concept of natural controls and gives guidelines and examples to aid in identifying suitable sites, how to collect data from the sites and then to process that data to arrive at a discharge for a given stage. It is intended to be used by both engineers and non-engineers, especially aiding those who have to study rivers and river discharges but don't have the underlining engineering theory as background.

## 2 NATURAL CONTROLS

### 2.1 Definition of Natural Controls

A control section is defined as being any section in a watercourse where a unique and known relationship exists between the water level (stage) and the discharge. This unique relationship enables the discharge to be calculated from the measured water level, which makes it an ideal place for continuous discharge measurement.

Controls most commonly used for discharge measurement are sections where flow passes from subcritical (slow and deep flowing) to supercritical (fast and shallow flowing). Figure 1. This transition results in a unique depth being established called the critical depth, from which the discharge can be calculated. These controls are called critical controls and common examples are weirs, flumes and spillways.

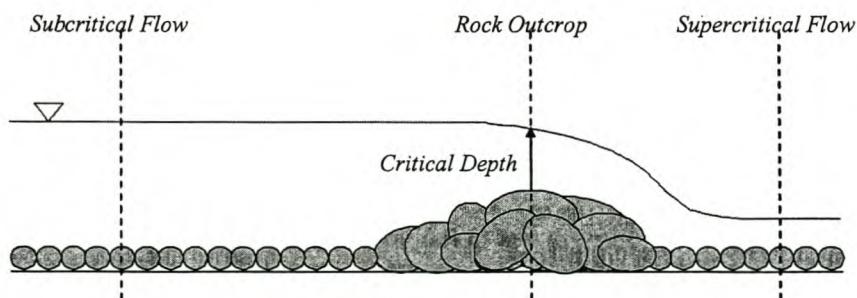


**Figure 1: Flow through critical control section.**

Another, not so commonly used in South Africa, type of control is found where the flow in and cross-sectional shape of a watercourse is uniform for a reasonable length (Figure 2). Uniform controls are not associated with particular localised features, as is the case with critical controls, but are rather characterised by the constant depth which the flow tends to assume when no other controls are present (Henderson, 1966).

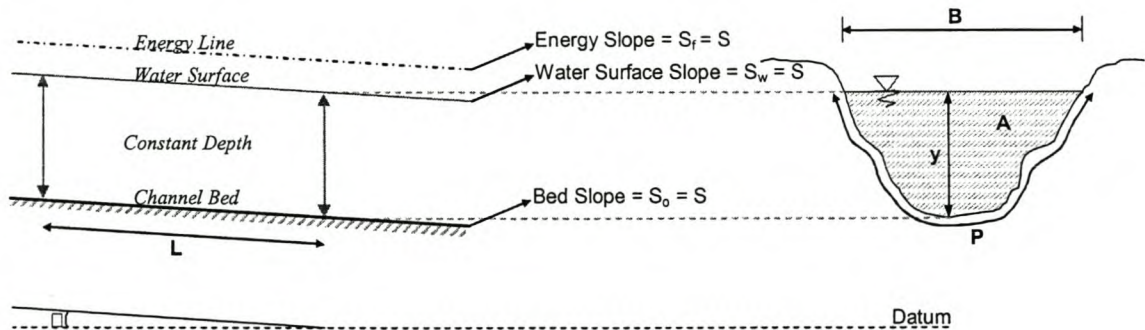


**Figure 2: Flow through uniform flow control (Ven Te Chow, 1959).**

Controls may be either natural or artificial, depending upon whether they are of natural origin or constructed by man. Natural controls can be formed by single topographic features such as reefs of bedrock extending across a stream or clasts of boulders constricting the flow, this forming a critical control; or by long reaches of river having essentially uniform characteristics, this inducing uniform flow.

## 2.2 Types of Natural Controls

The following photographs show examples of various natural controls. Figure 3 is a step-pool control formed by boulders forming a transverse barrier across the river. Figure 4 is a horizontal constriction control formed by clasts of boulder constricting the flow enough to induce critical depth. Figure 5 is an example of a plane bed control which is a uniform reach of river in a cobble bed river. Figure 6 shows a uniform section in a sand bed river.

### 1. Step-pool controls (Critical control)



**Figure 3: Example of step-pool control.**

### 2. Horizontal constriction controls (Critical control)

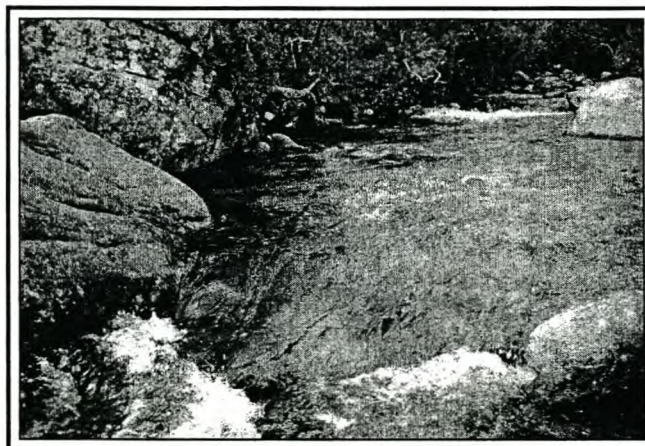


**Figure 4: Example of horizontal constriction control.**

**3. Plane bed reach in cobble bed river (Uniform control)**



**Figure 5: Example of plane bed uniform flow control.**

**4. Uniform flow reach in sand bed river (Uniform control)**

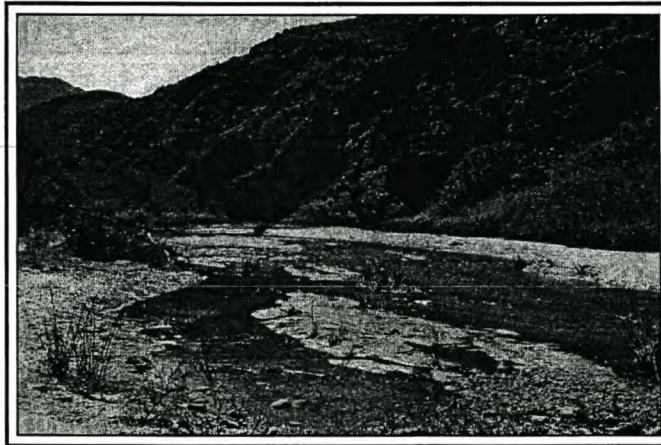


**Figure 6: Example of a sandbed river.**

Each of these types of controls has a unique approach to its use for discharge measurement and will thus be discussed separately in later sections.

### 3 GENERAL CRITERIA FOR SELECTING NATURAL CONTROL SITES

In searching for suitable natural control sites the following general criteria, as suggested by the USGS (1982), should be used as a guideline:

1. The general course of the river should be straight for approximately 100m upstream and downstream of the site.
2. The total river flow to be measured must be contained in the main channel.
3. The streambed should be stable.
4. An unchanging natural control must be present.
5. A pool must be present upstream from the control at low flows to ensure the recording of stage at these flows and to avoid high velocities in the approach channel during high flows.
6. Should a suitable site be situated between two tributaries, it should be far enough downstream from the upper tributary so that flow is fairly uniformly established across the entire width of the river, and far enough upstream from the lower tributary to avoid variable backwater effect.
7. Access to the site must be easy.
8. The control section should be far enough upstream from bridges, dams, etc. that could influence the water level at the control section through backwater effects.

An ideal measurement site is seldom found and judgment has to be exercised in choosing suitable sites, each of which will have shortcomings. Often, adverse conditions exist at all possible sites and a poor site has to be accepted.

In mountainous rivers with its large boulders and general nature to form a series of steps and pools, the best type of natural control is generally a critical control. To find such a control look for a section where large boulders form a transverse barrier across the river, thus forming a step-pool control with a reasonable deep pool area and a continuous step across the width of the river (Figure 3). Controls which are particularly good in terms of

flow measurement are sections where large boulders constrict the flow horizontally to form a horizontal constriction control (Figure 4). These two types of controls are reasonably accurate and can be used over a wide range of flows.

Where mountainous rivers become less steep and the distribution and grading of the bed particles are more even, the presence of critical controls will become scarce. In these conditions it is better to find a reach of river forming a plane bed control (Figure 5) where the theory of large scale roughness, as researched by Jonker (2002), can be applied to near uniform flow.

Even further downstream, the river gradient becomes flat and the cobbles and boulders are replaced by sand and gravel (Figure 6). In these areas the theory for sandbed rivers, as set out by Rooseboom and Le Grange (2000), should be used.

The following section will discuss the data collection involved for each type of natural control. Section 5 will deal with the processing of this data.

---



## 4 DATA COLLECTION

### 4.1 General Site Data

After suitable control sites are identified, they must be clearly marked with permanent markings. The surrounding area at each site must be explored to ascertain the nature of the river, extent of vegetation, flood plain shape and its overall dimensions. Flood plains should be investigated to determine the debris line indicating high water marks from previous flood events. Any back channels or parallel channels must be identified and their connectivity on the main channel investigated.

Benchmarks should be established and clearly indicated above these debris lines, ensuring that the benchmarks are not compromised by regularly occurring floods. High water marks also provide a good indication of the level at which a permanent stage recorder must be placed to avoid being damaged by floodwaters.

### 4.2 Cross Sections

After establishing benchmarks, each site must be carefully surveyed and as much detail as possible documented. The control section is taken at the section having the minimum flow area and the pool section in the deepest and slowest flowing part of the site (Figures 9,10,11 and 12). The location of each cross-section should be marked clearly for re-surveying especially after flood events.

In the case of uniform flow controls at least three cross-sections should be taken. One at the most upstream end of the reach, one in the middle of the reach and one at the downstream end. The slopes of the river bed and water surface should be surveyed at constant intervals along the reach. For uniform flow control sites in cobble and boulder-bed rivers, the particle distribution must be determined by sampling the particles in a 0.5 or 1m square grid (Figure 7) stretching from the upper-most cross-section to the most downstream cross section.

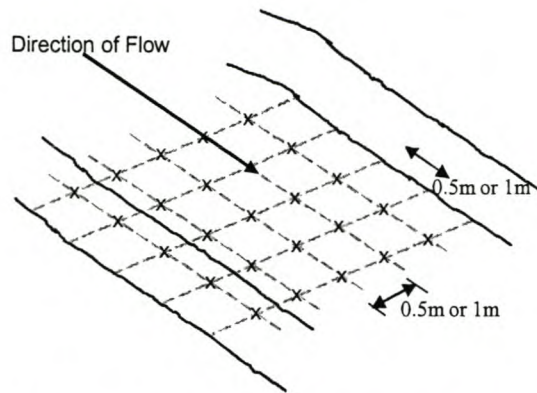


**Figure 7: Particle size measurement grid (Malan, 2002).**

Photographs should be taken at regular intervals of the sites, especially after flood events to visually assess the site stability.

### 4.3 Stage Measurement

The location of the water level measurement position materially affects the calculated discharge. If the water level is taken too close to the control section the water surface profile forms a drawdown curve and pressures are not hydrostatic. If it is taken too far upstream from the control section the frictional forces produce a water surface slope towards the control section (Ackers et al., 1978). An appropriate water level measurement position should avoid the area of drawdown, but should not be too far upstream from the control section to allow frictional losses to play a significant role (Figure 8).

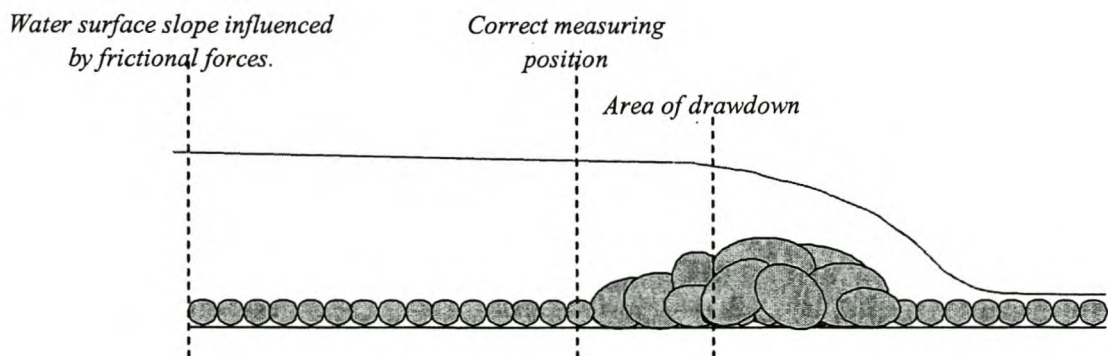


**Figure 8: Correct measuring position at critical control.**

Stage measurements at a critical control site should be taken in the deepest and most tranquil part of the pool section, at least 2 times the maximum head expected upstream of the critical section, but not further than 3 times. At least three levels should be taken across the cross-section to get an average depth and to eliminate reading errors. Downstream water levels should be taken to determine the modular limit.

For uniform controls the stage measurements should be taken at each cross-section (upper-most, middle and downstream section) to form a good average depth of flow and to determine the slope of the water surface.

The following photographs show some examples of stage measurement points for different types of controls.



**Figure 9: Water level measurement at a Step-Pool critical control.**

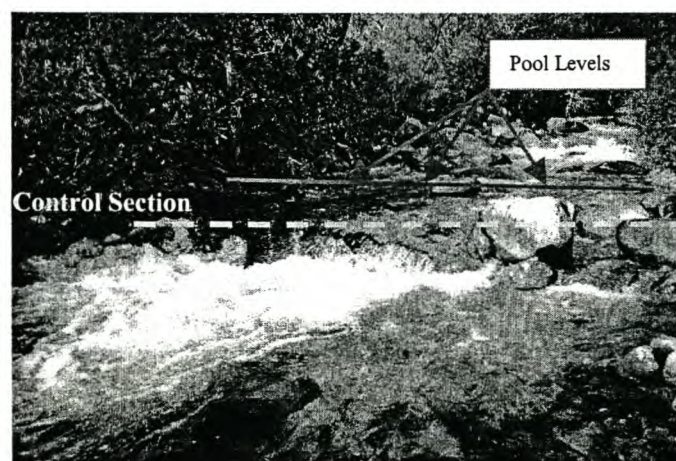


**Figure 10: Water level measurement Step-Pool control.**

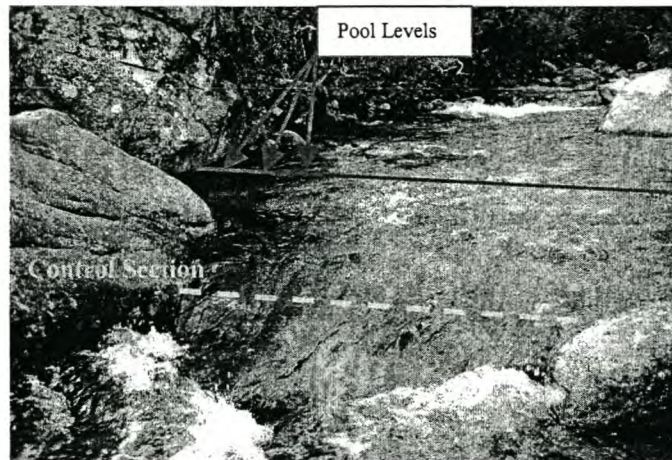


**Figure 11: Water level measurement at Horizontal Constriction control.**

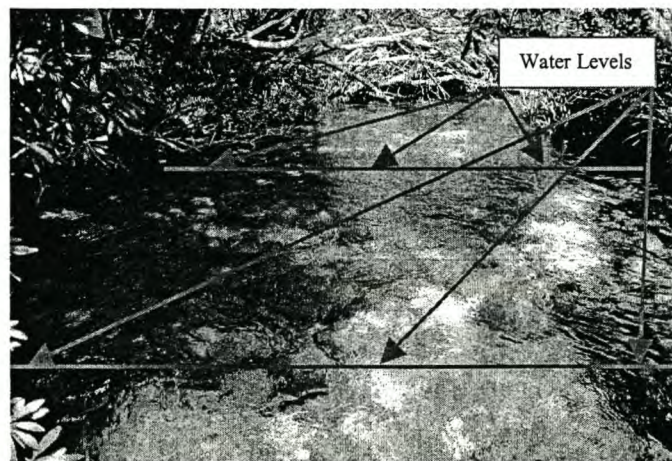


**Figure 12: Water level measurement Uniform Flow control (Plane bed control).**

#### **4.4 Problems Encountered with Collection of Data**

Water surfaces in pools can be very unstable and surveying is difficult. Multiple readings have to be taken to ensure an average value and to minimise error. This can be a lengthy process and very time consuming.

Without a permanent gauging plate, in order to survey the water levels, a person has to physically enter the river and hold a surveying staff in the river. This seriously limits

the range of flows that can be measured. High flow velocities and the slippery surface of cobbles and boulders make it unsafe for entry even at moderate flows.

Human error can cause readings to be discarded, mostly because benchmark levels are not surveyed along with the water levels and so levels can not be compared to other measurements.

#### **4.5 Recommendations**

It is strongly recommended that a permanent gauging plate be installed at sites. This will eliminate the need to physically enter the river and will greatly increase the range of flows that can be measured and save time.

Regular surveys of the sites should be done, especially after a high flow- or flood event occurred to determine the stability of the site. Controls consisting of bedrock outcrops or large boulders are much less susceptible to cross-sectional changes than controls formed by cobbles or smaller boulders. Key cross-sectional boulders should be marked and photos taken of the site at regular intervals, especially after a high flow event. These photos can then be compared digitally to determine if movement of the boulders had taken place.

Should a control to be used for long-term measurement, consist of a combination of large and small boulders or cobbles, it is advised that the small boulders or cobbles be stabilised or fastened in some way to establish site stability.

Surveying of the site should preferably be done in the dry season to capture as much detail as possible. During the wet season most of the site is normally under water and detailed surveying is difficult. Should surveying be done in the wet season, it must be repeated in the dry season.

## 5 DATA PROCESSING

### 5.1 Critical Controls

In order to determine the theoretical discharge ( $Q$ ) from the measured stage ( $h$ ) the energy equation between the pool section and the control section needs to be balanced. It is assumed that critical flow occurs in the control section and that energy losses between the two sections are negligible. Because the flow area in the control section does not change proportionally to a change in flow depth, the procedure is iterative.

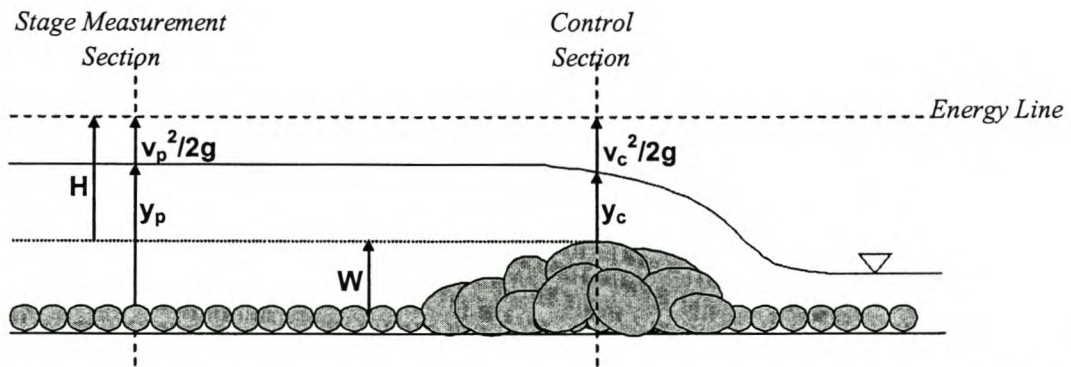


**Figure 13: Definition sketch for application of the Bernoulli (energy) equation.**

By applying the Bernoulli equation between the two sections and assuming ideal flow conditions, leads to the following equation:

$$H = h_p + \frac{\alpha_p v_p^2}{2g} = y_c + \frac{\alpha_c v_c^2}{2g}$$

with

$$h_p = y_p - W$$

The iterative procedure is as follows:

- 1) Estimate a value for flow depth in the control section ( $y_c$ ).
- 2) Determine the flow area in the control section ( $A_c$ ) and surface width of flow ( $B_c$ ) for flow depth  $y_c$ .

- 3) Calculate the discharge by assuming critical flow ( $Fr = 1$ ) in the control section:

$$Q = \sqrt{\frac{gA_c^3}{B_c}}$$

- 4) Calculate velocity head at control section: Equal to  $\frac{v_c^2}{2g}$
- 5) Calculate the energy head at control section:  $H_c = y_c + \frac{v_c^2}{2g}$
- 6) Determine the flow area in the pool section ( $A_p$ ) from the measured stage ( $h$ ).
- 7) Calculate the flow velocity in the pool section:  $v_p = \frac{Q}{A_p}$
- 8) Calculate the velocity head in the pool section: Equal to  $\frac{v_p^2}{2g}$
- 9) Determine the energy head at the pool section:  $H_p = y_p - W + \frac{v_p^2}{2g}$
- 10) Compare  $H_c$  and  $H_p$ . If  $H_c$  and  $H_p$  are not equal, guess another value for  $y_c$  and iterate until  $H_c$  equals  $H_p$ , i.e. until the energy equation, between the pool and control sections, is balanced.

The final discharge calculated in step 3 is the theoretical discharge for a given stage. This discharge was calculated by assuming uniform velocity distribution, straight and parallel streamlines, and no energy losses due to friction or by boundary layer development. But these assumptions are not completely valid and the theoretical discharge must be multiplied by a coefficient that corrects for the non-ideal flow conditions, namely the discharge coefficient  $C_d$ . The real discharge at the control section is thus equal to  $Q_{real} = C_d \times Q_{theoretical}$ .

Each type of critical control has its own unique discharge coefficient and it can vary with varying water levels. The next two sections give the discharge coefficients to be used for step-pool and horizontal constriction controls.

### 5.1.1 Step-Pool Controls

Wessels (1996) stated that discharge coefficients at vertically constricted controls are mainly contraction coefficients correcting for the idealised assumptions of a horizontal water surface and straight streamlines between the pool and control section. Thus discharge coefficients for these controls should be similar in value to the contraction coefficient for a rectangular orifice, which is in the order of 0.6.

The average discharge coefficients obtained from two sites calibrated in the field are 0.618 and 0.601 respectively (See Tables 1 and 2). These results agree with and confirm the above statement by Wessels. It is recommended that a first estimate value of 0.61 be used as discharge coefficient for step-pool controls.

**Table 1: Summary of Results obtained from first site.**

Theoretical Discharge [m <sup>3</sup> /s]	Real Discharge [m <sup>3</sup> /s]	Cd Discharge Coefficient
0.142	0.092	0.645
0.338	0.264	0.782
0.389	0.220	0.567
0.816	0.428	0.525
1.010	0.577	0.572
		<b>0.618</b>

= Average  $C_d$

**Table 2: Summary of Results obtained from second site.**

Theoretical Discharge [m <sup>3</sup> /s]	Real Discharge [m <sup>3</sup> /s]	Cd Discharge Coefficient
0.379	0.220	0.582
0.503	0.311	0.617
0.785	0.428	0.545
1.015	0.577	0.569
1.060	0.623	0.588
2.121	1.489	0.702
		<b>0.601</b>

= Average  $C_d$

Applying this average discharge coefficient to the data obtained in the field, it was found that the discharge could be predicted within 10% accuracy with an average error of 9.1%.



### 5.1.2 Horizontal Constriction Controls

The theoretical discharge calculated at this type of control in the field, consistently underestimates the measured value by an average of 21% (See Table 3) without employing a discharge coefficient.

**Table 3: % Error in Theoretical Calculation of Discharge**

Theoretical Discharge [m <sup>3</sup> /s]	Real Discharge [m <sup>3</sup> /s]	Cd Discharge Coefficient	% Deviation between Theoretical and Real Q
0.173	0.220	1.273	-21%
0.345	0.428	1.242	-20%
0.423	0.564	1.334	-25%
0.460	0.610	1.326	-25%
1.252	1.489	1.189	-16%
0.255	0.311	1.221	-18%
			<b>21 %</b>
			<b>25 %</b>

**Average % Error**  
**Maximum % Error**

The discharge coefficient values obtained all lie within the range  $C_d = 1.19$  to  $1.33$ . An average discharge coefficient value equal to  $1.26$  was employed and by using this value the accuracy of measurement was improved to an average error of  $3.7\%$  and a maximum error of  $6\%$ , bringing it well within  $10\%$  accuracy. A discharge coefficient value of  $1.26$  can be used for this type of critical control.

## 5.2 Uniform Controls

### 5.2.1 Cobble-Bed Rivers

Cobble and boulder bed rivers are characterised by steep gradients and relatively low flow depths in relation to bed particle size, and as a result display complex velocity-depth relations. Flow in these rivers is very turbulent and particularly so at low flows when bed elements protrude out of the water and affect the free water surface. Malan (2002) stated that the bed roughness could be classified as large-scale if the roughness elements affect the free surface.

Under these large-scale roughness conditions the boundary resistance becomes less dominant, while form drag around the individual particles composing the river bed and disturbance of the free water surface become more significant (Jonker, 2002). Malan (2002) stated that in the case of large-scale roughness, the roughness elements tend to act individually and that the total resistance to flow is mainly the sum of their form drags.

Conventional friction based uniform flow formulas, like the Chézy and Manning formulas, are not applicable to the large scale roughness situation as these equations underestimate channel resistance significantly (Jonker, 2002). New equations thus had to be formulated of which the most are empirically based. A study conducted by Jonker (2002) did just that, as he formulated a discharge equation to be used for large-scale roughness. This equation is universally applicable since it was derived theoretically.

Discharge should be calculated by using the following equation:

$$Q = A \sqrt{\frac{2gd_{50}S_o}{0.5285\left(\frac{R}{d_{50}}\right)^{-2.166}}}$$

Where

- $Q$  = Discharge [ $\text{m}^3/\text{s}$ ]  
 $g$  = Gravitational acceleration [ $\text{m}/\text{s}^2$ ]

$d_{50}$	=	Median particle diameter [m]
$S_o$	=	Bed slope
$R$	=	Hydraulic radius [m]
$A$	=	Cross sectional flow area = $W_T \bar{D}$ [m <sup>2</sup> ] (See Figure 2.5)
$R/d_{50}$	=	Relative submergence

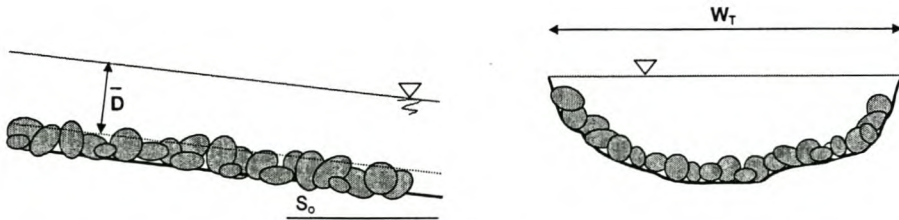


**Figure 14: Definition sketch for Jonker's large-scale roughness equation. (Jonker, 2002)**

The following input data for the equation should be determined:

1. Average size of the bedmaterial ( $d_{50}$ ) as well as the size for which 84% of the particles are smaller ( $d_{84}$ ) should be determined by measuring the size of the particles in a grid as showed in Section 4.2.
2. Flow area, width of flow, hydraulic radius, bed slope and wetted perimeter for each measured water level ( $y$ ).

Jonker (2002) proved that the equation is able to consistently provide fairly accurate estimates ( $\pm 25\%$ ) of mean flow velocity under conditions of large-scale roughness. Since the development of the equation is theoretical, which makes it generally applicable and not site specific as most other, previously developed, empirical and semi-empirical equations.

### 5.2.2 Sand-Bed Rivers

“Sand bed rivers continuously adjust their water- and sediment transport balance. This occurs by virtue of the considerable flexibility of an added import variable, namely the form roughness of the bed” (Rooseboom and Le Grange, 2000). Bedform roughness is the result of variations in flow depth, flow velocity and sediment concentration. Sediment being transported will lead to a change in the resistance of flow by changing the bed roughness and the suspended sediment concentration.

A sand bed river is inclined to assume a condition of minimum energy, i.e. minimization of applied stream power. The presence, however, of sediment in the river provides an alternative mechanism whereby scour is limited, that is the deformation of the river bed. As a river bed is deformed and the value of  $k_s$  increases, the applied unit stream power along the bed is decreased (Rooseboom and Le Grange, 2000).

Rooseboom (1974) stated, “that whenever alternative modes of flow exist, that mode which requires the least amount of applied unit power will be adopted. It follows that fluid flowing over transportable material will not transport such material unless this would result in less power being applied than without sediment transport.”

#### *The influence of sediment transport on flow resistance*

A major problem when working with sand bed rivers is its roughness function. If a river bed is flat and no roughness of the bedform is present, the absolute roughness value  $k_s$  is represented by an equivalent value of the radius  $R_o$  of the eddies formed right next to the bed and having a size of the same order of magnitude as the irregularities on the bed (Figure 15). This equivalent roughness  $R_o$  is generally regarded to be a function of the particle diameter  $d$ .

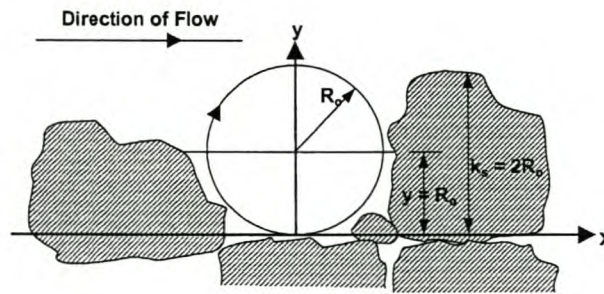


**Figure 15: Eddy formed in between irregularities on channel bottom.**

According to the unit stream power theory, the applied stream power will tend to increase as the discharge increases. It is also recognised that increasing flow in an erodible channel generates a complexity of bed forms along the channel bed.

When sediment is being transported, the amount of stream power applied along the bed can be reduced by (Rooseboom, 1974):

- 1) the formation of a pseudo-viscous zone of high concentration suspension along the bed which acts in a similar fashion to a true laminar sub-layer, or
- 2) deformation of the bed through the formation of bed forms whereby eddies with larger radii are formed along the bed i.e. the value of  $k_s$  increases.

When the value of  $k_s$  increases, it represents a decrease in the amount of applied power along the bed for maintaining motion.

The resistance to flow is a complex function of discharge, fluid and sediment characteristics and is dependent on the variations in bed forms. Changes in flow resistance for a sand bed river under steady flow, are considered to be due to change in the degree of bed deformation and the consequent roughness of the bed.

Bedforms vary as the flow regime varies and their influence in determining the total resistance is far more significant than that of particle roughness within certain flow regimes.

Rooseboom and Le Grange (2000) classified bedforms into three main categories comprising various flow regimes or flow classes:

- 1) The lower flow regime (small stream power) consisting of ripples, bars, dunes with ripples superimposed and dunes.
- 2) The transition zone comprising a flat bed with no bedforms.
- 3) The upper flow regime, comprising the upper regime plane bed, antidunes (standing waves and breaking antidunes), chutes and pools, etc.

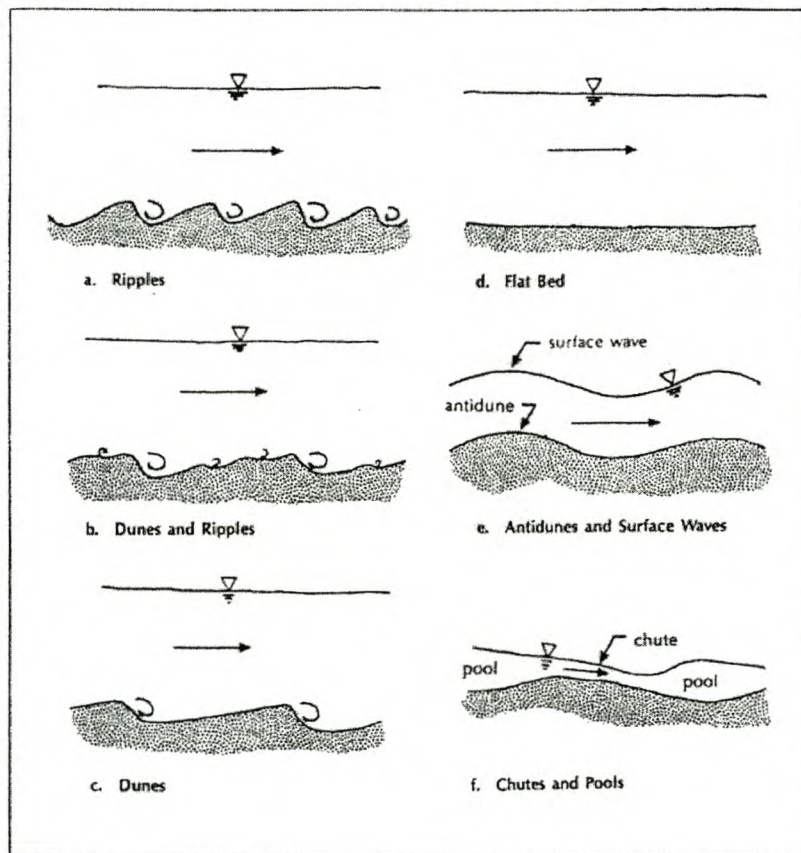


**Figure 16: Bedforms in sand bed rivers.**  
(Rooseboom and Le Grange, 2000)

At low flows and low sediment transport concentrations, the bed deforms into a series of bedforms known as ripples and dunes. (Figure 16)

At higher flows and higher sediment concentrations, the amplitude of the bedforms rapidly becomes smaller and for fine sands the bedforms may disappear leaving a flat bed with a minimum friction factor for the given flow. (Figure 16)

At the upper flow regime, standing waves tend to form with associated bedforms known as antidunes. (Figure 16)

At still higher flows, breaking waves form and the flow becomes difficult to describe quantitatively.

At low discharges and depths of flow the resistance to flow is in accordance with the relationships that describe non-sediment carrying flows. At high discharges and depths of flow, however, the friction factors are primarily determined by the interaction between the transported sediment and flowing fluid, i.e. the absolute roughness value  $k_s$ .

Rooseboom and Le Grange (2000) explained the progressive development of the total flow regime spectrum for a mobile bed consisting of a single particle diameter  $d$  by means of a diagram (Figure 17) showing the unique relationship between the two parameters  $\frac{\sqrt{gD_s}}{v_{ss}}$  (representing the unit power being applied along the bed relative to the power required to suspend the particles of a given density and diameter) and  $\frac{\sqrt{gD_s} k_s}{\nu}$  (representing the ratio between applied stream power for laminar conditions and the applied stream power for turbulent boundary conditions along an uneven bed).

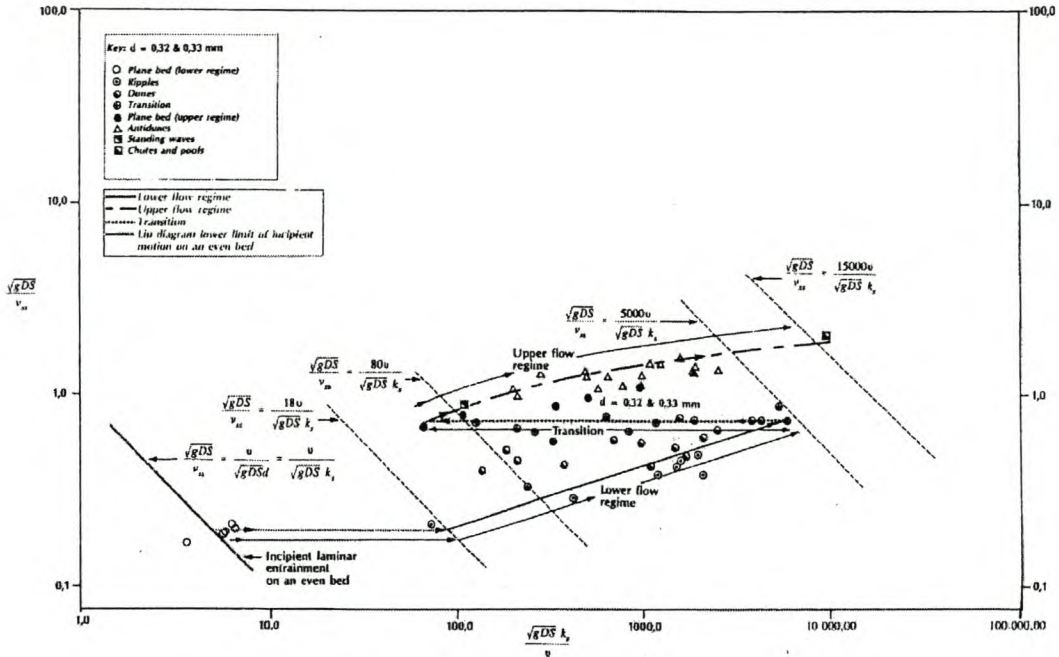


**Figure 17: Progressive development of the total flow regime spectrum for a mobile bed consisting of single size particles. (Rooseboom and Le Grange, 2000)**

The diagram is explained by Rooseboom and Le Grange (2000) as follows:

Starting at the lower limit of incipient motion and a flat bed, with increasing  $\sqrt{gDs}$  values the mobile bed is deformed under lower flow regime condition into ripples and subsequently dunes. These bedforms go hand in hand with increasing values of  $k_s$  or  $\frac{\sqrt{gDs} k_s}{v}$  values until the right-hand turning point is reached. Bed deformation under the low flow regime reaches a maximum value at this stage.

Transition from the lower to the higher flow regime and associated flattening of the bed is represented by the horizontal part of the line. Whilst  $\frac{\sqrt{gDs}}{v_{ss}}$  values remain constant,  $k_s$ -values decrease dramatically until a new turning point is reached where bed deformation is a minimum for upper regime conditions.



“Lower flow regime bedforms are associated with laminar boundary conditions. As the value of  $\frac{\sqrt{gDs} k_s}{\nu}$  increases, a point is reached where the laminar stream power becomes greater than that which is required to maintain turbulent flow at the boundary. Once the boundary conditions in the hollows between the bedforms switch to being turbulent, the bed suddenly becomes unstable. Less power is required to entrain particles when the flow at the bed switches from laminar to turbulent. The existing bedforms are thus seen to be washed away” (Rooseboom and Le Grange, 2000).

Bed deformation again increases from the left hand turning point under upper flow regime conditions, progressing through flat bed, antidunes, standing waves, etc. and associated increases in the value of  $k_s$ .

Rooseboom and Le Grange (2000) translated Figure 17 into a user-friendly set of graphs for easy practical application. This diagram (Figure 18) provides a complete averaged picture of resistance values and indicates the bedforms that will prevail.

The diagram should be used in the following manner:

- 1) Estimate a value for the flow depth  $D$ .
- 2) Read the corresponding  $\Delta$ -value from the diagram (particle diameter to be known)
- 3) Use the associated  $k_s$  value in the Chézy equation and iterate until it yields the same flow depth estimated in step 1.
- 4) The value of  $k_s$  as found will be the correct roughness coefficient to use under the specified flow conditions.

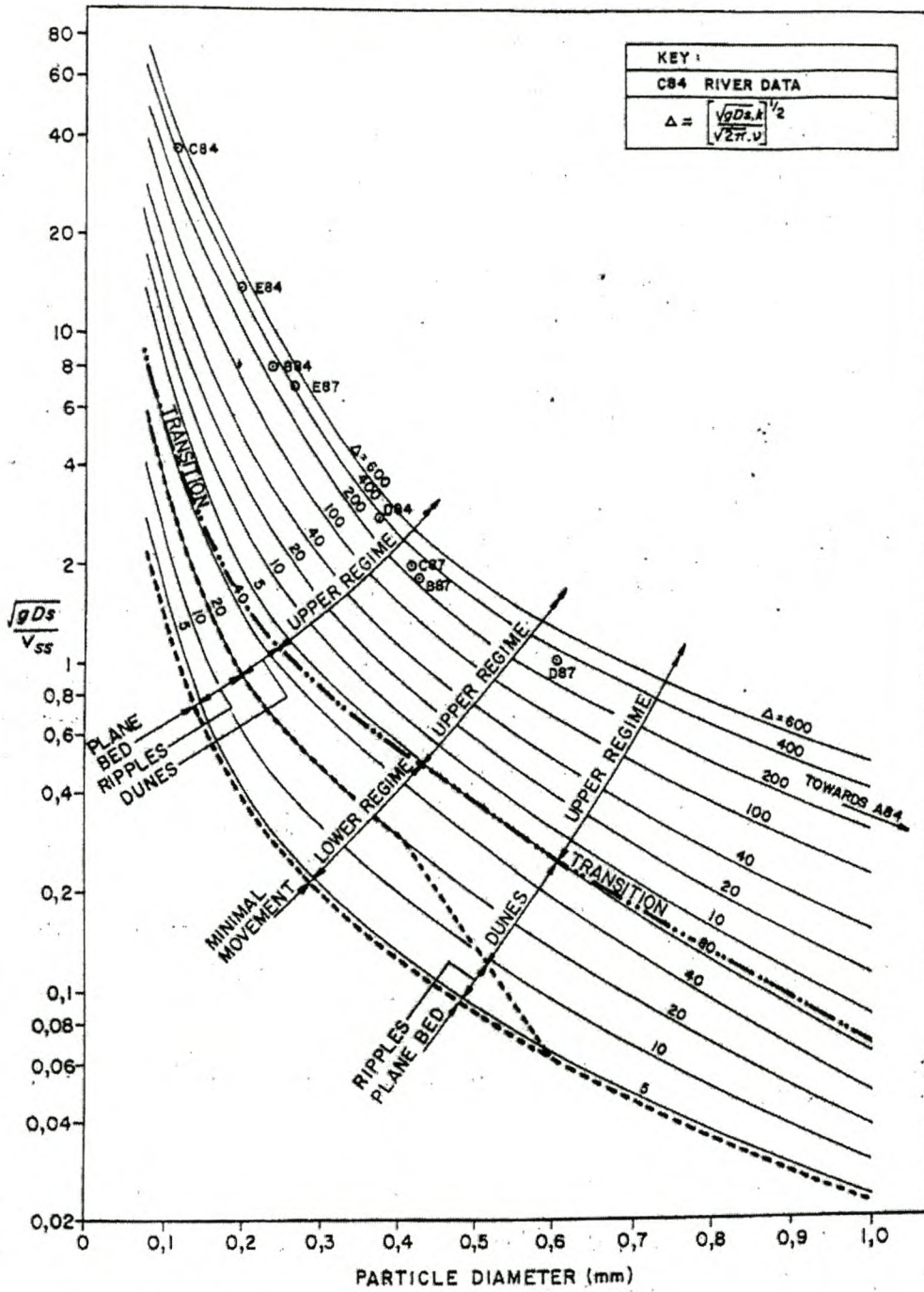


Figure 18: Resistance values and bedforms. (Rooseboom and Le Grange 2000)

## 6 REFERENCES

Ackers, P., W.R. White, J.A. Perkins and A.J.M. Harrison. *Weirs and Flumes for Flow Measurement*. New York: John Wiley and Sons, 1978.

Issam A. Al-Khatib, "Head-Discharge Relationship in Flumes of Compound Sections," *Journal of Irrigation and Drainage Engineering* 124, no. 3 (1998) : 177-179.

Wubbo Boiten and Remmet H. Pitlo, "The V-Shaped Broad-Crested Weir," *Journal of the Irrigation and Drainage Division Proceedings ASCE* 108, no. 2 (1982) : 142-160.

Bos, M.G. *Discharge Measurement Structures*. Wageningen: International Institute for Land Reclamation and Improvement/ILRI, 1<sup>st</sup> ed.1976; 2<sup>d</sup> ed. 1978; 3<sup>rd</sup> Revised ed. 1989.

Bos, M.G., J.A. Replogle and A.J. Clemmens. *Flow Measuring Flumes for Open Channel Systems*. New York: John Wiley and Sons, 1984.

British Standards Institution, BS3680: Part 4: 1981 *Methods for Measurement of Liquid Flow in Open Channels*

Chadwick, A. and J. Morfett. *Hydraulics in Civil and Environmental Engineering*. London: E & FN Spon, 1998.

Clark, D. *Plane and Geodetic Surveying*. London: Constable and Company Ltd, 1957.

J. Clemmens and M. G. Bos, "Critical Depth Relations for Flow Measuring Design," *Journal of Irrigation and Drainage Engineering* 118, no. 4 (1992) : 640-644.

Featherstone, R.E. and C. Nalluri. *Civil Engineering Hydraulics*. Oxford: Blackwell Science Ltd, 1995.

Vito Ferro, "Friction Factor for Gravel-bed Channel with high Boulder Concentration," *Journal of Hydraulic Engineering* 125, no. 7 (1999) : 771-778.

Vito Ferro, "Flow Measurement with Rectangular Free Overfall," *Journal of Irrigation and Drainage Engineering* 118, no. 6 (1992) : 956-964.

Mustafa Gögüş and Dogan Altmbilek, "Flow Measurement Structures of Compound Cross Section for Rivers," *Journal of Irrigation and Drainage Engineering* 120, no. 1 (1994) : 110-127.

Mustafa Gögüş and Issam A. Al-Khatib, "Flow Measurement Flumes of Rectangular Compound Cross Section," *Journal of Irrigation and Drainage Engineering* 121, no. 2 (1993) : 135-142.

Grover, N.C. and A.W. Harrington. *Stream Flow*. New York: John Wiley and Sons, 1949.

W.H. Hager, "Venturi Flume of Minimum Space Requirements," *Journal of Irrigation and Drainage Engineering* 114, no. 2 (1988) : 226-243.

Willi H. Hager, "Hydraulics of plane free overfall," *Journal of Hydraulic Engineering* 109, no.12 (1983) : 1683-1697.

W. Hager, "Modified, Trapezoidal Venturi Channel," *Journal of Irrigation and Drainage Engineering* 112, no. 3 (1986) : 225-241.

W.H. Hager, "Modified Venturi Channel," *Journal of Irrigation and Drainage Engineering* 111, no. 1 (1985) : 19-35.

Henderson, F.M. *Open Channel Flow*. New York: Macmillan Company, 1966.

Institute for Water and Environmental Engineering in association with the South African National Committee on Large Dams. 2002. *Design and Rehabilitation of Dams*. University of Stellenbosch, Stellenbosch.

International Association for Hydraulic Research. *Hydraulic Structures Design Manual: Discharge Characteristics*. Rotterdam: A.A. Balkema, 1994.

Robert D. Jarrett, "Hydraulics of High-Gradient Streams," *Journal of Hydraulic Engineering* 110, no. 11 (1984) : 1519-1539.

Jonker, V., A. Rooseboom and A.H.M. Görgens. *Environmentally Significant Morphological and Hydraulic Characteristics of Cobble and Boulder Bed Rivers in the Western Cape*. Pretoria: Water Research Commission, 2002.

Le Grange, A. Du P. *Techniques for Predicting the Deformation and Hydraulic Resistance of Sand-bed Flow Channels*. Dissertation, 1994. University of Stellenbosch.

Lotriet, H.H. 1996. *River Discharge Measurement at South African Compound Weirs in Rivers with High Sediment Loads: The Development of an Improved Method for Measurement*. Ph.D. diss., Department of Civil Engineering, University of Stellenbosch, Stellenbosch.

Lotriet, H.H. and A. Rooseboom. *River Discharge Measurement in South African Rivers: The Development of Improved Measuring Techniques*. Pretoria: Water Research Commission, 1995.

Malan, J.G. 2002. *Flow resistance of large-scale roughness in mountain rivers of the Western Cape*. MscIng Thesis, Department of Civil Engineering, University of Stellenbosch, Stellenbosch.

- Malan, J.G. and J.W. van Huyssteen. 1999. *Vloeiemeting deur middel van Natuurlike Kontroles*. B.Sc. Eng final year essay, Department of Civil Engineering, University of Stellenbosch, Stellenbosch.
- Rooseboom *et al.* 1984. *National Transport Commission: Road Drainage Manual*. 1<sup>st</sup> ed. Pretoria: National Transport Commission. Directorate Land Transport.
- Rooseboom, A. 2001. *Class notes for Advanced Hydraulics MT06*. Stellenbosch : University of Stellenbosch.
- Rooseboom, A. *Open Channel Fluid Mechanics*. Pretoria: Department of Environment Affairs, 1974.
- Rooseboom, A. and A duP Le Grange. "The Hydraulic Resistance of Sand Stream Beds under Steady Flow Conditions," *Journal of Hydraulic Research* 38, no. 1 (2000) : 27-35.
- Rowntree, K.M. and R.A. Wadson. 1999. *A Hierarchical Geomorphological Model for the Classification of Selected South African Rivers*. Report no. 497/1/99, Water Research Commission, Pretoria.
- M. B. Rubin, "Relationship of Critical Flow in Waterfall to Minimum Energy Head," *Journal of Hydraulic Engineering* 123, no. 1 (1997) : 82-84.
- Z. Samani, S. Jorat and M. Yousaf, "Hydraulic Characteristics of Circular Flume," *Journal of Irrigation and Drainage Engineering* 117, no. 4 (1991) : 558-566.
- Z. Samani and H. Magallanez, "Measuring Water in Trapezoidal Canals," *Journal of Irrigation and Drainage Engineering* 119, no. 1 (1993) : 181-186.
- Z. Samani and H. Magallanez, "Simple Flume for Flow Measurement in Open Channel," *Journal of Irrigation and Drainage Engineering* 126, no. 2 (2000) : 127-129.
- South African Department of Transport. Directorate: Roads. 1997. *Road Drainage Manual*. Pretoria.
- United States Department of the Interior, United States Geological Survey. Geological Survey Water-Supply Paper 2175. 1982. *Measurement and Computation of Streamflow*. Washington, D.C.: Government Printing Office.
- Vicente L. Lopes and Edward D. Shirley, "Computation of Flow Transitions in Open Channels with Steady Uniform Lateral Inflow," *Journal of Irrigation and Drainage Engineering* 119, no. 1 (1993) : 187-200.
- Ven Te Chow. *Open-Channel Hydraulics*. New York: McGraw-Hill Book Company Inc., 1959.
- Webber, N.B. *Fluid Mechanics for Civil Engineers*. London: Chapman and Hall, 1971.

Wessels, P. 1996. The Calibration of Compound Crump and Sharp-Crested Gauging Weirs in South Africa. Ph.D. diss., Department of Civil Engineering, University of Stellenbosch, Stellenbosch.

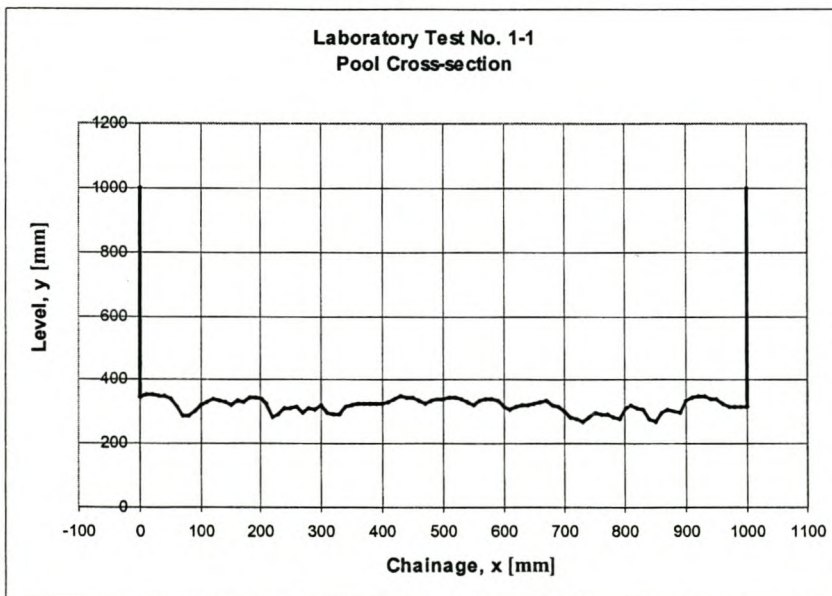
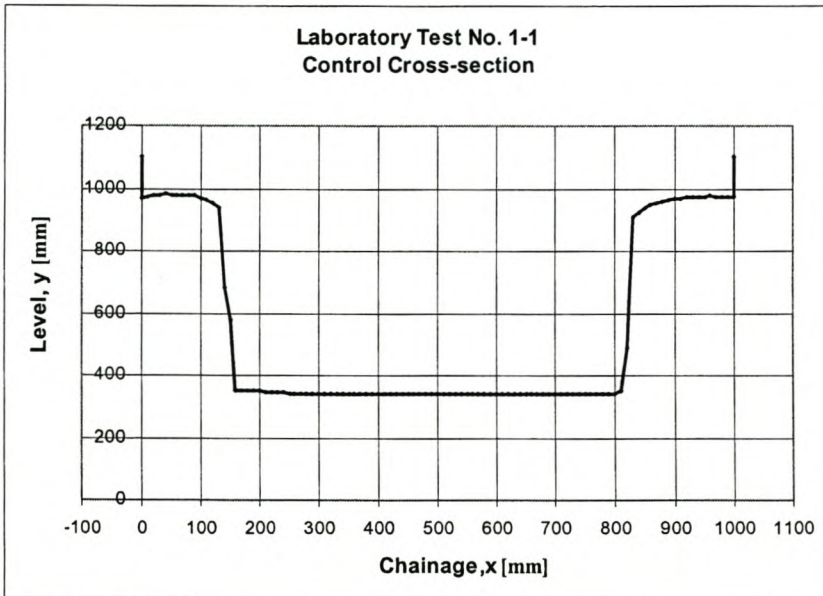
## **APPENDIX B**

### **Raw Data from Laboratory Tests**

**Laboratory Test No. 1-1**  
**Constriction with Vertical Sides:  $B/b = 1.5$**   
**26 Augustus 2002**  
**Waterlevels**

$H_{V\text{-notch}}$ [mm]	$H_3$ [mm]	$H_2$ [mm]	$H_{\text{control}}$ [mm]
1032	441	440	423
1099	486	484	463
1146	524	523	499
1187	556	555	529
1222	585	584	557
1245	605	602	574

Min. Control Level	340 mm
Min. Pool Level	270 mm
Min. V-notch Level	806 mm





**Laboratory Test No. 1-1**  
**26 Augustus 2002**  
**Cross-sections**

<b>CONTROL</b>		(Levels are in mm)	
<b>Chainage</b>	<b>Level</b>	<b>Chainage</b>	<b>Level</b>
0	1100	510	340
0	970	520	340
10	975	530	340
20	977	540	340
30	979	550	340
40	982	560	340
50	980	570	340
60	980	580	340
70	980	590	340
80	980	600	340
90	976	610	340
100	970	620	340
110	962	630	340
120	955	640	340
130	937	650	340
140	680	660	340
150	580	670	340
160	353	680	340
170	353	690	340
180	353	700	340
190	350	710	340
200	350	720	340
210	348	730	340
220	348	740	340
230	347	750	340
240	347	760	340
250	343	770	340
260	343	780	340
270	341	790	340
280	340	800	340
290	340	810	350
300	340	820	490
310	340	830	910
320	340	840	925
330	340	850	938
340	340	860	946
350	340	870	952
360	340	880	960
370	340	890	963
380	340	900	966
390	340	910	970
400	340	920	972
410	340	930	973
420	340	940	974
430	340	950	975
440	340	960	976
450	340	970	974
460	340	980	974
470	340	990	974
480	340	1000	974
490	340	1000	1100
500	340		

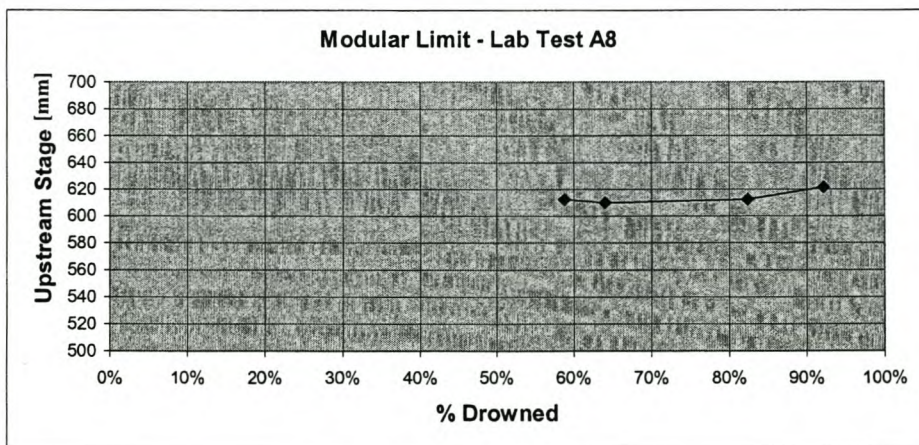
<b>POOL</b>		(Levels are in mm)	
<b>Chainage</b>	<b>Level</b>	<b>Chainage</b>	<b>Level</b>
0	1000	510	343
0	345	520	342
10	355	530	340
20	352	540	328
30	350	550	320
40	350	560	333
50	340	570	340
60	315	580	339
70	286	590	336
80	285	600	315
90	300	610	308
100	320	620	316
110	330	630	321
120	338	640	322
130	335	650	326
140	332	660	329
150	320	670	335
160	333	680	319
170	330	690	315
180	345	700	300
190	342	710	280
200	341	720	277
210	325	730	270
220	280	740	283
230	290	750	295
240	310	760	294
250	310	770	290
260	315	780	283
270	295	790	279
280	310	800	311
290	305	810	320
300	320	820	309
310	295	830	306
320	293	840	278
330	290	850	270
340	316	860	297
350	322	870	305
360	323	880	301
370	326	890	298
380	325	900	336
390	325	910	345
400	327	920	348
410	330	930	350
420	341	940	341
430	348	950	339
440	345	960	325
450	342	970	316
460	335	980	316
470	327	990	316
480	337	1000	316
490	340	1000	1000
500	341		

Laboratory Test No. 1-1  
 26 Augustus 2002  
 Modular Limit

H <sub>upstream</sub>	H <sub>downstream</sub>	%Drowned
612	500	58.8%
610	513	64.1%
612	564	82.4%
621	599	92.2%

Min. Control Level	340
--------------------	-----

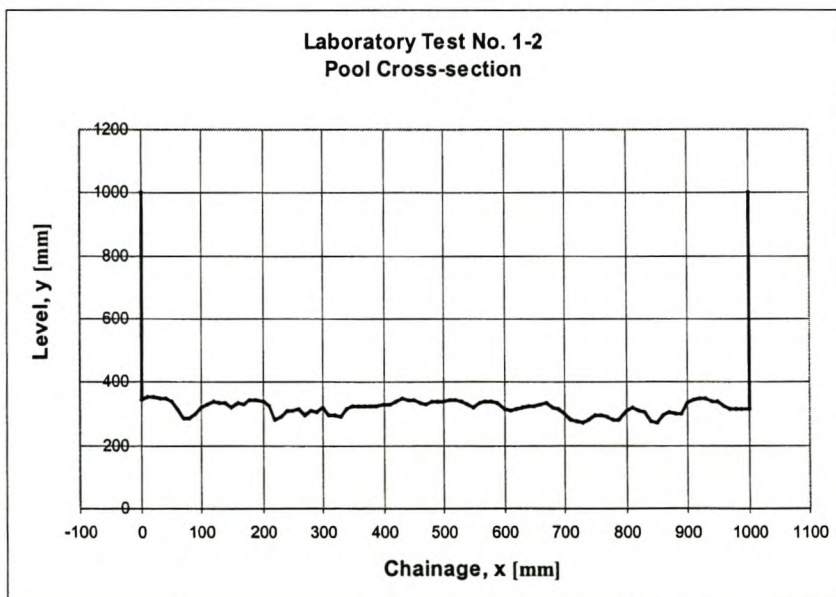
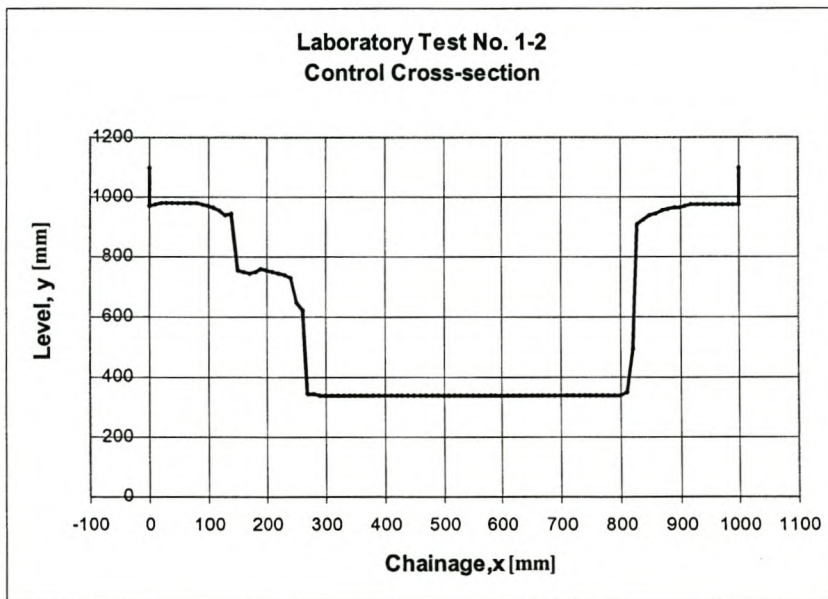
**Modular Limit = 82%**



**Laboratory Test No. 1-2**  
**Constriction with Vertical Sides: B/b = 1.8**  
**29 Augustus 2002**  
**Waterlevels**

H <sub>V-notch</sub> [mm]	H <sub>3</sub> [mm]	H <sub>2</sub> [mm]	H <sub>control</sub> [mm]
924	383	382	374
960	404	404	393
984	418	418	403
1004	433.5	433	416
1029	450	449	432
1096	503	502	481
1146	547	546	520
1188	586	585	556
1223	621	620	587
1245	643	642	610
1273	681	680	648

Min. Control Level	340 mm
Min. Pool Level	270 mm
Min. V-notch Level	806 mm



**Laboratory Test No. 1-2**  
**29 Augustus 2002**  
**Cross-sections**

CONTROL		(Levels are in mm)	
Chainage	Level	Chainage	Level
0	1100	510	340
0	970	520	340
10	975	530	340
20	977	540	340
30	979	550	340
40	982	560	340
50	980	570	340
60	980	580	340
70	980	590	340
80	980	600	340
90	976	610	340
100	970	620	340
110	962	630	340
120	955	640	340
130	937	650	340
140	944	660	340
150	756	670	340
160	750	680	340
170	742	690	340
180	750	700	340
190	761	710	340
200	752	720	340
210	750	730	340
220	746	740	340
230	738	750	340
240	726	760	340
250	647	770	340
260	623	780	340
270	344	790	340
280	342	800	340
290	340	810	350
300	340	820	490
310	340	830	910
320	340	840	925
330	340	850	938
340	340	860	946
350	340	870	952
360	340	880	960
370	340	890	963
380	340	900	966
390	340	910	970
400	340	920	972
410	340	930	973
420	340	940	974
430	340	950	975
440	340	960	976
450	340	970	974
460	340	980	974
470	340	990	974
480	340	1000	974
490	340	1000	1100
500	340		

POOL		(Levels are in mm)	
Chainage	Level	Chainage	Level
0	1000	510	343
0	345	520	342
10	355	530	340
20	352	540	328
30	350	550	320
40	350	560	333
50	340	570	340
60	315	580	339
70	286	590	336
80	285	600	315
90	300	610	308
100	320	620	316
110	330	630	321
120	338	640	322
130	335	650	326
140	332	660	329
150	320	670	335
160	333	680	319
170	330	690	315
180	345	700	300
190	342	710	280
200	341	720	277
210	325	730	270
220	280	740	283
230	290	750	295
240	310	760	294
250	310	770	290
260	315	780	283
270	295	790	279
280	310	800	311
290	305	810	320
300	320	820	309
310	295	830	306
320	293	840	278
330	290	850	270
340	316	860	297
350	322	870	305
360	323	880	301
370	326	890	298
380	325	900	336
390	325	910	345
400	327	920	348
410	330	930	350
420	341	940	341
430	348	950	339
440	345	960	325
450	342	970	316
460	335	980	316
470	327	990	316
480	337	1000	316
490	340	1000	1000
500	341		

**Laboratory Test No. 1-2**  
**29 Augustus 2002**  
**Modular Limit**

<b>H<sub>upstream</sub></b>	<b>H<sub>downstream</sub></b>	<b>%Drowned</b>
685	622	81.7%

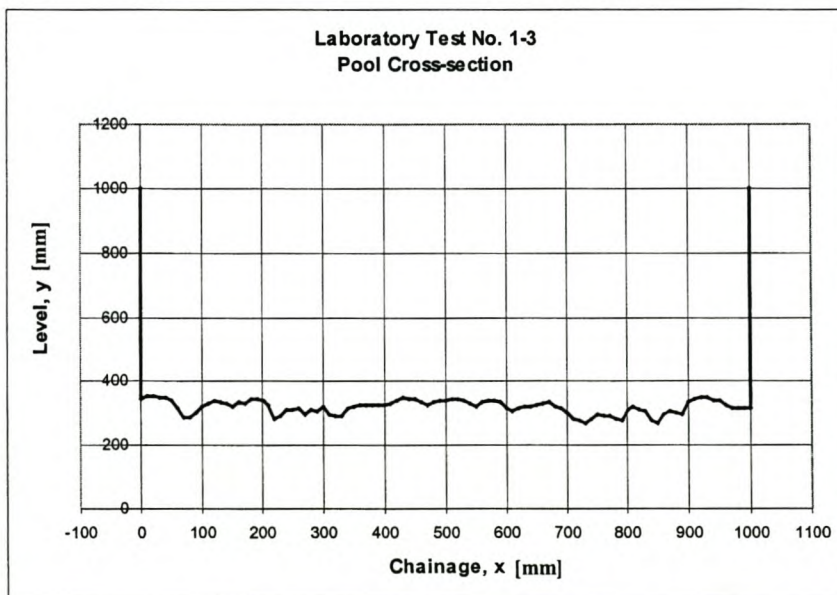
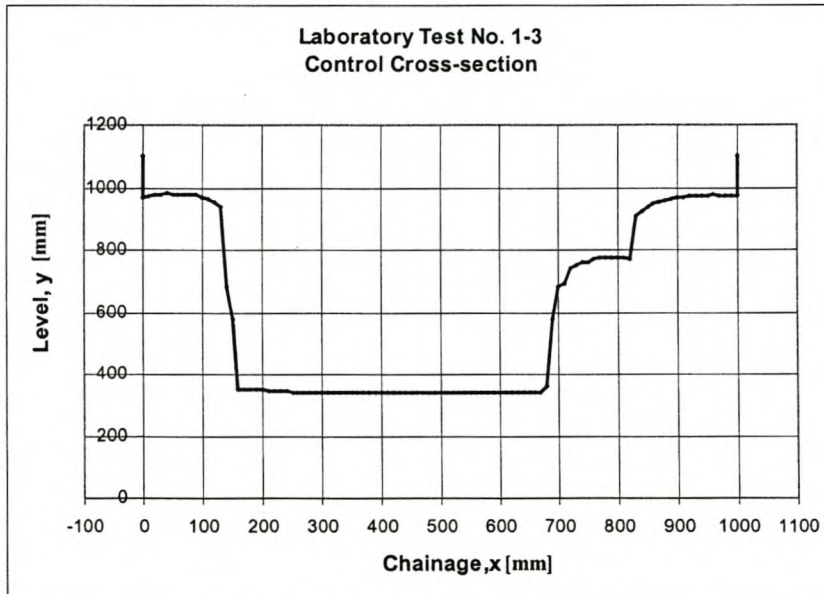
Min. Control Level	340
--------------------	-----

<b>Modular Limit =</b>	<b>82%</b>
------------------------	------------

**Laboratory Test No. 1-3**  
**Constriction with Vertical Sides:  $B/b = 2.3$**   
**18 September 2002**  
**Waterlevels**

$H_{V\text{-notch}}$ [mm]	$H_3$ [mm]	$H_2$ [mm]	$H_{\text{control}}$ [mm]
921	388	388	381
956	412	411	399
990	439	439	424
1015	460	460	441
1042	485	484	464
1075	514	513	490
1009	538	538	513
1124	564	563	536
1146	587	586	555
1166	610	610	577
1187	634	633	598
1222	675	674	641
1246	704	703	664

Min. Control Level	340 mm
Min. Pool Level	270 mm
Min. V-notch Level	806 mm



**Laboratory Test No. 1-3****16 September 2002****Cross-sections**

<b>CONTROL</b>		(Levels are in mm)	
<b>Chainage</b>	<b>Level</b>	<b>Chainage</b>	<b>Level</b>
0	1100	510	340
0	970	520	340
10	975	530	340
20	977	540	340
30	979	550	340
40	982	560	340
50	980	570	340
60	980	580	340
70	980	590	340
80	980	600	340
90	976	610	340
100	970	620	340
110	962	630	340
120	955	640	340
130	937	650	340
140	680	660	340
150	580	670	340
160	353	680	362
170	353	690	576
180	353	700	681
190	350	710	692
200	350	720	740
210	348	730	752
220	348	740	759
230	347	750	762
240	347	760	772
250	343	770	776
260	343	780	777
270	341	790	776
280	340	800	774
290	340	810	775
300	340	820	772
310	340	830	908
320	340	840	925
330	340	850	938
340	340	860	946
350	340	870	952
360	340	880	960
370	340	890	963
380	340	900	966
390	340	910	970
400	340	920	972
410	340	930	973
420	340	940	974
430	340	950	975
440	340	960	976
450	340	970	974
460	340	980	974
470	340	990	974
480	340	1000	974
490	340	1000	1100
500	340		

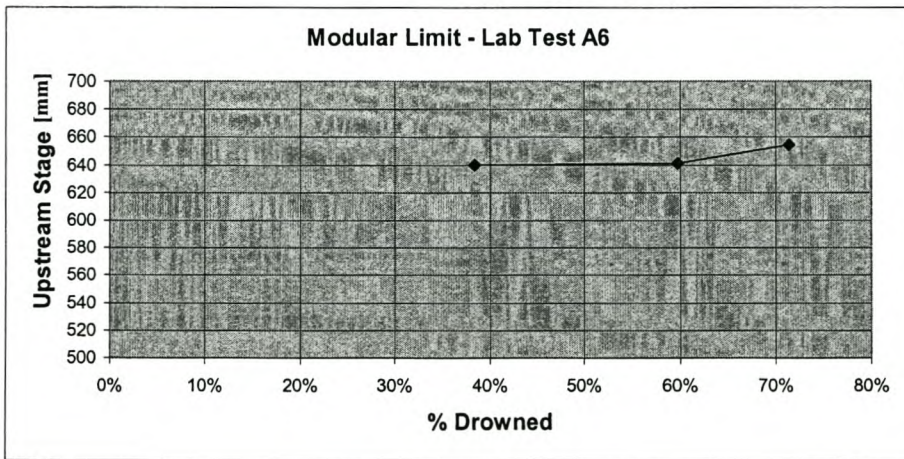
<b>POOL</b>		(Levels are in mm)	
<b>Chainage</b>	<b>Level</b>	<b>Chainage</b>	<b>Level</b>
0	1000	510	343
0	345	520	342
10	355	530	340
20	352	540	328
30	350	550	320
40	350	560	333
50	340	570	340
60	315	580	339
70	286	590	336
80	285	600	315
90	300	610	308
100	320	620	316
110	330	630	321
120	338	640	322
130	335	650	326
140	332	660	329
150	320	670	335
160	333	680	319
170	330	690	315
180	345	700	300
190	342	710	280
200	341	720	277
210	325	730	270
220	280	740	283
230	290	750	295
240	310	760	294
250	310	770	290
260	315	780	283
270	295	790	279
280	310	800	311
290	305	810	320
300	320	820	309
310	295	830	306
320	293	840	278
330	290	850	270
340	316	860	297
350	322	870	305
360	323	880	301
370	326	890	298
380	325	900	336
390	325	910	345
400	327	920	348
410	330	930	350
420	341	940	341
430	348	950	339
440	345	960	325
450	342	970	316
460	335	980	316
470	327	990	316
480	337	1000	316
490	340	1000	1000
500	341		

18 September 2002  
 Modular Limit

H <sub>upstream</sub>	H <sub>downstream</sub>	%Drowned
640	455	38.3%
641	520	59.8%
654	564	71.3%

Min. Control Level	340
--------------------	-----

**Modular Limit = 60%**

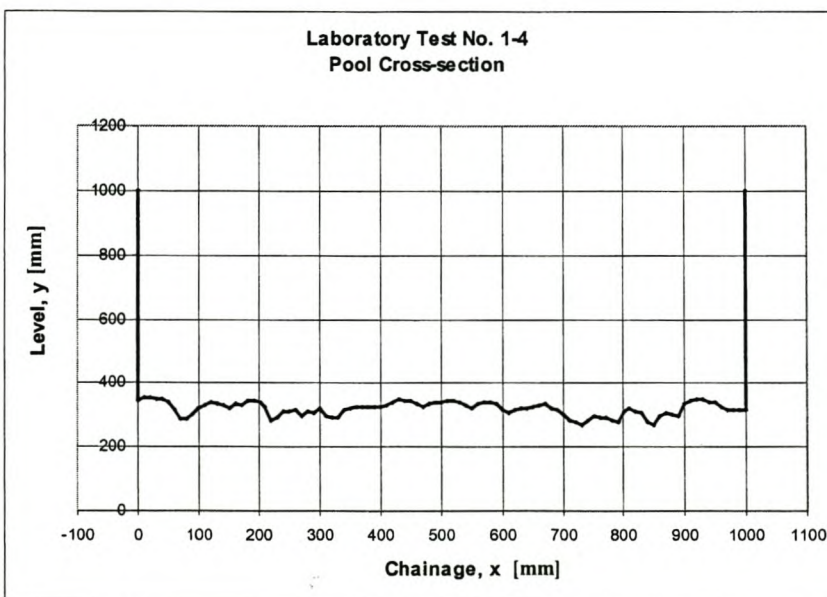
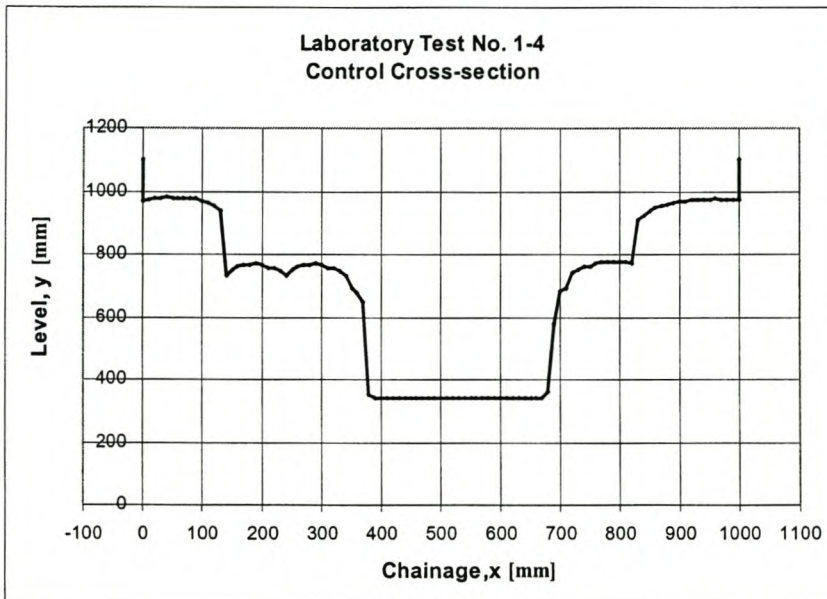




**Laboratory Test No. 1-4**  
**Constriction with Vertical Sides:  $B/b = 3.2$**   
**24 September 2002**  
**Waterlevels**

$H_{V\text{-notch}}$ [mm]	$H_3$ [mm]	$H_2$ [mm]	$H_{\text{control}}$ [mm]
923	404	403	390
991	518	518	487
1047	459	459	435
1101	578	578	543
1146	630	629	590
1186	678	678	642
1229	738	739	702

Min. Control Level	340 mm
Min. Pool Level	270 mm
V-notch height	806 mm



**Laboratory Test No. 1-4**  
**24 September 2002**  
**Cross-sections**

<b>CONTROL</b>		(Levels are in mm)	
<b>Chainage</b>	<b>Level</b>	<b>Chainage</b>	<b>Level</b>
0	1100	510	340
0	970	520	340
10	975	530	340
20	977	540	340
30	979	550	340
40	982	560	340
50	980	570	340
60	980	580	340
70	980	590	340
80	980	600	340
90	976	610	340
100	970	620	340
110	962	630	340
120	955	640	340
130	937	650	340
140	729	660	340
150	750	670	340
160	759	680	362
170	763	690	576
180	766	700	681
190	768	710	692
200	767	720	740
210	758	730	752
220	754	740	759
230	744	750	762
240	729	760	772
250	750	770	776
260	759	780	777
270	763	790	776
280	766	800	774
290	768	810	775
300	767	820	772
310	758	830	908
320	754	840	925
330	744	850	938
340	730	860	946
350	692	870	952
360	676	880	960
370	645	890	963
380	352	900	966
390	343	910	970
400	340	920	972
410	340	930	973
420	340	940	974
430	340	950	975
440	340	960	976
450	340	970	974
460	340	980	974
470	340	990	974
480	340	1000	974
490	340	1000	1100
500	340		

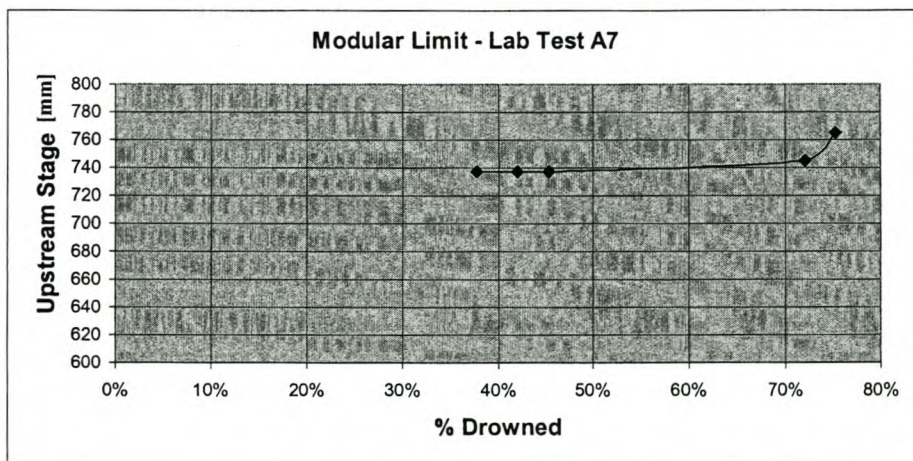
<b>POOL</b>		(Levels are in mm)	
<b>Chainage</b>	<b>Level</b>	<b>Chainage</b>	<b>Level</b>
0	1000	510	343
0	345	520	342
10	355	530	340
20	352	540	328
30	350	550	320
40	350	560	333
50	340	570	340
60	315	580	339
70	286	590	336
80	285	600	315
90	300	610	308
100	320	620	316
110	330	630	321
120	338	640	322
130	335	650	326
140	332	660	329
150	320	670	335
160	333	680	319
170	330	690	315
180	345	700	300
190	342	710	280
200	341	720	277
210	325	730	270
220	280	740	283
230	290	750	295
240	310	760	294
250	310	770	290
260	315	780	283
270	295	790	279
280	310	800	311
290	305	810	320
300	320	820	309
310	295	830	306
320	293	840	278
330	290	850	270
340	316	860	297
350	322	870	305
360	323	880	301
370	326	890	298
380	325	900	336
390	325	910	345
400	327	920	348
410	330	930	350
420	341	940	341
430	348	950	339
440	345	960	325
450	342	970	316
460	335	980	316
470	327	990	316
480	337	1000	316
490	340	1000	1000
500	341		

**Laboratory Test No. 1-4**  
**24 September 2002**  
**Modular Limit**

H <sub>upstream</sub>	H <sub>downstream</sub>	%Drowned
737	490	37.8%
737	507	42.1%
737	520	45.3%
745	632	72.1%
765	660	75.3%

Min. Control Level	340
--------------------	-----

**Modular Limit = 45%**



**Laboratory Test No. 2-1**

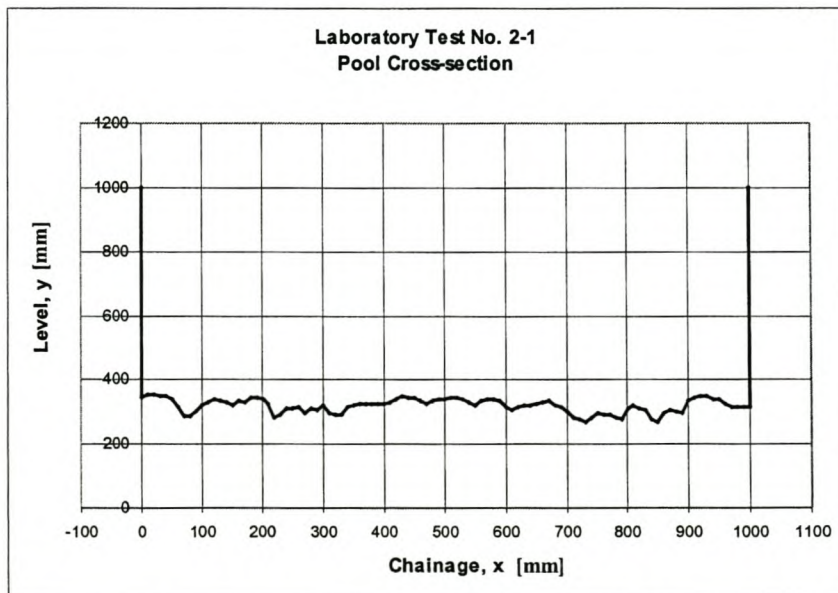
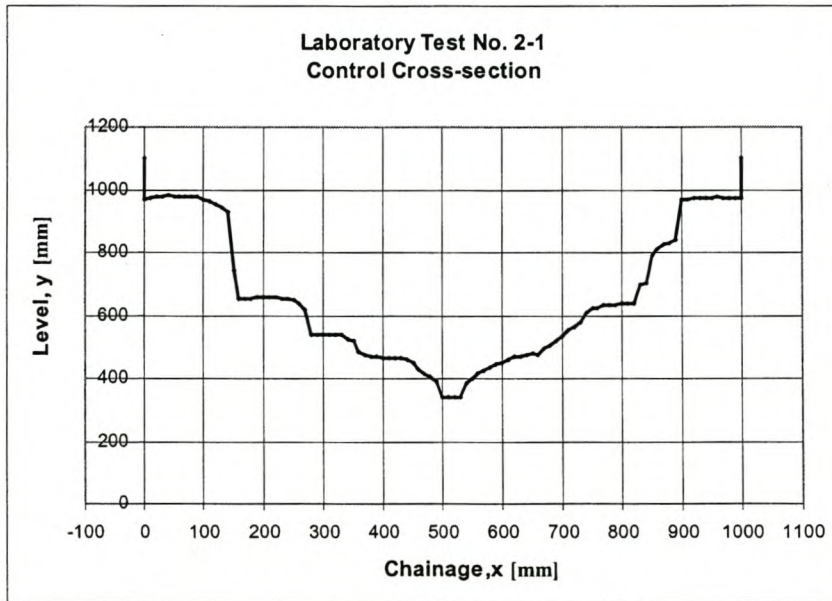
**Constriction with Sloped Sides: Slope = 53°**

**8 Oktober 2002**

**Waterlevels**

H <sub>V-notch</sub> [mm]	H <sub>3</sub> [mm]	H <sub>2</sub> [mm]	H <sub>control</sub> [mm]
922	483	483	466
957	512	512	492
1009	554	554	530
1067	604	603	570
1166	691	691	645
1200	724	723	680
1117	651	651	614
1096	631	630	594

Min. Control Level	340 mm
Min. Pool Level	270 mm
V-notch height	806 mm



**Laboratory Test No. 2-1**  
**8 Oktober 2002**  
**Cross-sections**

CONTROL		(Levels are in mm)	
Chainage	Level	Chainage	Level
0	1100	510	341
0	970	520	340
10	975	530	343
20	977	540	386
30	979	550	402
40	982	560	416
50	980	570	424
60	980	580	433
70	980	590	446
80	980	600	451
90	976	610	460
100	970	620	467
110	962	630	470
120	955	640	475
130	942	650	478
140	927	660	476
150	740	670	494
160	652	680	504
170	653	690	520
180	652	700	535
190	655	710	555
200	657	720	563
210	658	730	579
220	656	740	607
230	653	750	620
240	650	760	623
250	645	770	630
260	635	780	632
270	619	790	633
280	539	800	636
290	537	810	636
300	537	820	637
310	539	830	695
320	536	840	703
330	536	850	788
340	525	860	810
350	517	870	825
360	484	880	830
370	474	890	840
380	471	900	966
390	469	910	970
400	465	920	972
410	464	930	973
420	462	940	974
430	462	950	975
440	459	960	976
450	451	970	974
460	430	980	974
470	413	990	974
480	404	1000	974
490	388	1000	1100
500	340		

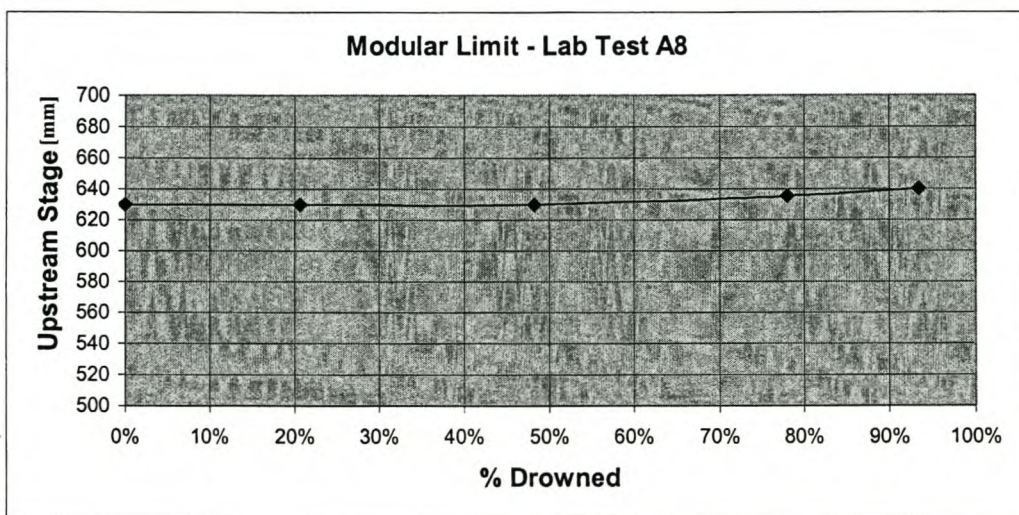
POOL		(Levels are in mm)	
Chainage	Level	Chainage	Level
0	1000	510	343
0	345	520	342
10	355	530	340
20	352	540	328
30	350	550	320
40	350	560	333
50	340	570	340
60	315	580	339
70	286	590	336
80	285	600	315
90	300	610	308
100	320	620	316
110	330	630	321
120	338	640	322
130	335	650	326
140	332	660	329
150	320	670	335
160	333	680	319
170	330	690	315
180	345	700	300
190	342	710	280
200	341	720	277
210	325	730	270
220	280	740	283
230	290	750	295
240	310	760	294
250	310	770	290
260	315	780	283
270	295	790	279
280	310	800	311
290	305	810	320
300	320	820	309
310	295	830	306
320	293	840	278
330	290	850	270
340	316	860	297
350	322	870	305
360	323	880	301
370	326	890	298
380	325	900	336
390	325	910	345
400	327	920	348
410	330	930	350
420	341	940	341
430	348	950	339
440	345	960	325
450	342	970	316
460	335	980	316
470	327	990	316
480	337	1000	316
490	340	1000	1000
500	341		

**Laboratory Test No. 2-1**  
**8 Oktober 2002**  
**Modular Limit**

H <sub>upstream</sub>	H <sub>downstream</sub>	%Drowned
630	340	0.0%
630	400	20.7%
630	480	48.3%
635	570	78.0%
640	620	93.3%

Min. Control Level	340
--------------------	-----

**Modular Limit = 48%**



**Laboratory Test No. 2-2**

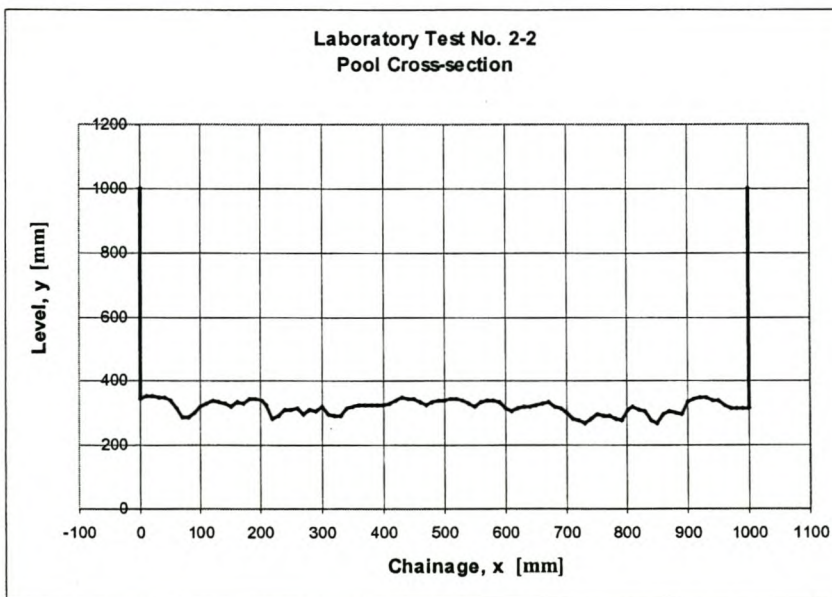
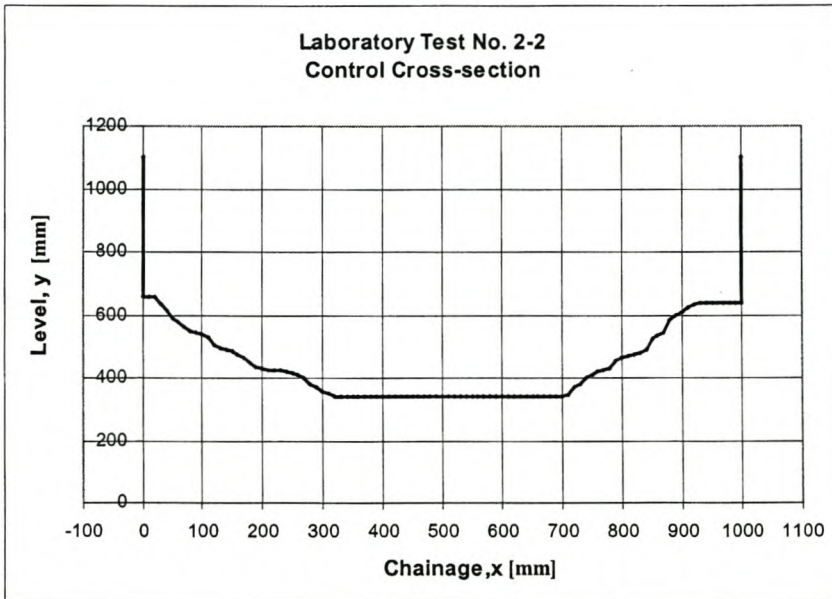
**Constriction with Sloped Sides: Slope = 45°**

**15 Oktober 2002**

**Waterlevels**

H <sub>V-notch</sub> [mm]	H <sub>3</sub> [mm]	H <sub>2</sub> [mm]	H <sub>control</sub> [mm]
925	392	391	383
959	415	415	402
1006	449	449	434
1060	489	488	466
1106	522	521	496
1157	560	559	532
1215	601	600	567

Min. Control Level	340 mm
Min. Pool Level	270 mm
V-notch height	806 mm



## Laboratory Test No. 2-2

15 Oktober 2002

## Cross-sections

CONTROL		(Levels are in mm)	
Chainage	Level	Chainage	Level
0	1100	510	340
0	657	520	340
10	657	530	340
20	657	540	340
30	632	550	340
40	610	560	340
50	587	570	340
60	579	580	340
70	562	590	340
80	546	600	340
90	543	610	340
100	537	620	340
110	527	630	340
120	502	640	340
130	496	650	340
140	487	660	340
150	482	670	340
160	472	680	340
170	465	690	340
180	449	700	340
190	437	710	346
200	430	720	370
210	423	730	381
220	427	740	401
230	427	750	410
240	421	760	418
250	415	770	426
260	410	780	431
270	398	790	455
280	379	800	464
290	370	810	470
300	358	820	476
310	350	830	480
320	340	840	489
330	340	850	522
340	340	860	535
350	340	870	542
360	340	880	581
370	340	890	599
380	340	900	608
390	340	910	621
400	340	920	632
410	340	930	636
420	340	940	638
430	340	950	638
440	340	960	638
450	340	970	638
460	340	980	638
470	340	990	638
480	340	1000	638
490	340	1000	1100
500	340		

POOL		(Levels are in mm)	
Chainage	Level	Chainage	Level
0	1000	510	343
0	345	520	342
10	355	530	340
20	352	540	328
30	350	550	320
40	350	560	333
50	340	570	340
60	315	580	339
70	286	590	336
80	285	600	315
90	300	610	308
100	320	620	316
110	330	630	321
120	338	640	322
130	335	650	326
140	332	660	329
150	320	670	335
160	333	680	319
170	330	690	315
180	345	700	300
190	342	710	280
200	341	720	277
210	325	730	270
220	280	740	283
230	290	750	295
240	310	760	294
250	310	770	290
260	315	780	283
270	295	790	279
280	310	800	311
290	305	810	320
300	320	820	309
310	295	830	306
320	293	840	278
330	290	850	270
340	316	860	297
350	322	870	305
360	323	880	301
370	326	890	298
380	325	900	336
390	325	910	345
400	327	920	348
410	330	930	350
420	341	940	341
430	348	950	339
440	345	960	325
450	342	970	316
460	335	980	316
470	327	990	316
480	337	1000	316
490	340	1000	1000
500	341		

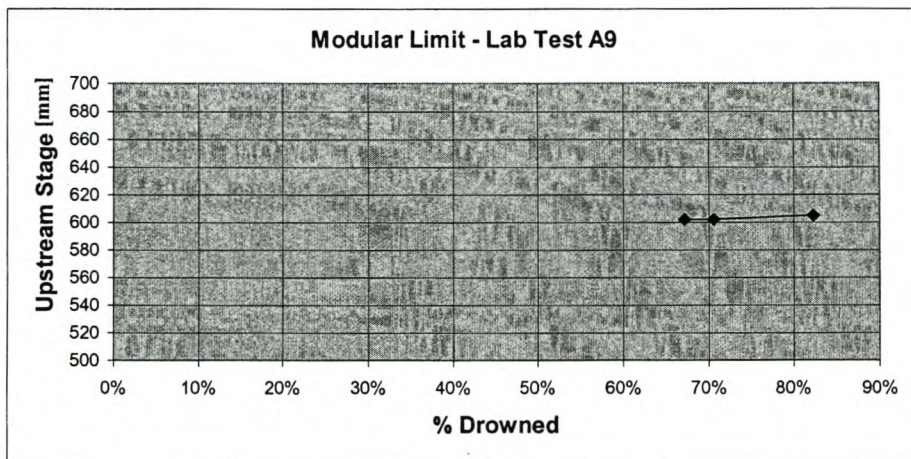


Laboratory Test No. 2-2  
 15 Oktober 2002  
 Modular Limit

H <sub>upstream</sub>	H <sub>downstream</sub>	%Drowned
602	516	67.2%
602	525	70.6%
605	558	82.3%

Min. Control Level	340
--------------------	-----

<b>Modular Limit = 71%</b>
----------------------------



**Laboratory Test No. 2-3**

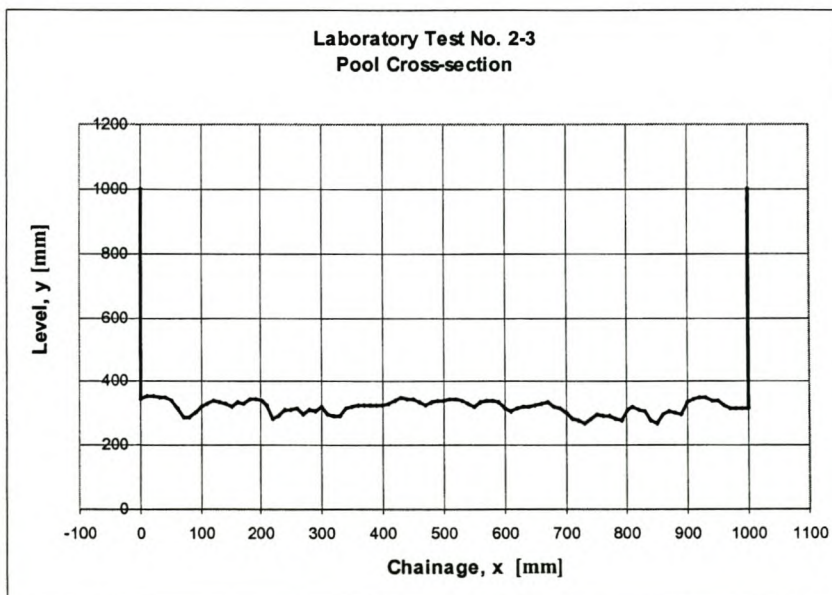
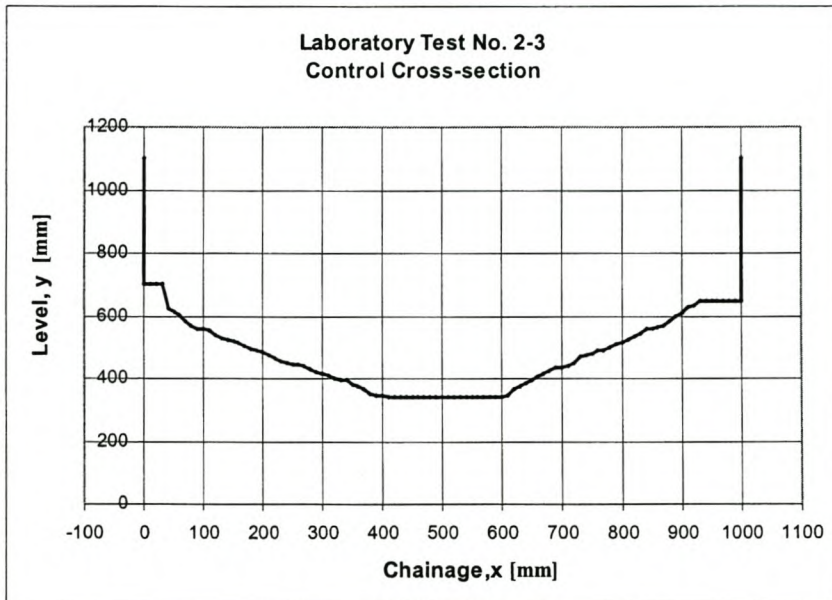
**Constriction with Sloped Sides: Slope = 38°**

**22 Oktober 2002**

**Waterlevels**

H <sub>V-notch</sub> [mm]	H <sub>3</sub> [mm]	H <sub>2</sub> [mm]	H <sub>control</sub> [mm]
923	408	408	396
962	440	440	425
1008	474	474	456
1060	516	515	490
1119	559	558	531
1164	590	590	558
1202	618	618	580

Min. Control Level	340 mm
Min. Pool Level	270 mm
V-notch height	806 mm



**Laboratory Test No. 2-3**  
**22 Oktober 2002**  
**Cross-sections**

<b>CONTROL</b>		(Levels are in mm)	
<b>Chainage</b>	<b>Level</b>	<b>Chainage</b>	<b>Level</b>
0	1100	510	340
0	700	520	340
10	700	530	340
20	700	540	340
30	700	550	340
40	620	560	340
50	610	570	340
60	601	580	340
70	584	590	340
80	570	600	340
90	560	610	345
100	559	620	365
110	553	630	375
120	540	640	384
130	526	650	394
140	522	660	407
150	520	670	413
160	512	680	426
170	506	690	434
180	496	700	436
190	490	710	441
200	482	720	447
210	473	730	468
220	465	740	475
230	455	750	481
240	451	760	487
250	445	770	491
260	444	780	500
270	438	790	508
280	432	800	516
290	419	810	525
300	414	820	532
310	409	830	542
320	402	840	556
330	396	850	560
340	393	860	565
350	382	870	569
360	375	880	585
370	364	890	596
380	350	900	609
390	345	910	625
400	345	920	633
410	340	930	649
420	340	940	649
430	340	950	649
440	340	960	649
450	340	970	649
460	340	980	649
470	340	990	649
480	340	1000	649
490	340	1000	1100
500	340		

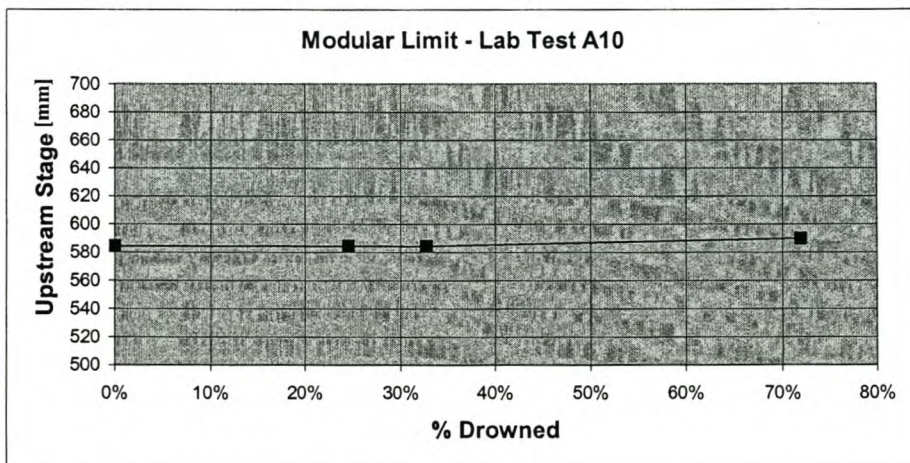
<b>POOL</b>		(Levels are in mm)	
<b>Chainage</b>	<b>Level</b>	<b>Chainage</b>	<b>Level</b>
0	1000	510	343
0	345	520	342
10	355	530	340
20	352	540	328
30	350	550	320
40	350	560	333
50	340	570	340
60	315	580	339
70	286	590	336
80	285	600	315
90	300	610	308
100	320	620	316
110	330	630	321
120	338	640	322
130	335	650	326
140	332	660	329
150	320	670	335
160	333	680	319
170	330	690	315
180	345	700	300
190	342	710	280
200	341	720	277
210	325	730	270
220	280	740	283
230	290	750	295
240	310	760	294
250	310	770	290
260	315	780	283
270	295	790	279
280	310	800	311
290	305	810	320
300	320	820	309
310	295	830	306
320	293	840	278
330	290	850	270
340	316	860	297
350	322	870	305
360	323	880	301
370	326	890	298
380	325	900	336
390	325	910	345
400	327	920	348
410	330	930	350
420	341	940	341
430	348	950	339
440	345	960	325
450	342	970	316
460	335	980	316
470	327	990	316
480	337	1000	316
490	340	1000	1000
500	341		

**Laboratory Test No. 2-3**  
**22 Oktober 2002**  
**Modular Limit**

H <sub>upstream</sub>	H <sub>downstream</sub>	%Drowned
584	340	0.0%
584	400	24.6%
584	420	32.8%
590	520	72.0%

Min. Control Level	340
--------------------	-----

**Modular Limit = 33%**



## **APPENDIX C**

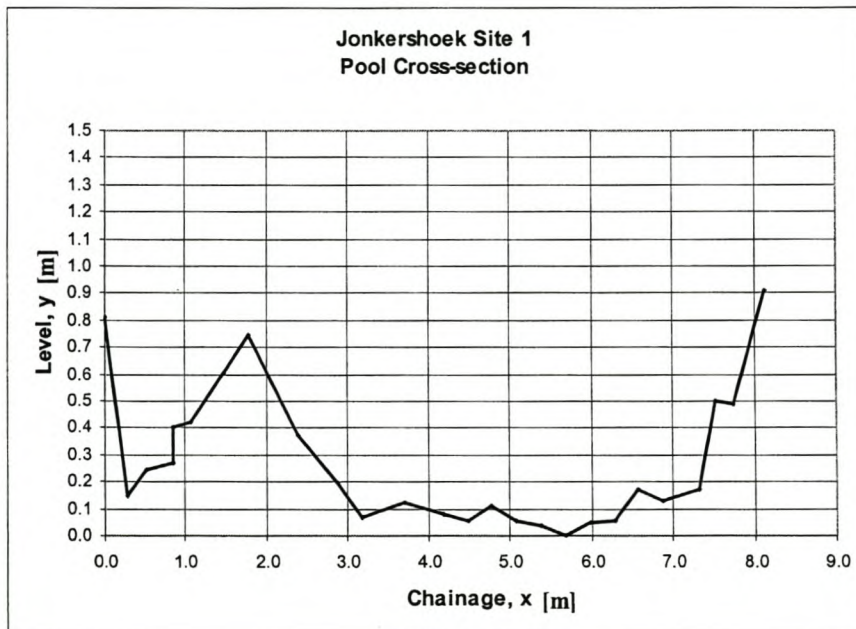
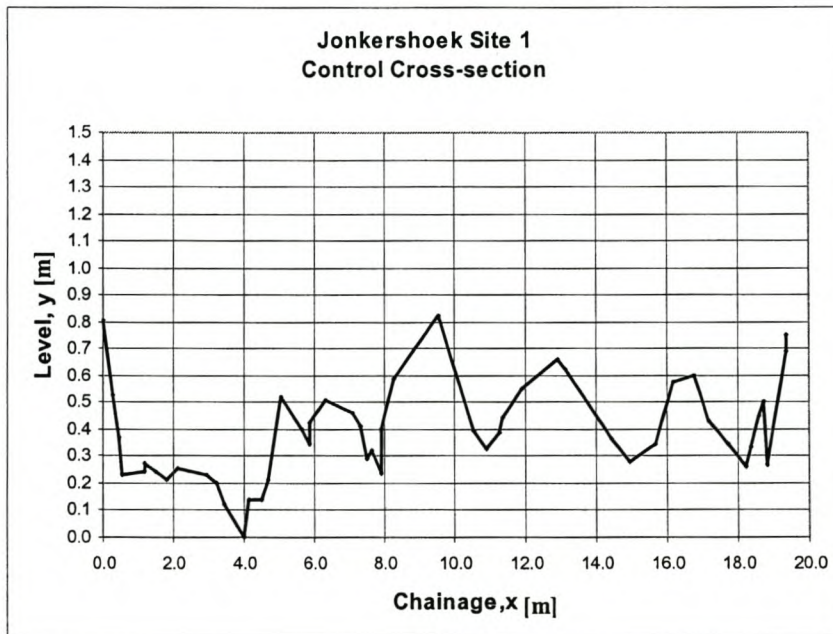
### **Raw Data from Fieldwork**

**Jonkershoek Site 1**

**Waterlevels**

Measurements in meters

Date	Waterlevel	Benchmark Level at Pool	Waterlevel above lowest point in Pool	Weir reading	Qweir
28/11/2002	1.401	0.811	0.320	0.039	0.092
12/10/2002	1.341	0.811	0.380	0.079	0.264
22/01/2002	1.309	0.790	0.391	0.070	0.220
25/10/2002	1.253	0.799	0.456	0.109	0.428
04/10/2002	1.247	0.811	0.474	0.133	0.577



## Jonkershoek Site 1

## Control Section

Chainage [m]	Level [m]	Level above lowest point
0.000	0.858	0.802
0.283	1.132	0.528
0.456	1.290	0.370
0.561	1.432	0.228
1.178	1.418	0.242
1.199	1.390	0.270
1.499	1.418	0.242
1.809	1.448	0.212
2.133	1.408	0.252
2.935	1.431	0.229
3.215	1.460	0.200
3.452	1.542	0.118
3.988	1.660	0.000
4.149	1.521	0.139
4.489	1.521	0.139
4.691	1.447	0.213
5.041	1.141	0.519
5.653	1.260	0.400
5.851	1.317	0.343
5.851	1.237	0.423
6.310	1.149	0.511
7.112	1.203	0.457
7.309	1.251	0.409
7.513	1.368	0.292
7.653	1.341	0.319
7.923	1.423	0.237
7.923	1.260	0.400
8.271	1.071	0.589
9.531	0.838	0.822
10.546	1.269	0.391
10.911	1.331	0.329
11.259	1.271	0.389
11.362	1.220	0.440
11.917	1.112	0.548
12.914	1.000	0.660
13.137	1.040	0.620
14.458	1.300	0.360
14.965	1.383	0.277
15.704	1.316	0.344
16.186	1.083	0.577
16.782	1.059	0.601
17.173	1.232	0.428
17.725	1.315	0.345
18.229	1.399	0.261
18.354	1.328	0.332
18.607	1.212	0.448
18.707	1.160	0.500
18.829	1.395	0.265
19.375	0.969	0.691
19.375	0.911	0.749

## Pool Section

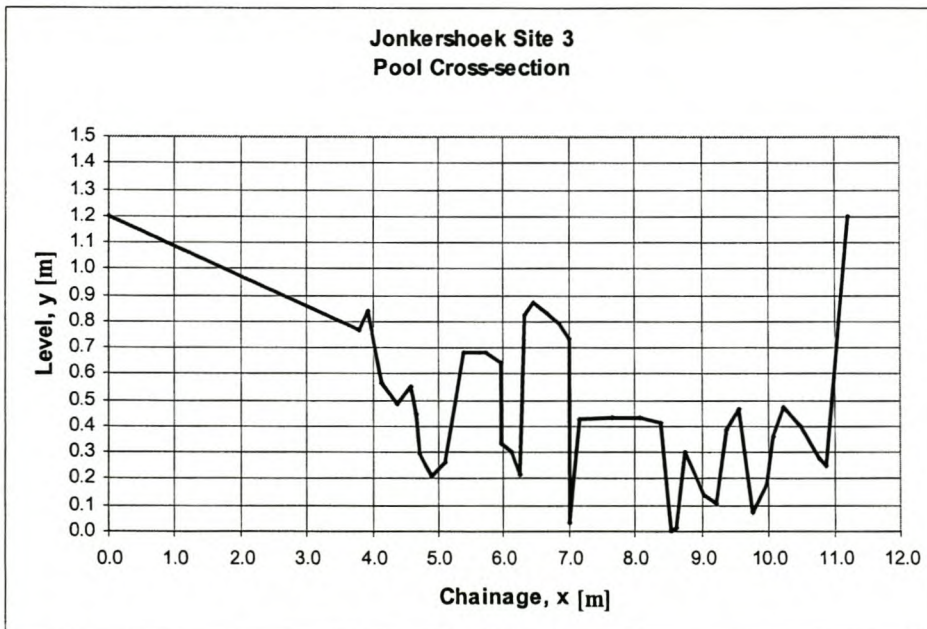
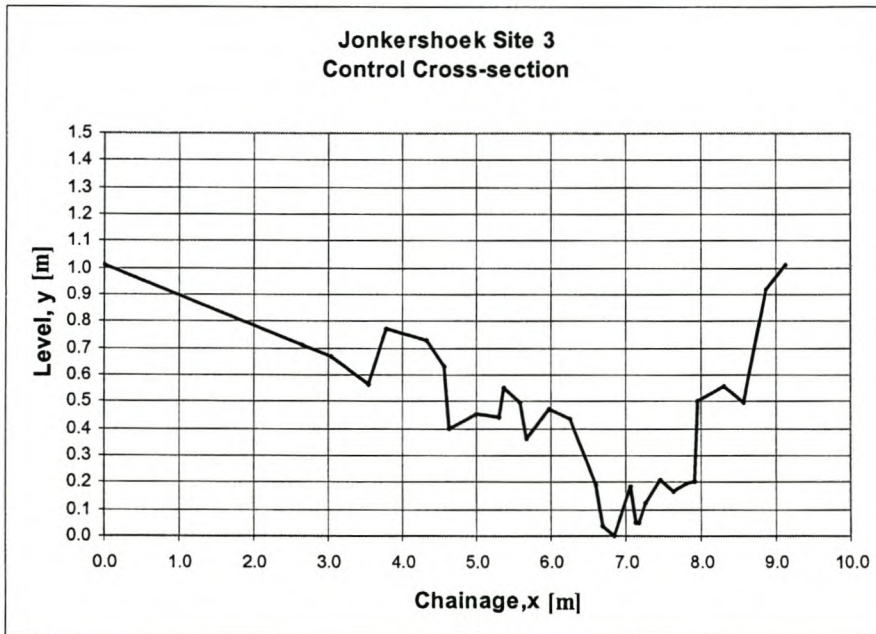
Chainage [m]	Level [m]	Level above lowest point
0.000	0.911	0.810
0.280	1.572	0.149
0.530	1.479	0.242
0.850	1.452	0.269
0.850	1.321	0.400
1.080	1.301	0.420
1.480	1.115	0.606
1.780	0.976	0.745
2.380	1.349	0.372
2.880	1.528	0.193
3.180	1.653	0.068
3.700	1.599	0.122
4.180	1.640	0.081
4.480	1.665	0.056
4.780	1.613	0.108
5.080	1.669	0.052
5.380	1.685	0.036
5.680	1.721	0.000
5.980	1.673	0.048
6.280	1.669	0.052
6.580	1.548	0.173
6.880	1.590	0.131
7.320	1.550	0.171
7.530	1.221	0.500
7.750	1.236	0.485
8.130	0.811	0.910

**Jonkershoek Site 3**

**Waterlevels**

Measurements in meters

Date	Waterlevel	Benchmark Level at Pool	Waterlevel above lowest point in Pool	Weir reading	Qweir
22/01/2002	1.055	0.515	0.525	0.070	0.220
21/01/2002	0.855	0.354	0.564	0.088	0.311
25/10/2001	0.975	0.532	0.622	0.109	0.428
04/10/2001	0.985	0.573	0.653	0.133	0.577
03/10/2001	0.909	0.506	0.662	0.140	0.623
19/01/2002	0.968	0.681	0.778	0.250	1.489





## Jonkershoek Site 3

## Control Section

Chainage [m]	Level [m]	Level above lowest point
0.000	0.448	1.008
2.650	0.746	0.710
3.050	0.791	0.665
3.550	0.891	0.565
3.790	0.686	0.770
4.330	0.730	0.726
4.560	0.828	0.628
4.640	1.059	0.397
5.000	1.001	0.455
5.300	1.017	0.439
5.380	0.905	0.551
5.590	0.963	0.493
5.670	1.094	0.362
5.970	0.984	0.472
6.260	1.019	0.437
6.600	1.265	0.191
6.700	1.420	0.036
6.850	1.456	0.000
7.060	1.275	0.181
7.140	1.409	0.047
7.180	1.409	0.047
7.250	1.332	0.124
7.450	1.249	0.207
7.640	1.293	0.163
7.810	1.261	0.195
7.910	1.252	0.204
7.950	0.952	0.504
8.300	0.899	0.557
8.570	0.958	0.498
8.880	0.538	0.918
9.120	0.448	1.008

## Pool Section

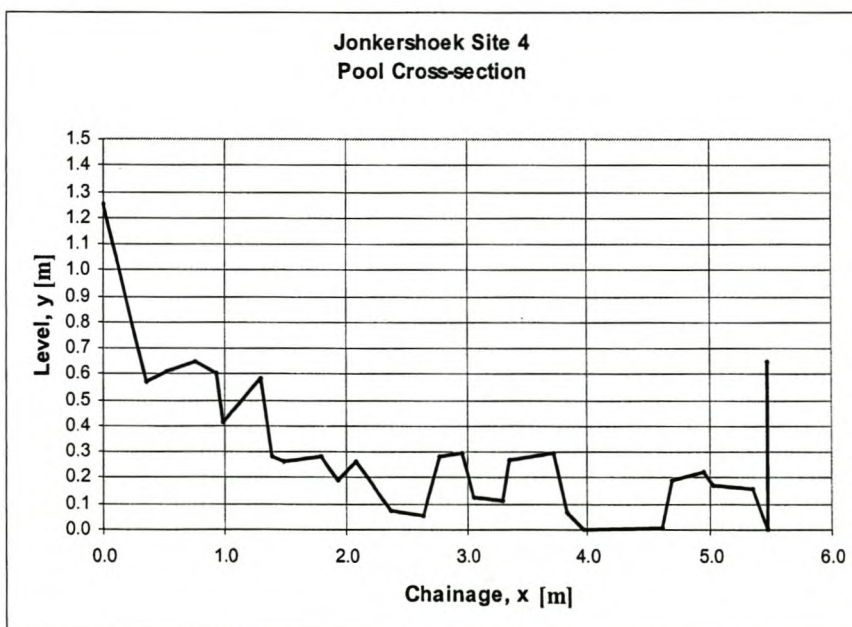
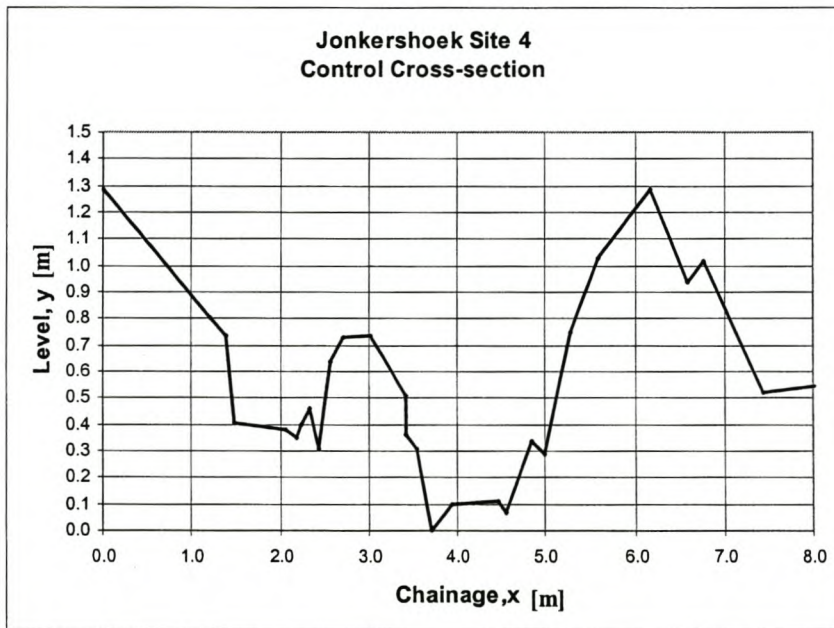
Chainage [m]	Level [m]	Level above lowest point
0.000	0.134	1.197
3.804	0.562	0.769
3.919	0.493	0.838
4.144	0.766	0.565
4.379	0.849	0.482
4.579	0.778	0.553
4.669	0.883	0.448
4.719	1.038	0.293
4.889	1.119	0.212
5.099	1.070	0.261
5.389	0.652	0.679
5.719	0.649	0.682
5.969	0.691	0.640
5.969	0.998	0.333
6.109	1.031	0.300
6.239	1.117	0.214
6.319	0.507	0.824
6.454	0.459	0.872
6.659	0.500	0.831
6.849	0.537	0.794
7.009	0.598	0.733
7.014	1.299	0.032
7.159	0.908	0.423
7.659	0.899	0.432
8.059	0.899	0.432
8.369	0.918	0.413
8.549	1.331	0.000
8.629	1.319	0.012
8.749	1.030	0.301
9.029	1.191	0.140
9.219	1.229	0.102
9.369	0.946	0.385
9.549	0.869	0.462
9.769	1.260	0.071
9.969	1.151	0.180
10.069	0.970	0.361
10.239	0.858	0.473
10.489	0.934	0.397
10.769	1.057	0.274
10.890	1.085	0.246
11.229	0.134	1.197

**Jonkershoek Site 4**

**Waterlevels**

Measurements in meters

Date	Waterlevel	Benchmark Level at Pool	Waterlevel above lowest point in Pool	Weir reading	Qweir
28/11/2001	1.605	0.514	0.308	0.039	0.092
22/01/2001	1.498	0.515	0.416	0.070	0.220
21/01/2001	1.283	0.407	0.470	0.088	0.311
25/10/2001	1.408	0.460	0.523	0.109	0.428
04/10/2001	1.415	0.576	0.560	0.128	0.564
03/10/2001	1.338	0.514	0.575	0.138	0.610
19/01/2001	1.303	0.681	0.777	0.250	1.489



## Jonkershoek Site 4

## Control Section

Chainage [m]	Level [m]	Level above lowest point
0.000	0.392	1.285
1.217	0.872	0.805
1.397	0.943	0.734
1.487	1.273	0.404
2.067	1.299	0.378
2.187	1.329	0.348
2.237	1.276	0.401
2.337	1.215	0.462
2.447	1.371	0.306
2.567	1.041	0.636
2.707	0.949	0.728
3.027	0.941	0.736
3.427	1.171	0.506
3.427	1.314	0.363
3.547	1.371	0.306
3.717	1.677	0.000
3.947	1.579	0.098
4.467	1.569	0.108
4.557	1.607	0.070
4.847	1.338	0.339
4.997	1.392	0.285
5.287	0.927	0.750
5.597	0.650	1.027
6.167	0.392	1.285
6.587	0.741	0.936
6.777	0.659	1.018
7.447	1.157	0.520
8.017	1.135	0.542

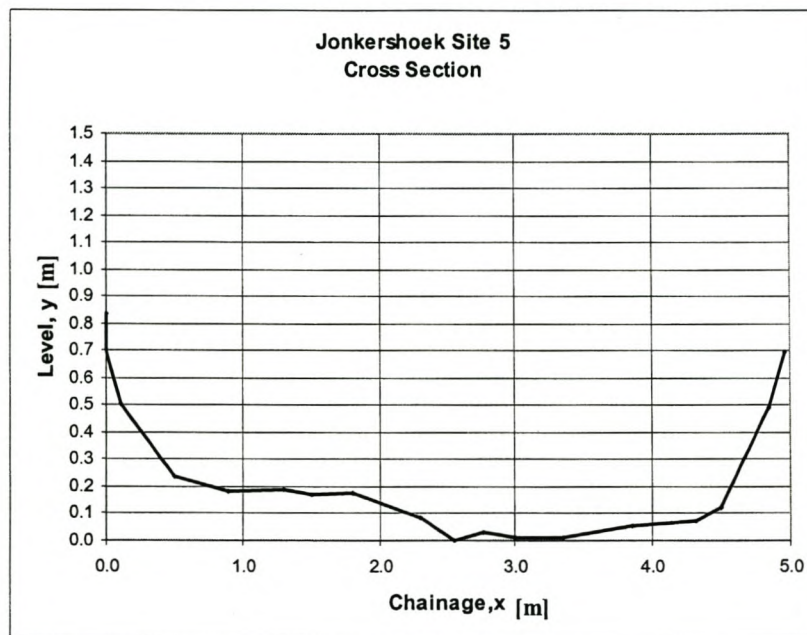
## Pool Section

Chainage [m]	Level [m]	Level above lowest point
0.000	0.543	1.249
0.350	1.220	0.572
0.510	1.181	0.611
0.760	1.144	0.648
0.930	1.189	0.603
0.990	1.378	0.414
1.300	1.210	0.582
1.400	1.508	0.284
1.490	1.527	0.265
1.800	1.510	0.282
1.940	1.599	0.193
2.090	1.529	0.263
2.370	1.721	0.071
2.640	1.741	0.051
2.780	1.509	0.283
2.970	1.500	0.292
3.060	1.668	0.124
3.300	1.678	0.114
3.360	1.522	0.270
3.720	1.495	0.297
3.830	1.726	0.066
3.970	1.790	0.002
4.600	1.783	0.009
4.680	1.600	0.192
4.940	1.571	0.221
5.020	1.622	0.170
5.350	1.632	0.160
5.470	1.792	0.000
5.470	1.144	0.648

**Jonkershoek Site 5****Waterlevels**

Measurements in meters

Date	Waterlevel	Benchmark Level at Pool	Waterlevel above lowest point in Pool	Weir reading	Qweir
14/01/2002	1.718	0.511	0.423	0.021	0.036
28/11/2001	1.295	0.119	0.454	0.039	0.092
25/10/2001	1.167	0.169	0.632	0.109	0.428
04/10/2001	1.818	0.859	0.671	0.128	0.545
03/10/2001	1.394	0.451	0.687	0.140	0.623
02/10/2001	1.053	0.119	0.696	0.148	0.678
19/01/2002	1.346	0.559	0.843	0.235	1.357
29/10/2001	1.781	1.064	0.913	0.292	1.949



**Jonkershoek Site 5****Control Section**

Chainage [m]	Level [m]
0.000	0.832
0.000	0.699
0.110	0.503
0.500	0.238
0.900	0.181
1.300	0.188
1.500	0.170
1.800	0.173
2.300	0.084
2.550	0.000
2.770	0.030
3.000	0.012
3.350	0.010
3.850	0.056
4.320	0.073
4.500	0.121
4.850	0.492
4.970	0.698

## **APPENDIX D**

### **Calculations**

**Laboratory Test no. 1-1****Constriction with Vertical Sides: B/b = 1.5****26 August 2002****POOL**

hmeasure [m]	hp [m]	Ap [m <sup>2</sup> ]	Average hp [m]	Average B [m]	Vp [m/s]	$\alpha Vp^2/2g$ [m]	Htheory [m]
441.000	0.171	0.122	0.122	1.000	0.300	0.005	0.176
485.000	0.215	0.166	0.166	1.000	0.386	0.008	0.223
524.000	0.254	0.205	0.205	1.000	0.454	0.011	0.265
556.000	0.286	0.237	0.237	1.000	0.504	0.014	0.300
585.000	0.315	0.266	0.266	1.000	0.545	0.016	0.331
605.000	0.335	0.286	0.286	1.000	0.573	0.018	0.353

**CONTROL**

yc [m]	Ac [m <sup>2</sup> ]	Bc [m]	Average yc [m]	Average b [m]	Qctheory [m <sup>3</sup> /s]	Vc [m/s]	$\alpha Vc^2/2g$ [m]	Htheory [m]	Qreal [m <sup>3</sup> /s]
0.070	0.045	0.657	0.068	0.653	0.037	0.817	0.036	0.176	0.034
0.101	0.065	0.660	0.099	0.655	0.064	0.983	0.052	0.223	0.065
0.129	0.084	0.664	0.127	0.657	0.093	1.112	0.066	0.265	0.094
0.152	0.099	0.666	0.148	0.668	0.119	1.207	0.078	0.300	0.125
0.173	0.113	0.668	0.169	0.668	0.145	1.286	0.089	0.331	0.156
0.187	0.122	0.669	0.183	0.668	0.164	1.340	0.096	0.353	0.178

Cd	B/b	H/b
0.927	1.5	0.269
1.012	1.5	0.340
1.010	1.5	0.404
1.046	1.5	0.449
1.074	1.5	0.496
1.086	1.5	0.529

**Laboratory Test no. 1-2****Constriction with Vertical Sides:  $B/b = 1.8$** **29 August 2002****POOL**

hmeasure [m]	hp [m]	Ap [m <sup>2</sup> ]	Average hp [m]	Average B [m]	Vp [m/s]	$\alpha Vp^2/2g$ [m]	Htheory [m]
502.000	0.232	0.180	0.183	0.987	0.404	0.009	0.241
642.000	0.372	0.319	0.323	0.987	0.512	0.014	0.386
620.000	0.350	0.297	0.301	0.987	0.487	0.013	0.363
546.000	0.276	0.224	0.227	0.987	0.401	0.009	0.285
585.000	0.315	0.262	0.266	0.987	0.447	0.011	0.326
449.000	0.179	0.128	0.130	0.989	0.272	0.004	0.183
433.000	0.163	0.112	0.114	0.981	0.234	0.003	0.166
404.000	0.134	0.083	0.085	0.981	0.188	0.002	0.136
418.000	0.148	0.097	0.099	0.981	0.207	0.002	0.150
382.000	0.112	0.061	0.063	0.981	0.135	0.001	0.113

**CONTROL**

yc [m]	Ac [m <sup>2</sup> ]	Bc [m]	Average yc [m]	Average b [m]	Qctheory [m <sup>3</sup> /s]	Vc [m/s]	$\alpha Vc^2/2g$ [m]	Htheory [m]	Qreal [m <sup>3</sup> /s]
0.112	0.070	0.621	0.112	0.623	0.073	1.048	0.059	0.241	0.062
0.208	0.114	0.548	0.205	0.556	0.163	1.428	0.109	0.387	0.175
0.192	0.105	0.548	0.189	0.557	0.144	1.372	0.101	0.363	0.153
0.140	0.076	0.546	0.140	0.547	0.090	1.172	0.074	0.284	0.092
0.168	0.091	0.544	0.165	0.554	0.117	1.284	0.088	0.326	0.122
0.075	0.041	0.543	0.075	0.545	0.035	0.858	0.039	0.184	0.032
0.062	0.034	0.541	0.062	0.543	0.026	0.780	0.033	0.165	0.024
0.044	0.024	0.539	0.044	0.543	0.016	0.657	0.023	0.137	0.013
0.052	0.028	0.539	0.052	0.542	0.020	0.714	0.027	0.149	0.019
0.029	0.016	0.537	0.029	0.543	0.008	0.533	0.015	0.114	0.007

Cd	B/b	H/b
0.844	1.6	0.387
1.074	1.8	0.696
1.058	1.8	0.652
1.025	1.8	0.518
1.044	1.8	0.589
0.907	1.8	0.339
0.930	1.8	0.303
0.832	1.8	0.252
0.930	1.8	0.275
0.802	1.8	0.211



**Laboratory Test no. 1-3****Constriction with Vertical Sides: B/b = 2.3****18 September 2002****POOL**

hmeasure [m]	hp [m]	Ap [m <sup>2</sup> ]	Average hp [m]	Average B [m]	Vp [m/s]	$\alpha Vp^2/2g$ [m]	Htheory [m]
388.000	0.118	0.068	0.069	0.987	0.107	0.001	0.119
411.000	0.141	0.090	0.092	0.986	0.144	0.001	0.142
439.000	0.169	0.118	0.120	0.985	0.191	0.002	0.171
460.000	0.190	0.139	0.141	0.985	0.210	0.002	0.192
484.000	0.214	0.162	0.165	0.985	0.236	0.003	0.217
513.000	0.243	0.191	0.194	0.985	0.268	0.004	0.247
538.000	0.268	0.215	0.219	0.985	0.292	0.005	0.273
563.000	0.293	0.240	0.244	0.985	0.314	0.005	0.298
586.000	0.316	0.263	0.267	0.985	0.335	0.006	0.322
610.000	0.340	0.286	0.291	0.985	0.350	0.007	0.347
633.000	0.363	0.309	0.314	0.986	0.369	0.007	0.370
674.000	0.404	0.350	0.355	0.986	0.399	0.009	0.413
703.000	0.433	0.378	0.384	0.986	0.418	0.009	0.442

**CONTROL**

yc [m]	Ac [m <sup>2</sup> ]	Bc [m]	Average yc [m]	Average b [m]	Qctheory [m <sup>3</sup> /s]	Vc [m/s]	$\alpha Vc^2/2g$ [m]	Htheory [m]	Qreal [m <sup>3</sup> /s]
0.032	0.013	0.406	0.030	0.437	0.007	0.560	0.017	0.119	0.006
0.047	0.019	0.408	0.045	0.428	0.013	0.679	0.025	0.142	0.012
0.067	0.028	0.413	0.065	0.428	0.022	0.811	0.035	0.172	0.019
0.080	0.033	0.411	0.078	0.422	0.029	0.886	0.042	0.192	0.027
0.096	0.040	0.412	0.094	0.421	0.038	0.970	0.050	0.216	0.037
0.116	0.048	0.413	0.114	0.421	0.051	1.067	0.061	0.247	0.051
0.133	0.055	0.413	0.131	0.420	0.063	1.142	0.070	0.273	0.069
0.150	0.062	0.414	0.148	0.421	0.075	1.213	0.079	0.299	0.078
0.166	0.069	0.415	0.164	0.421	0.088	1.276	0.087	0.323	0.092
0.181	0.075	0.416	0.179	0.421	0.100	1.333	0.095	0.346	0.106
0.197	0.082	0.416	0.195	0.421	0.114	1.390	0.103	0.370	0.122
0.225	0.094	0.418	0.223	0.422	0.140	1.486	0.118	0.413	0.153
0.244	0.102	0.419	0.233	0.438	0.158	1.547	0.128	0.442	0.176

Cd	B/b	H/b
0.803	2.3	0.272
0.888	2.3	0.331
0.865	2.3	0.403
0.922	2.3	0.455
0.953	2.3	0.514
0.996	2.3	0.587
1.094	2.3	0.649
1.029	2.3	0.710
1.045	2.3	0.768
1.059	2.3	0.822
1.074	2.3	0.880
1.095	2.3	0.980
1.114	2.3	1.009

**Laboratory Test no. 1-4**  
**Constriction with Vertical Sides: B/b = 3.2**  
**24 September 2002**

**POOL**

h <sub>measure</sub> [m]	h <sub>p</sub> [m]	A <sub>p</sub> [m <sup>2</sup> ]	Average h <sub>p</sub> [m]	Average B [m]	V <sub>p</sub> [m/s]	$\alpha V_p^2/2g$ [m]	H <sub>theory</sub> [m]
403.000	0.133	0.083	0.084	0.992	0.092	0.000	0.133
459.000	0.189	0.138	0.140	0.988	0.148	0.001	0.190
518.000	0.248	0.196	0.199	0.987	0.195	0.002	0.250
578.000	0.308	0.255	0.259	0.987	0.234	0.003	0.311
629.000	0.359	0.306	0.310	0.987	0.263	0.004	0.363
678.000	0.408	0.354	0.359	0.987	0.289	0.004	0.412
737.000	0.467	0.413	0.418	0.988	0.316	0.005	0.472

**CONTROL**

y <sub>c</sub> [m]	A <sub>c</sub> [m <sup>2</sup> ]	B <sub>c</sub> [m]	Average y <sub>c</sub> [m]	Average b [m]	Q <sub>c</sub> theory [m <sup>3</sup> /s]	V <sub>c</sub> [m/s]	$\alpha V_c^2/2g$ [m]	H <sub>theory</sub> [m]	Q <sub>real</sub> [m <sup>3</sup> /s]
0.041	0.012	0.294	0.040	0.303	0.008	0.634	0.022	0.133	0.006
0.078	0.023	0.299	0.077	0.304	0.020	0.875	0.041	0.189	0.020
0.118	0.036	0.301	0.117	0.305	0.038	1.076	0.062	0.250	0.039
0.158	0.048	0.303	0.157	0.306	0.060	1.245	0.083	0.311	0.064
0.192	0.059	0.305	0.191	0.307	0.080	1.372	0.101	0.363	0.092
0.225	0.069	0.307	0.224	0.308	0.102	1.486	0.118	0.413	0.122
0.263	0.081	0.308	0.254	0.319	0.130	1.606	0.138	0.471	0.159

C <sub>d</sub>	B/b	H/b
0.800	3.3	0.437
0.966	3.3	0.622
1.006	3.2	0.821
1.076	3.2	1.017
1.143	3.2	1.182
1.187	3.2	1.341
1.223	3.1	1.478

**Laboratory Test no. 2-1****Constriction with Sloped Sides: Slope = 53°****8 October 2002****POOL**

hmeasure [m]	hp [m]	Ap [m <sup>2</sup> ]	Average hp [m]	Average B [m]	Vp [m/s]	$\alpha Vp^2/2g$ [m]	Htheory [m]
483.000	0.213	0.162	0.164	0.987	0.035	0.000	0.213
512.000	0.242	0.190	0.193	0.986	0.045	0.000	0.242
554.000	0.284	0.231	0.235	0.986	0.073	0.000	0.284
604.000	0.334	0.281	0.285	0.987	0.117	0.001	0.335
631.000	0.361	0.308	0.312	0.987	0.135	0.001	0.362
651.000	0.381	0.327	0.332	0.987	0.156	0.001	0.382
691.000	0.421	0.367	0.372	0.987	0.196	0.002	0.423
724.000	0.454	0.400	0.405	0.988	0.228	0.003	0.457

**CONTROL**

yc [m]	Ac [m <sup>2</sup> ]	Bc [m]	Average yc [m]	Average b [m]	Qctheory [m <sup>3</sup> /s]	Vc [m/s]	$\alpha Vc^2/2g$ [m]	Htheory [m]	Qreal [m <sup>3</sup> /s]
0.094	0.006	0.062	0.045	0.130	0.006	0.960	0.049	0.213	0.006
0.112	0.008	0.073	0.052	0.159	0.009	1.048	0.059	0.241	0.012
0.140	0.014	0.103	0.048	0.299	0.017	1.172	0.074	0.284	0.025
0.174	0.025	0.145	0.076	0.330	0.033	1.306	0.091	0.335	0.047
0.191	0.030	0.159	0.086	0.350	0.041	1.369	0.100	0.361	0.062
0.204	0.036	0.177	0.084	0.429	0.051	1.415	0.107	0.381	0.073
0.231	0.048	0.207	0.107	0.447	0.072	1.505	0.121	0.422	0.106
0.253	0.058	0.229	0.126	0.458	0.091	1.575	0.133	0.456	0.133

Cd	B/b	H/b
1.068	7.6	1.637
1.368	6.2	1.514
1.482	3.3	0.948
1.431	3.0	1.016
1.483	2.8	1.031
1.433	2.3	0.888
1.474	2.2	0.944
1.460	2.2	0.995

**Laboratory Test no. 2-2****Constriction with Sloped Sides: Slope = 45°****15 October 2002****POOL**

hmeasure [m]	hp [m]	Ap [m <sup>2</sup> ]	Average hp [m]	Average B [m]	Vp [m/s]	$\alpha Vp^2/2g$ [m]	Htheory [m]
391.000	0.121	0.071	0.072	0.993	0.114	0.001	0.122
415.000	0.145	0.095	0.096	0.990	0.157	0.001	0.146
449.000	0.179	0.128	0.130	0.988	0.209	0.002	0.181
489.000	0.219	0.168	0.170	0.987	0.279	0.004	0.223
522.000	0.252	0.200	0.203	0.987	0.335	0.006	0.258
560.000	0.290	0.238	0.241	0.987	0.403	0.009	0.299
601.000	0.331	0.278	0.282	0.987	0.477	0.012	0.343

**CONTROL**

yc [m]	Ac [m <sup>2</sup> ]	Bc [m]	Average yc [m]	Average b [m]	Qctheory [m <sup>3</sup> /s]	Vc [m/s]	$\alpha Vc^2/2g$ [m]	Htheory [m]	Qreal [m <sup>3</sup> /s]
0.034	0.014	0.413	0.032	0.440	0.008	0.578	0.018	0.122	0.006
0.050	0.021	0.425	0.046	0.459	0.015	0.700	0.026	0.146	0.012
0.073	0.032	0.434	0.064	0.492	0.027	0.846	0.038	0.181	0.024
0.100	0.047	0.471	0.079	0.600	0.047	0.990	0.053	0.223	0.044
0.123	0.061	0.497	0.099	0.620	0.067	1.098	0.065	0.258	0.067
0.150	0.079	0.526	0.111	0.708	0.096	1.213	0.079	0.299	0.100
0.179	0.100	0.559	0.137	0.729	0.133	1.325	0.094	0.343	0.146

Cd	B/b	H/b
0.788	2.26	0.277
0.817	2.16	0.318
0.896	2.01	0.368
0.942	1.64	0.371
0.998	1.59	0.416
1.040	1.39	0.422
1.104	1.35	0.470

**Laboratory Test no. 2-3****Constriction with Sloped Sides: Slope = 38°****22 October 2002****POOL**

hmeasure [m]	hp [m]	Ap [m <sup>2</sup> ]	Average hp [m]	Average B [m]	Vp [m/s]	$\alpha Vp^2/2g$ [m]	Htheory [m]
408.000	0.138	0.088	0.089	0.990	0.082	0.000	0.138
440.000	0.170	0.119	0.121	0.988	0.120	0.001	0.171
474.000	0.204	0.153	0.155	0.987	0.159	0.001	0.205
515.000	0.245	0.193	0.196	0.986	0.215	0.002	0.247
558.000	0.288	0.235	0.239	0.986	0.281	0.004	0.292
590.000	0.320	0.267	0.271	0.986	0.336	0.006	0.326
618.000	0.348	0.295	0.299	0.987	0.388	0.008	0.356

**CONTROL**

yc [m]	Ac [m <sup>2</sup> ]	Bc [m]	Average yc [m]	Average b [m]	Qctheory [m <sup>3</sup> /s]	Vc [m/s]	$\alpha Vc^2/2g$ [m]	Htheory [m]	Qreal [m <sup>3</sup> /s]
0.044	0.011	0.247	0.038	0.290	0.007	0.657	0.023	0.137	0.006
0.066	0.018	0.270	0.053	0.339	0.014	0.805	0.035	0.171	0.013
0.088	0.026	0.297	0.065	0.400	0.024	0.929	0.046	0.204	0.025
0.116	0.039	0.335	0.077	0.502	0.042	1.067	0.061	0.247	0.044
0.146	0.055	0.379	0.097	0.569	0.066	1.197	0.077	0.293	0.075
0.168	0.070	0.415	0.109	0.641	0.090	1.284	0.088	0.326	0.105
0.188	0.084	0.447	0.117	0.720	0.114	1.358	0.099	0.357	0.135

Cd	B/b	H/b
0.855	3.42	0.473
0.889	2.91	0.503
1.013	2.47	0.511
1.060	1.96	0.492
1.127	1.73	0.515
1.168	1.54	0.509
1.182	1.37	0.496

## Fieldwork: Site 1

## POOL

hmeasure [m]	hp [m]	Ap [m <sup>2</sup> ]	Average hp [m]	Average B [m]	Vp [m/s]	$\alpha Vp^2/2g$ [m]	Htheory [m]
0.320	0.320	0.228	1.057	4.638	0.134	0.001	0.321
0.380	0.380	0.269	1.357	5.044	0.249	0.003	0.383
0.391	0.391	0.280	1.413	5.046	0.275	0.004	0.395
0.456	0.456	0.345	1.750	5.072	0.466	0.012	0.468
0.474	0.474	0.363	1.845	5.083	0.547	0.016	0.490

## CONTROL

yc [m]	Ac [m <sup>2</sup> ]	Bc [m]	Average yc [m]	Average b [m]	Qctheory [m <sup>3</sup> /s]	Vc [m/s]	$\alpha Vc^2/2g$ [m]	Htheory [m]	Qreal [m <sup>3</sup> /s]
0.211	0.148	1.571	0.091	1.620	0.142	0.961	0.049	0.321	0.092
0.280	0.376	4.561	0.073	5.167	0.338	0.899	0.043	0.384	0.264
0.290	0.423	4.931	0.083	5.119	0.389	0.918	0.045	0.396	0.220
0.350	0.787	7.184	0.107	7.343	0.816	1.037	0.058	0.469	0.428
0.370	0.939	7.951	0.118	7.969	1.010	1.076	0.062	0.493	0.577

Cd	B/b	H/b
0.645	2.862	0.198
0.782	0.976	0.074
0.567	0.986	0.077
0.525	0.691	0.064
0.572	0.638	0.062

## Fieldwork: Site 3

## POOL

hmeasure [m]	hp [m]	Ap [m <sup>2</sup> ]	Average hp [m]	Average B [m]	Vp [m/s]	$\alpha Vp^2/2g$ [m]	Htheory [m]
1.055	0.525	0.241	0.728	3.026	0.533	0.015	0.540
0.855	0.564	0.270	0.877	3.250	0.579	0.018	0.582
0.975	0.622	0.319	1.124	3.528	1.914	0.196	0.818
0.985	0.653	0.338	1.266	3.742	0.601	0.019	0.672
0.909	0.662	0.347	1.309	3.768	0.906	0.044	0.706
0.968	0.778	0.416	1.966	4.724	0.752	0.030	0.808

## CONTROL

yc [m]	Ac [m <sup>2</sup> ]	Bc [m]	Average yc [m]	Average b [m]	Qctheory [m <sup>3</sup> /s]	Vc [m/s]	$\alpha Vc^2/2g$ [m]	Htheory [m]	Qreal [m <sup>3</sup> /s]
0.350	0.342	2.604	0.223	1.532	0.378	1.135	0.069	0.540	0.220
0.380	0.420	2.810	0.234	1.797	0.504	1.211	0.078	0.582	0.311
0.590	1.377	5.526	0.280	4.913	0.786	1.563	0.131	0.818	0.428
0.460	0.605	3.750	0.248	2.439	1.015	1.258	0.085	0.672	0.577
0.480	0.813	3.750	0.247	3.289	1.060	1.459	0.114	0.706	0.623
0.550	0.942	3.750	0.247	3.809	2.121	1.570	0.132	0.808	1.489

Cd	B/b	H/b
0.582	1.419	0.537
0.617	1.409	0.511
0.545	0.775	0.267
0.569	1.475	0.497
0.588	1.167	0.391
0.702	1.475	0.454

## Fieldwork: Site 4

## POOL

hmeasure	hp	Avg hp	Ap	Avg Bp	Vp	aVp2/2g	Htheory
0.308	0.308	0.136	0.605	4.444	0.095	0.000	0.308
0.416	0.416	0.244	1.047	4.290	0.165	0.001	0.417
0.523	0.523	0.340	1.050	3.088	0.328	0.006	0.529
0.560	0.560	0.377	1.214	3.220	0.348	0.006	0.566
0.575	0.575	0.392	1.282	3.269	0.359	0.007	0.582
0.777	0.777	0.502	2.302	4.581	0.544	0.016	0.793
0.470	0.470	0.287	0.831	2.894	0.306	0.005	0.475

## CONTROL

yc	Ac	b	Avg yc	Avg b	Qctheory	Vc	aVc2/2g	Htheory	Qreal
0.157	0.070	1.021	0.088	0.795	0.057	0.820	0.036	0.308	0.092
0.233	0.152	1.144	0.164	0.928	0.173	1.140	0.070	0.417	0.220
0.319	0.259	1.435	0.151	1.710	0.345	1.330	0.095	0.529	0.428
0.353	0.312	1.666	0.146	2.131	0.423	1.355	0.098	0.566	0.564
0.368	0.338	1.787	0.161	2.094	0.460	1.362	0.099	0.582	0.610
0.537	0.770	2.860	0.231	3.340	1.252	1.626	0.141	0.793	1.489
0.274	0.200	1.211	0.205	0.978	0.255	1.273	0.087	0.475	0.311

Cd	B/b	H/b
1.600	5.589	0.387
1.273	4.624	0.450
1.242	1.806	0.309
1.334	1.511	0.266
1.326	1.561	0.278
1.189	1.371	0.237
1.221	2.959	0.486